

AD-A048 891

HUGHES HELICOPTERS CULVER CITY CALIF
ADVANCED TECHNOLOGY HELICOPTER LANDING GEAR.(U)
OCT 77 R E GOODALL

F/G 1/3

UNCLASSIFIED

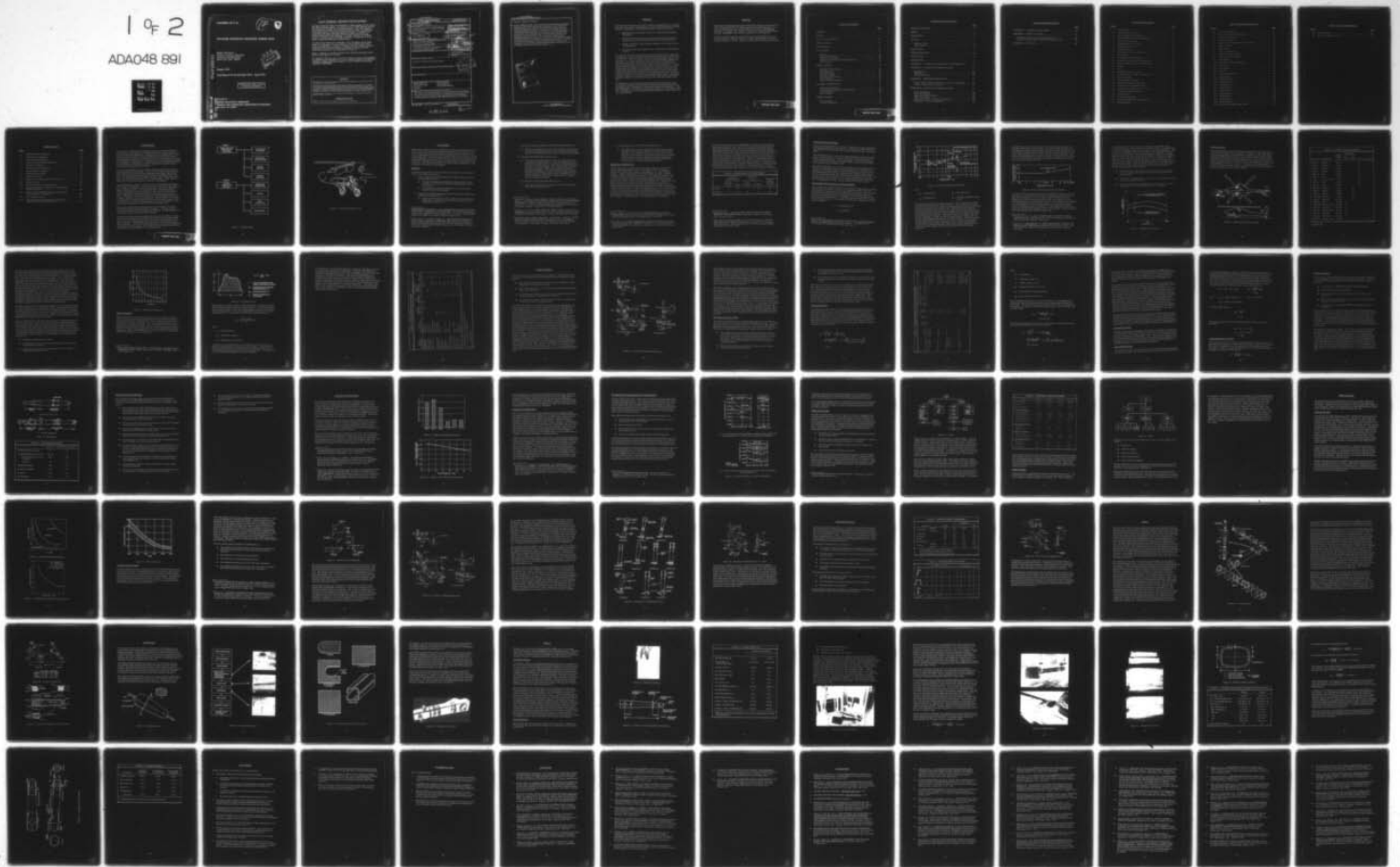
HH-77-41

USAAMRDL-TR-77-27

DAAJ02-75-C-0028
NL

1 of 2

ADAO48 891



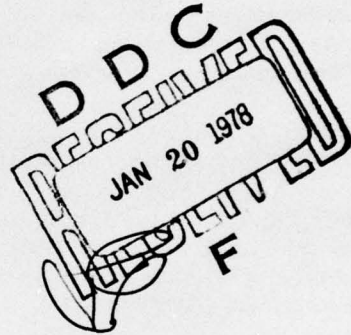
USAAMRDL-TR-77-27

12
B.S.



ADVANCED TECHNOLOGY HELICOPTER LANDING GEAR

Hughes Helicopters
Division of Summa Corporation
Centinela and Teale Streets
Culver City, Calif. 90230



AD A U 488 91

October 1977

Final Report for Period April 1975 - April 1977

Approved for public release;
distribution unlimited.

ADU NO.

DTIC FILE COPY

Prepared for
APPLIED TECHNOLOGY LABORATORY
RESEARCH AND TECHNOLOGY LABORATORIES (AVRADCOM)
Fort Eustis, Va. 23604

12

APPLIED TECHNOLOGY LABORATORY POSITION STATEMENT

This report presents the results of an investigation to design, fabricate, and test a landing gear made of composite materials. The main strut for the YAH-64 helicopter was used as the baseline for the design of the composite component. The primary objectives that were satisfied during the course of this effort were as follows: (a) Establishment of the design criteria for a high-energy-absorbing landing gear. (b) Selection of an advanced structural material and design techniques to satisfy the structural and functional requirements for the landing gear. (c) Design, fabrication, and laboratory testing of a wheel-type composite helicopter landing gear. (d) Evaluation of the test results to assure conformance with the design criteria.

This effort further revealed that the application of the wet filament winding (WFW) process in the fabrication of the gear produced a more cost-effective gear than the current steel baseline gear. In summary, it has been shown that a graphite composite landing gear can be successfully designed and fabricated to withstand the design criteria loads developed for a high-energy-absorbing landing gear.

William T. Alexander, Jr., Structures Technical Area, Technology Applications Division, served as project engineer for this effort.

On 1 September 1977, after this report had been prepared, the name of this organization was changed from Eustis Directorate, U.S. Army Air Mobility Research and Development Laboratory to Applied Technology Laboratory, U.S. Army Research and Technology Laboratories (AVRADCOM).

DISCLAIMERS

The findings in this report are not to be construed as an official Department of the Army position unless so designated by other authorized documents.

When Government drawings, specifications, or other data are used for any purpose other than in connection with a definitely related Government procurement operation, the United States Government thereby incurs no responsibility nor any obligation whatsoever; and the fact that the Government may have formulated, furnished, or in any way supplied the said drawings, specifications, or other data is not to be regarded by implication or otherwise as in any manner licensing the holder or any other person or corporation, or conveying any rights or permission, to manufacture, use, or sell any patented invention that may in any way be related thereto.

Trade names cited in this report do not constitute an official endorsement or approval of the use of such commercial hardware or software.

DISPOSITION INSTRUCTIONS

Destroy this report when no longer needed. Do not return it to the originator.

UNCLASSIFIED

SECURITY CLASSIFICATION OF THIS PAGE (When Data Entered)

REPORT DOCUMENTATION PAGE		READ INSTRUCTIONS BEFORE COMPLETING FORM
1. REPORT NUMBER 18 USAAMRDL TR-77-27 ✓	2. GOVT ACCESSION NO.	3. RECIPIENT'S CATALOG NUMBER
4. TITLE (and Subtitle) 6 ADVANCED TECHNOLOGY HELICOPTER LANDING GEAR,	5. TYPE OF REPORT & PERIOD COVERED 9 Final rept Apr 1 1975 to Apr 1 1977	6. PERFORMING ORG. REPORT NUMBER 14 HH-77-41
7. AUTHOR(s) 10 Ralph E. Goodall	8. CONTRACT OR GRANT NUMBER(s) 15 DAAJ02-75-C-0028	9. PROGRAM ELEMENT, PROJECT, TASK AREA & WORK UNIT NUMBERS 16 62209A 1F262209AH76 00 059 24
11. CONTROLLING OFFICE NAME AND ADDRESS Applied Technology Laboratory, U.S. Army Research and Technology Laboratories (AVRADCOM) Fort Eustis, Virginia 23604	12. REPORT DATE 10 Oct 1 1977	13. NUMBER OF PAGES 17 151p
14. MONITORING AGENCY NAME & ADDRESS (if different from Controlling Office)	15. SECURITY CLASS. (of this report) UNCLASSIFIED	15a. DECLASSIFICATION/DOWNGRADING SCHEDULE
16. DISTRIBUTION STATEMENT (of this Report) Approved for public release; distribution unlimited.		
17. DISTRIBUTION STATEMENT (of the abstract entered in Block 20, if different from Report)		
18. SUPPLEMENTARY NOTES		
19. KEY WORDS (Continue on reverse side if necessary and identify by block number) Energy Absorption Design Analysis Baseline Helicopter Test Landing Gear Shock Strut Wet Filament Winding Graphite		
20. ABSTRACT (Continue on reverse side if necessary and identify by block number) This report covers the work performed on the advanced helicopter landing gear program by Hughes Helicopters. The objectives of the program were to design, fabricate, and test a wheel-type advanced main landing gear concept possessing high-energy-absorbing characteristics for helicopters →		

DDC
RECEIVED
JAN 20 1978
F

409164

Goodall

UNCLASSIFIED

SECURITY CLASSIFICATION OF THIS PAGE(When Data Entered)

Block 20. Abstract (continued)

in the 15,000-pound class. These objectives were achieved by formulating design criteria through a data search, choosing the most cost-effective composite material, and through a design analysis, selecting the most promising landing gear concept. This concept used graphite epoxy as a structural material to fabricate the trailing arm of the main landing gear of the Hughes YAH-64 helicopter by wet-filament winding (WFW). The graphite arm was successfully tested, demonstrating the practicality of employing composite structures in the construction of high-energy-attenuating landing gear components. The program showed that the graphite trailing arm was 11 percent lighter than the baseline steel arm. The weight of the baseline landing gear could be reduced by maximizing the use of composites: 7 percent by using existing WFW equipment, and 26 percent by developing and using a toroid winding machine.

ACCESSION for	
NTIS	White Section <input checked="" type="checkbox"/>
DDC	Buff Section <input type="checkbox"/>
UNANNOUNCED	
JUSTIFICATION	
BY	DISTRIBUTION/AVAILABILITY NOTES
Dist.	PHONE
A	

UNCLASSIFIED

SECURITY CLASSIFICATION OF THIS PAGE(When Data Entered)

SUMMARY

This report describes the work done to evaluate the applicability of composite materials in the design and fabrication of a wheel-type high-energy-absorbing helicopter landing gear. The following primary objectives were met:

- a. Establishment of the design criteria for a high-energy-absorbing landing gear.
- b. Selection of advanced structural material and design techniques to satisfy the structural and functional requirements for this gear.
- c. Design, fabrication, and laboratory testing of a wheel-type helicopter landing gear.
- d. Evaluation of the test results to assure conformance with the design criteria.

An evaluation of industry-established composite structural fibers applicable to landing gear design concluded that Thornel 300 graphite fiber was the most cost effective. This was based on industry-projected graphite material cost reductions. It was also concluded, using wet-filament-winding (WFW) cost experience gained from other projects such as tail boom and main rotor blade fabrication, that a graphite gear would be more cost effective than the present steel baseline gear. The capabilities of a graphite gear were demonstrated using the trailing arm of the most cost-effective configuration that could be fabricated using available WFW equipment. The arm successfully withstood the high dynamic and static loads associated with reserve energy drops and crash forces required by the advanced design criteria. Subsequent evaluation, based on a 33-percent ultimate static load margin, showed that a graphite trailing arm would weigh 11 percent less than the baseline metal arm.

In summation, it was shown that a graphite composite landing gear can be successfully designed and fabricated to withstand the loads associated with the design criteria developed for a high-energy-absorbing landing gear. The final landing gear, consisting of a composite trailing arm, shock strut, cross tube, and wheel was 7 percent lighter than the baseline metal gear and proved to be cost effective.

PREFACE

The Advanced Technology Helicopter Landing Gear Program was carried out under Contract DAAJ02-75-C-0028 issued by the Eustis Directorate, U. S. Army Air Mobility Research and Development Laboratory (USAAMRDL), Fort Eustis, Virginia. Mr. William T. Alexander, Technology Applications Division, USAAMRDL, had technical cognizance over the program.

The author acknowledges the contributions made by Mr. Herbert T. Lund, Program Manager, and Mr. Robert A. Wagner, R&D Manager, both from Hughes Helicopters, and Mr. William T. Alexander of the Eustis Directorate.

PRECEDING PAGE BLANK

TABLE OF CONTENTS

	<u>Page</u>
SUMMARY	3
PREFACE	5
LIST OF ILLUSTRATIONS	10
LIST OF TABLES	13
INTRODUCTION	15
DATA SEARCH	18
Reports	18
Improved Crash Safety	20
Military Specifications	22
Evaluation of MIL-STD-1290 Requirements	22
Shock Absorber	29
DESIGN CRITERIA	33
MIL-STD-1290 Evaluation	35
Fuselage Impact	36
Airframe Damage	39
Main Rotor Blade	39
Unsymmetrical Landings	40
Shock Absorber	41
Design Criteria Summation	43
MATERIAL INVESTIGATION	45
Composite Fabrication	47
Environmental Degradation of Composites	48
Fiber Evaluation	50
Resin Systems	52
DESIGN ANALYSIS	55
Fiber Selection	55
Concept Evaluations	57

TABLE OF CONTENTS (CONT)

	<u>Page</u>
CONCEPT SELECTION	64
DESIGN	67
FABRICATION	71
TESTING	75
Dynamic Testing	75
Static Testing	75
CONCLUSIONS	86
RECOMMENDATIONS	88
REFERENCES	89
BIBLIOGRAPHY	92
APPENDIX A - LANDING GEAR STRUCTURAL REQUIREMENTS	101
APPENDIX B - LANDING GEAR SPECIFICATIONS	103
Specifications	103
Standards	104
Other Publications	105
APPENDIX C - PROCESS SPECIFICATIONS	106
Resins, Epoxy, Filament Winding, for Structural Applications . . .	106
Filament Wound Landing Gear Strut	114
APPENDIX D - TRAILING ARM STRESS ANALYSIS	122
Design Calculations	122
Basic Arm Analysis	122
Upper Pivot Stress Analysis	124
Pivot Lug Analysis	125
Attachment of Axle to Trailing Arm Analysis	128
Attachment of Strut to Trailing Arm	131

TABLE OF CONTENTS (CONT)

	<u>Page</u>
APPENDIX E - LANDING GEAR DRAWINGS	133
APPENDIX F - WEIGHT ANALYSIS	145
Composite Trailing Arm Weight Breakdown (lb)	145
Weight Analysis of Final Composite Trailing Arm (lb)	146
APPENDIX G - TEST PLAN	147

LIST OF ILLUSTRATIONS

<u>Figure</u>		<u>Page</u>
1	Program Plan	16
2	Advanced Composite Gear	17
3	Inherent Landing Gear Capability	23
4	Recommended Ground Contact Velocities	24
5	Helicopter Energy Ratio	25
6	Landing Gear Turnover Angle	26
7	Landing Gear Efficiency	29
8	Load Stroke Curve	30
9	Three-View of Baseline Main Gear	34
10	Shock Struts	42
11	Materials Strength Comparison	46
12	Graphite Versus Steel Cost Comparison	46
13	Moisture Effects on Composite Materials	49
14	Fibers	51
15	Resin	53
16	Materials Weight Comparison	56
17	Graphite Versus S-Glass Cost Comparison	56
18	Price of Graphite	57
19	Baseline Gear Components	59
20	Geometry of Baseline Main Gear	60
21	Trailing Arm Configuration Review	62
22	Geometry of Configurations 3, 5, and 6	63
23	Three-View of Configuration 6	66
24	Composite Arm	68
25	Geometry Comparison	70
26	Construction Schematic of Trailing Arm	70
27	Winding Mandrel	71

LIST OF ILLUSTRATIONS (CONT)

<u>Figure</u>		<u>Page</u>
28	Fabrication Sequence	72
29	Brooms and Doublers Configuration	73
30	Trailing Arm Assembly	74
31	Dynamic Test Setup	76
32	Location of Strain Gages and Accelerometer	76
33	Static Test Setup	78
34	Static Failure	80
35	Trailing Arm Sections	81
36	Section at Failure Location	82
37	Trailing Arm Final Design	84
D-1	Gear Loading	123
D-2	Upper Pivot Loads and Reactions	125
D-3	Pivot Hole	126
D-4	Axle Loading	129
D-5	Axle Hole	130
D-6	Shock Strut Attachment	132
E-1	Configuration 1	133
E-2	Configuration 1A	134
E-3	Configuration 1B	135
E-4	Configuration 2	136
E-5	Configuration 3	137
E-6	Configuration 4	138
E-7	Configuration 4A	139
E-8	Configuration 5	140
E-9	Configuration 6	141
E-10	Configuration 6A	142
E-11	Arm Assembly Main Landing Gear	143

LIST OF ILLUSTRATIONS (CONT)

<u>Figure</u>		<u>Page</u>
G-1	Basic Dimensions	148
G-2	Static Load Deflection Curve	150

LIST OF TABLES

<u>Table</u>		<u>Page</u>
1	Crashworthiness Comparison	21
2	Landing Gear Comparison	27
3	Shock Absorber Evaluation	32
4	Baseline Vertical Impact Capabilities	37
5	Absorber Comparison	42
6	Composite Fiber Comparison	52
7	Concept Weight Comparison	65
8	Configuration Evaluation	65
9	Dynamic Test Data	77
10	Applied Versus Design Loads at Failed Section	82
11	Weight Summary	85
A-1	Landing Gear Structural Requirements	101
C-1	Physical and Reactive Properties of Liquid Resins/ Hardener Systems	108
C-2	Mechanical and Physical Properties of Glass Cloth Base Laminates - Wet Layup	109
D-1	Test and Design Loads	123
D-2	Fiber Properties at Their Respective Orientation Angles for a Fiber Volume Ratio of 0.5	127

INTRODUCTION

The demand for improving helicopter payload fraction has been satisfied in recent years by using advanced composite materials to replace metal in a variety of structural applications. Generally this has brought about a weight savings of 10 to 25 percent. The Eustis Directorate realized that the helicopter landing gear generally represented 3 to 5 percent of gross weight, and that the possible weight saved by a composite gear was significant and worthy of investigation. Consequently, a contract was awarded to Hughes Helicopters to evaluate the use of advanced composite materials as applied to a high-energy-absorbing helicopter landing gear.

A review of past design practices clearly showed the need to improve the crashworthiness of the helicopter. This can be accomplished by increasing ground contact velocities and energy absorption capabilities of the landing gear. The baseline helicopter airframe (YAH-64), including blades, was shown by analysis and test to be flightworthy after high ground contact velocities, such as 31 feet per second, with no weight penalty. These improvements will pay off by reducing costs, injuries, and fatalities.

Hughes Helicopters, as prime contractor, was responsible for the design and program administration. Two subcontractors were used. Fiber Science, Inc., Gardena, California, was selected for their expertise in WFW techniques, and Menasco, Inc., Burbank, California, was chosen for their extensive landing gear testing capabilities. The advanced technology helicopter landing gear program was divided into two phases over a 2-year period. Each phase was divided into tasks for orderly administration and reporting. Figure 1 shows the program plan. During Phase 1, as a result of a data search, advanced design criteria were formulated. Three composite materials were evaluated; graphite epoxy, the most cost effective, was selected as the material to fabricate the advanced landing gear.

The program continued by selecting the gear of the YAH-64, the Hughes Helicopters advanced attack helicopter, as baseline. The gear shown in Figure 2 was selected for fabrication and testing after a design analysis and a comparison with two other promising concepts.

The final gear configuration developed under this program differs from the baseline in that the shock strut is longer and attaches lower on the trailing arm. Also, graphite epoxy composite was used for the structural material rather than steel. During Phase 2 one trailing arm was fabricated using WFW techniques. It was dynamically tested at limit and reserve energy loads and statically tested to failure. The trailing arm successfully withstood the design loads, failing statically at 2.1 times limit load.

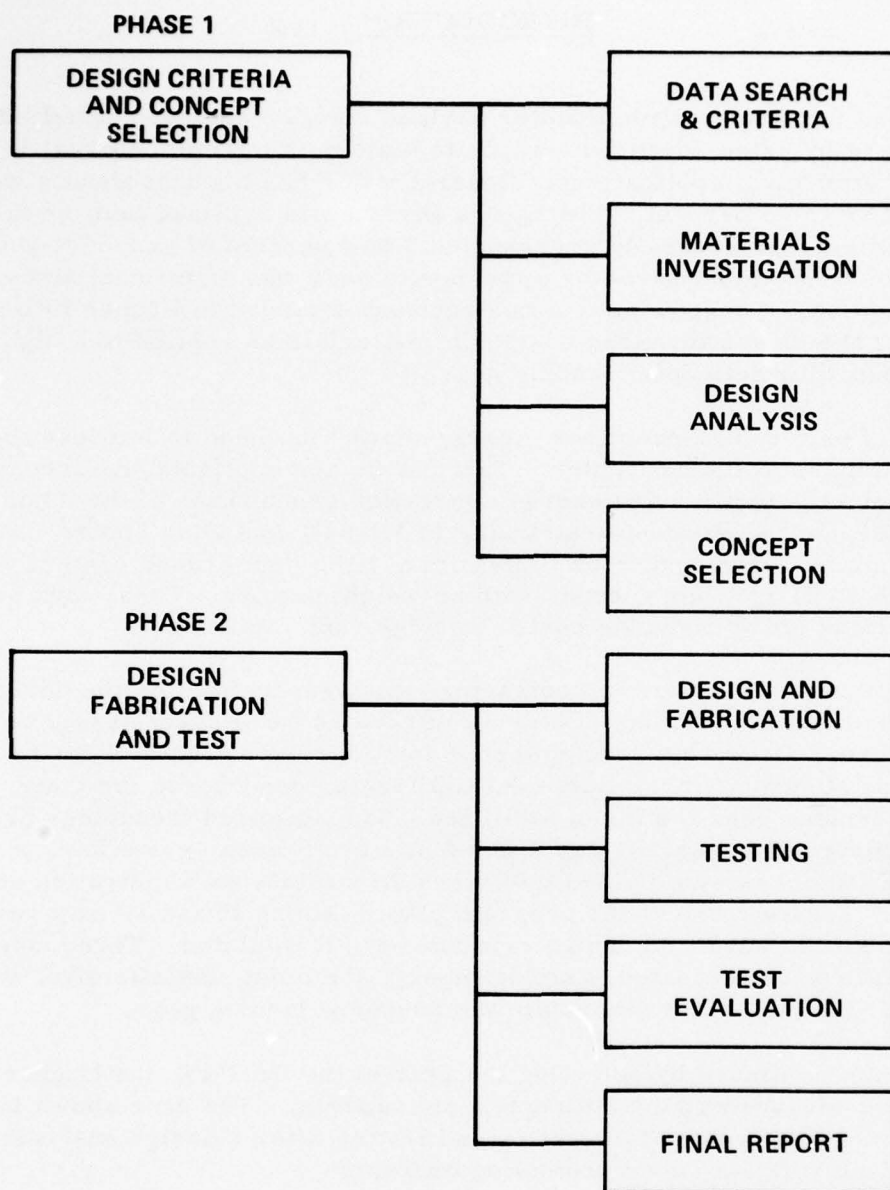


Figure 1. Program Plan.

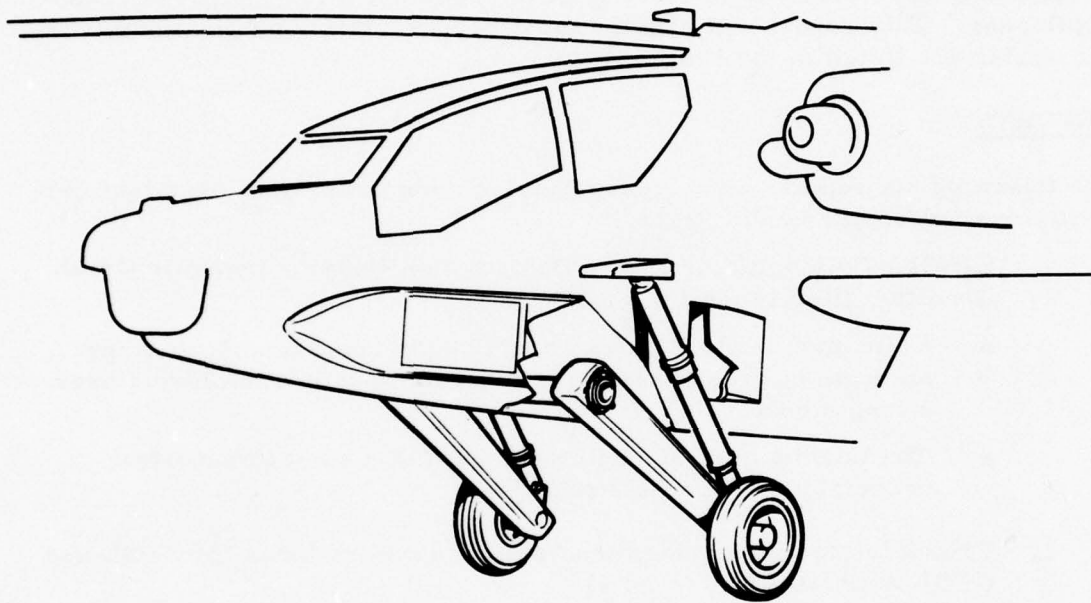


Figure 2. Advanced Composite Gear.

DATA SEARCH

Data from all practical sources relevant to helicopter landing gear experience was surveyed. The information gained pertaining to failures, design, and energy-absorbing methods was used to formulate advanced landing gear criteria. Approximately 130 reports and specifications were reviewed, covering 1960 through 1976. During this period, great strides were made in the awareness and definition of crash survival techniques. Many reports outlined those traits that a helicopter and its landing gear should have for improved crashworthiness. This report will cite the most representative publications. The remainder are listed in the Bibliography.

REPORTS

The following six reports, with accompanying comments, give excellent criteria for a helicopter landing gear.

1. CH-21A Helicopter Airframe Deformation Under a Dynamic Crash Condition (Reference 1)
 - Helicopter landing gears should be designed to absorb large amounts of crash energy at moderate acceleration levels over a long stroke.
 - The landing gear should be designed so as not to penetrate occupiable areas of the fuselage.
2. Principles for Improving Structural Crashworthiness for STOL and CTOL Aircraft (Reference 2)
 - All new aircraft designs should be monitored from the earliest design stages in order to ensure that the principles of crashworthiness are adhered to.

¹ EXPERIMENTAL RESEARCH, CH-21 HELICOPTER AIRFRAME DEFORMATION UNDER A DYNAMIC CRASH CONDITION, Aviation Safety Engineering and Research; TRECOM Technical Report 63-77, U.S. Army Transportation Research Command, Fort Eustis, Virginia, January 1964.

² Avery, James P., and Reed, William H., PRINCIPLES FOR IMPROVING STRUCTURAL CRASHWORTHINESS FOR STOL AND CTOL AIRCRAFT, Aviation Safety Engineering and Research; USAAVLABS Technical Report 66-39, U.S. Army Aviation Materiel Laboratories, Fort Eustis, Virginia, June 1966, AD 637133.

3. Analysis of Helicopter Structural Crashworthiness (Reference 3)
 - The floor accelerations for an aircraft similar to the UH-1D/H may be reduced 65 percent by the use of energy-absorbing techniques in the landing gear system and in the belly of the fuselage.
4. Crash Survival Design Guide (Reference 4)
 - The design of a landing gear for improving crashworthiness presents two definite problems. First, the landing gear must protect the fuselage against contact with the impact surface to as great an extent as possible. This requires that the landing gear possess certain strength characteristics and energy-absorbing capabilities. The second problem arises once the strength of the landing gear and its energy-absorbing capabilities are exceeded. The designer must then attempt to ensure that the landing gear failure does not give rise to occupant injury or postcrash hazards.
5. Crashworthy Landing Gear Study (Reference 5)
 - The landing gear should be considered as only one portion of a total impact protection system.

³ Drummond, John K., Gatlin, Clifford I., Goebel, Donald E., and Larsen, Stuart E., ANALYSIS OF HELICOPTER STRUCTURAL CRASHWORTHINESS, VOLUMES I-II, Dynamic Science; USAAVLABS Technical Reports 70-71A and 70-71B, U. S. Army Air Mobility Research and Development Laboratory, Fort Eustis, Virginia, January 1971, AD 880680/880678.

⁴ Turnbow, J. W., et al, CRASH SURVIVAL DESIGN GUIDE, Dynamic Science; USAAMRDL Technical Report 71-22, U. S. Army Air Mobility Research and Development Laboratory, Fort Eustis, Virginia, October 1971, AD 733358.

⁵ Carr, Richard W., Phillips, Norman S., and Scranton, Richard S., CRASH-WORTHY LANDING GEAR STUDY, Beta Industries, Inc.; USAAMRDL Technical Report 72-61, U. S. Army Air Mobility Research and Development Laboratory, Fort Eustis, Virginia, April 1973, AD 765489.

6. Crash Testing of a CH-47C Helicopter (Reference 6)

- The landing gear should be designed to absorb crash energy by stroking over the available distance at a limit load no greater than the critical collapse load for the airframe. The velocity sensitivity of the stroking load should be minimized to avoid the landing gear becoming a rigid link during high velocity sink rates. Failure of the gear should not result in penetration of occupied areas or of flammable fluid containers.

IMPROVED CRASH SAFETY

The awareness of the need for improving crash safety was marked by six events. The Hughes OH-6A, from its inception in 1960, incorporated 30-feet-per-second contact velocity in its design as its crashworthiness criteria. It had a relatively high energy-absorbing gear and a crushable structure, which provided large amounts of crash energy attenuation. The crash performance of the OH-6A in service proved its design to be a step forward. In the early 1960's, Aviation Safety Engineering and Research dynamically crashed a CH-21 helicopter (see Reference 1). This test showed that for increased crash safety the helicopter landing gear should have improved energy attenuation capability, and that gear arrangements should preclude the possibility of fuselage penetration during a crash. This program emphasized the necessity to change past design practices. The improvement in the energy-absorbing capability of the helicopter landing gear was exemplified by a honeycomb shock absorber (Reference 7) added to a Sikorsky S61L. The absorber was installed in line with the existing main landing gear air-oil shock absorber, and increased the limit drop velocity by 237 percent.

⁶Singley, George T. III, FULL SCALE CRASH TESTING OF A CH-47C HELICOPTER, Paper presented to the 32nd National V/STOL Forum of the American Helicopter Society, Washington, D. C., May 1976.

⁷Rich, M. J., AN ENERGY ABSORPTION SAFETY ALIGHTING GEAR FOR HELICOPTER AND VTOL AIRCRAFT, Sikorsky Aircraft; IAS (AIAA) 62-16, American Institute of Aeronautics and Astronautics, New York, New York, January 1962.

In 1971 the Eustis Directorate, USAAMRDL, released the Crash Survival Design Guide (Reference 4). This report collects the known and pertinent information needed to improve the crashworthiness of helicopter design. MIL-STD-1290 (Reference 8), covering crashworthiness, was written and released in January 1974. This document establishes improved crashworthiness design criteria for military helicopters. Recently, two Army helicopters, the UTTAS and the AAH* were designed using the latest specifications and principles of crashworthiness. These new helicopters promise great improvements in personnel crash survival and the lowering of helicopter accident repair costs. The comparison in Table 1 shows a helicopter designed for crashworthiness in 1960 (the OH-6A) versus one designed to the latest 1974 specifications (the YAH-64). The trend has been to increase ground contact velocities and to attenuate more energy during gear stroking.

TABLE 1. CRASHWORTHINESS COMPARISON					
	Velocity, feet per second		Deflection, inches		Percent of Energy Attenuated by Gear
	Fuselage Contact	Crash	Shock Absorber	Structure	
OH-6A	12	30	9	33	15
YAH-64	31	42	45	11	57

⁸Military Standard - 1290 (AV), LIGHT FIXED- AND ROTARY-WING AIRCRAFT CRASHWORTHINESS, Department of Defense, Washington, D. C., 25 January 1974.

*Utility Tactical Transport System - Production Contract for YUH-60A Helicopter Awarded Sikorsky Aircraft Co. in December 1977; Advanced Attack Helicopter - Development Contract for YAH-64 Awarded Hughes Helicopters in December 1976.

MILITARY SPECIFICATIONS

Modern landing gear design for military helicopters has been controlled by approximately 32 Military Specifications. Specifications MIL-S-8698 and MIL-STD-1290 have had major effect on gear design and were reviewed in detail.

MIL-S-8698 (Reference 9) covers the static and dynamic structural design criteria for helicopters. It defines the minimum load requirements for flight, takeoff and landing. For the landing gear, it specifies limit and reserve energy drop heights, obstruction loads, unsymmetrical landings, and taxiing and ground handling loads.

MIL-STD-1290 (Reference 8) establishes minimum crashworthiness design criteria for light fixed-wing and rotary-wing aircraft. It controls gear design by specifying the angular alignment and maximum velocity at which the fuselage may just contact the landing surface and still remain flight-worthy. This specification also requires that a collapsed gear will not rupture flammable fluid containers, nor increase the danger to occupants. A further overall requirement, where the landing gear will play a dominant role, is attenuation of a crash contact velocity of 42 feet per second.

EVALUATION OF MIL-STD-1290 REQUIREMENTS

The requirements of MIL-STD-1290 were evaluated by determining a fuselage ground contact velocity for a number of existing helicopters. This was accomplished by assuming that the landing gear in each case could be altered to allow the shock strut to stroke through the total distance between the bottom of the extended gear and the fuselage. It was further assumed that the main rotor would provide 1g of lift and that the gear would have a reserve energy load factor of 3g. The resulting velocities were plotted and are presented in Figure 3.

$$\begin{aligned}V_c &= (N_Z \eta_G S_G 64.4)^{1/2} \\ &= (173.88 S_G)^{1/2}\end{aligned}$$

⁹ Military Specification MIL-S-8698(ASG), STRUCTURAL DESIGN REQUIREMENTS, HELICOPTERS, Department of Defense, Washington, D. C., 1 July 1954, with Amendment 1, 28 February 1958.

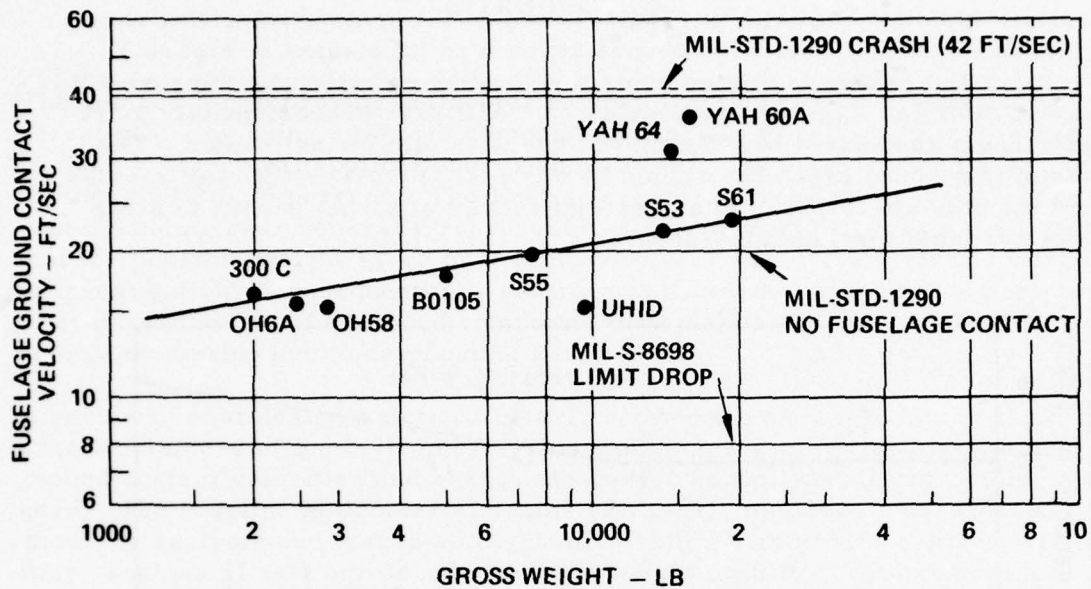


Figure 3. Inherent Landing Gear Capability.

where

$$N_Z = 3g \text{ Load Factor}$$

$$S_G = \text{Gear Stroke, ft}$$

$$\eta_G = 0.9 \text{ Efficiency}$$

$$V_C = \text{Fuselage Contact Velocity, ft/sec}$$

The figure shows that as helicopters increase in gross weight they can attenuate greater vertical landing contact velocities. This is due to an inherent trait that as helicopter size increases the fuselage/ground clearance increases. It also shows that many helicopters of over 7500 pounds gross weight can meet or exceed the 20-foot-per-second fuselage contact velocity requirement of MIL-STD-1290 by simply stroking the landing gear through all of the available fuselage/ground clearance. Helicopters with gross weights below 7500 pounds would suffer a weight increase by requiring larger landing load factors or by increasing clearances for more gear stroking. It can be concluded that MIL-STD-1290 requirements would result in relatively less cost and weight penalties for the larger helicopter. It can also be concluded that in order to use the inherent helicopter capabilities, landing velocity requirements for fuselage contact should increase as helicopter gross weight increases.

A suggested curve is shown in Figure 4, where the contact velocities vary for gross weights of over 7500 pounds at the rate illustrated in Figure 3. The suggested change in ground contact velocities not only will improve autorotation safety at higher gross weights, but will save proportionately more repair costs associated with the more expensive, larger helicopter. The costs of this added capability should be minimal in comparison with savings, since the only alteration is to add enough energy-absorber stroke to make use of available fuselage clearance.

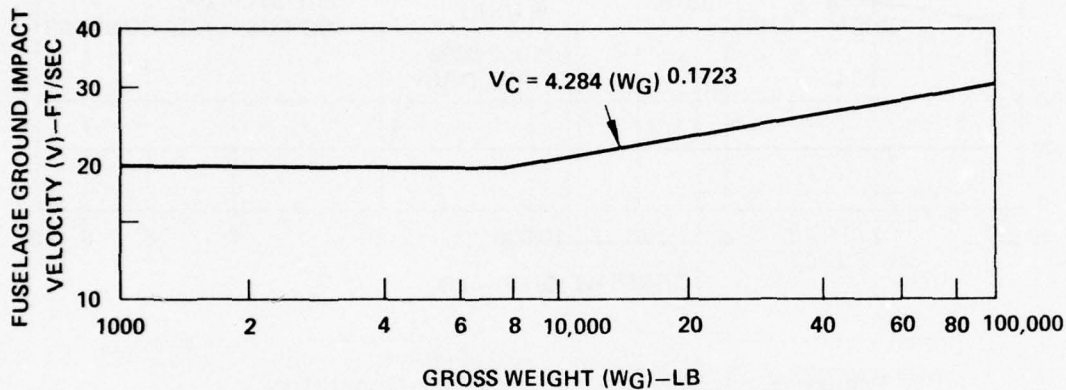


Figure 4. Recommended Ground Contact Velocities.

An example of how an advanced technology helicopter landing gear can significantly reduce accident costs, injuries, and fatalities was shown by evaluating Army accidents for the years 1970 through 1972 (Reference 10). Statistics show that 6.26 percent of all accidents have excessive vertical acceleration and are survivable (Reference 11). If a helicopter were designed to be flightworthy for vertical ground impacts of 31 feet per second, then 75 percent (Reference 4) of the reported survivable helicopter accidents would be classified as just hard landings. The worldwide active Army in the years 1970 through 1972 would have had 50 fewer fatalities, 93 fewer injuries, and would have saved \$13,500,000 in total costs.

¹⁰ Kimball, K. A., et al, ARMY AUTOROTATION ACCIDENTS, FISCAL YEARS 1970-1972, AARU Report 74-2, U. S. Army Aeromedical Research Unit, Fort Rucker, Alabama, August 1973.

¹¹ Haley, J. T., ANALYSIS OF U. S. ARMY HELICOPTER ACCIDENTS TO DEFINE INJURY PROBLEMS, AGARD Conference Preprint 88-71, U. S. Army Board for Aviation Accident Research, Fort Rucker, Alabama, June 1971.

The landing gear and main rotor energy attenuation capabilities can be combined to increase safety during the autorotation landing, and significantly reduce the limitations imposed by a helicopter height-velocity diagram. The comparative magnitude of the gear and rotor energy capabilities, shown in Figure 5, were estimated using the information from Figure 3, and using standard formulas for rotor inertia and autorotation calculations. Curve A, Figure 5, is the ratio of the energy stored in the main rotor to the vertical descent energy of an autorotating helicopter. It gives an estimate of the excess energy available to stop the vertical descent of typical helicopters at different gross weights. Curve B adds the landing gear to the rotor capabilities and shows a 30-percent improvement in available energy for a 15,000-pound helicopter. In summation:

- Present helicopter design produces helicopters that are progressively less safe in autorotation when their gross weight exceeds 15,000 pounds.
- The ability of the landing gear to absorb energy inherently increases as the gross weight increases.
- The energy attenuation capabilities of the landing gear can significantly improve the autorotation safety of the helicopter.

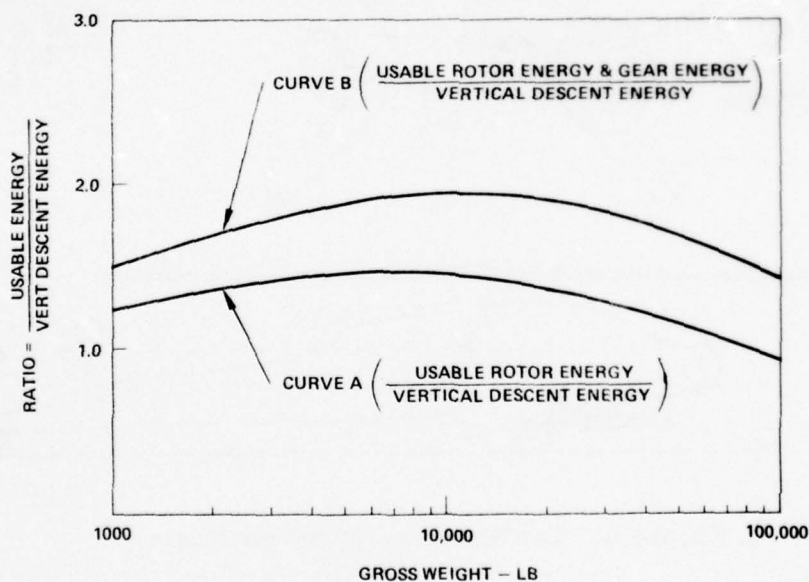


Figure 5. Helicopter Energy Ratio.

Helicopter Design

The helicopter landing gear arrangement is governed by many parameters, such as the minimum turnover angle shown in Figure 6. This angle affects stability during landing, ground handling, or parking, and has been established by Military Specifications for use on commercial as well as military helicopters. During the helicopter design process, most aircraft manufacturers and their customers have decided to use a skid gear for low gross weight rotorcraft, as shown in Table 2, since these helicopters can be easily ground handled with separate wheels. The skid gear also eliminates the weight and costs associated with the complexity of brakes and the associated hydraulic system found with wheeled gears.

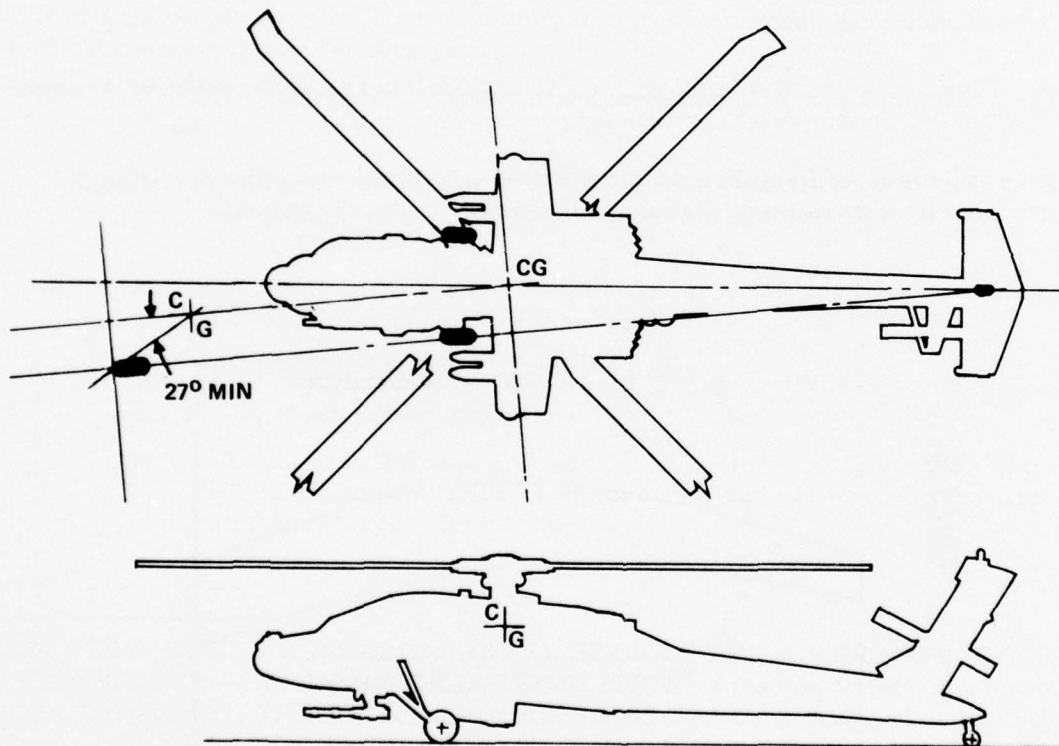


Figure 6. Landing Gear Turnover Angle.

TABLE 2. LANDING GEAR COMPARISON

Helicopter	Manufacturer	Gross Weight, lb	Tricycle			Quadricycle
			Nose Wheel	Tail Wheel	Skid	
300C	Hughes	2,050			X	
F28A	Enstrom	2,150			X	
OH-6A	Hughes	2,400			X	
500D	Hughes	3,000			X	
OH-58A	Bell	3,000			X	
206L	Bell	3,900			X	
105C	Boeing Vertol	5,070			X	
UH-1H	Bell	9,500			X	
AH-1T	Bell	14,000			X	
HH-52A	Sikorsky	7,900		X		
SH-2D	Kaman	12,800		X		
YAH-64	Hughes	13,200		X		
YUH-60A	Sikorsky	15,850		X		
SH-3D	Sikorsky	20,500		X		
YAH-63	Bell	15,000*	X			
YUH-61A	Boeing Vertol	15,000*	X			
CH-3E	Sikorsky	22,050	X			
CH-46E	Boeing Vertol	23,300	X			
RH-53	Sikorsky	41,126	X			
CH-54A	Sikorsky	42,000	X			
CH-47C	Boeing Vertol	46,000				X

*Approximate

The U. S. higher gross weight helicopters use wheels exclusively. This provides a taxi capability and eliminates ground handling problems associated with large separate wheels and jacking equipment. The tricycle type gear with a nose or tail wheel, rather than a quadricycle, is predominantly used. The nose wheel and quadricycle types give a more compact gear arrangement and are generally used on helicopters that rear-load large equipment. The tail wheel, rather than a nose wheel, is sometimes used in order to keep the main wheels closer together and to reduce the pitchover velocity that can be associated with high nose-up landings. Some helicopter pilots have found the tail wheel helpful as a ground proximity indicator when nap-of-the-earth and night flying is required. The type of main rotor system also affects the landing gear, since rotors with low lead-lag hinge resistance must have a shock strut to dampen a ground resonance condition. Two-bladed teetering main rotors similar to the OH-58A have not used landing gear shock struts. However, future helicopters designed to recent crash-worthiness criteria will probably require a shock strut for efficient energy absorption. Generally, the gear is configured or arranged to carry out the helicopter design mission with the greatest cost effectiveness.

The modern state-of-the-art landing gear attenuates large amounts of energy by using two methods, or a combination thereof. The most efficient method is to use a shock strut with a load limiter or energy absorber. A variety of load limiters are available, such as air-oil or honeycomb designs with efficiencies in the order of 90 to 95 percent. Another method is the use of yielding capabilities of the metal arm or cross strut. This configuration provides efficiencies in the range of 50 to 80 percent.

The relationship between load factor and gear energy-absorption efficiency, Figure 7, shows that when the efficiency drops 45 percent the load factor increases 90 percent. This has a significant impact on the empty weight of the helicopter, since high efficiency gives a lower load factor and a shorter gear, and therefore allows lower fuselage and gear weights. The importance of arriving at an efficient landing gear arrangement in the preliminary design of a helicopter must be emphasized, since the final cost and weight of the helicopter will be greatly affected. The landing gear can be optimized for efficiency by:

- Developing an efficient shock strut.
- Minimizing the change in mechanical advantage of the shock strut over the travel of the gear.
- Maximizing the gear movement that strokes the shock strut; i. e., minimizing bending deflection.

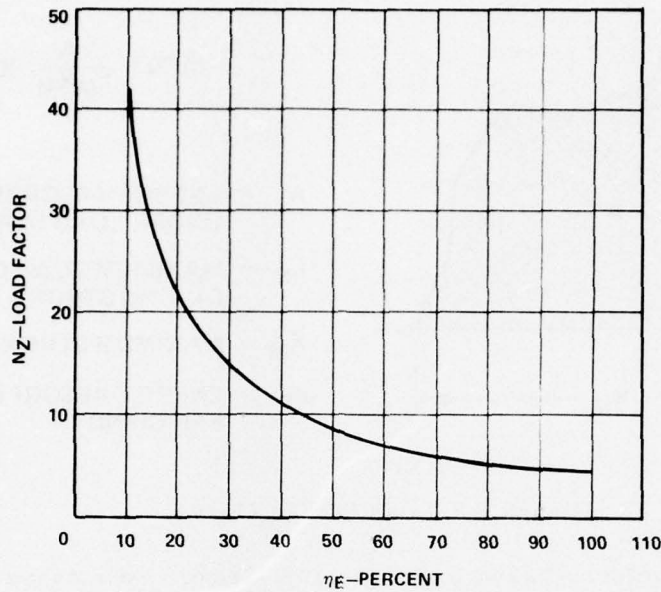
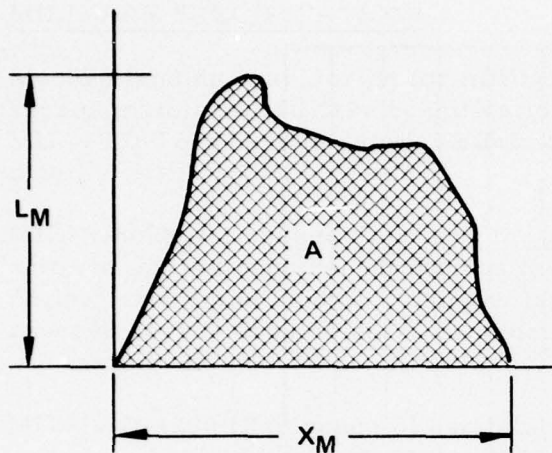


Figure 7. Landing Gear Efficiency.

SHOCK ABSORBER

The shock absorber, also called a damper or energy absorber, has been shown to be an important part of the landing gear. It must provide efficient energy attenuation and at the same time give a smooth ground roll for the helicopter at a minimum weight and cost. Three methods have been used to evaluate shock absorber efficiency. The most widely used is based on the quantity of energy absorbed. High efficiency in absorbing energy minimizes helicopter weight by limiting the load factor and the length of individual gear components. MIL-L-8552C (Reference 12) shows the method of computing efficiency; this method is shown in Figure 8.

¹² Military Specification MIL-L-8552C, LANDING GEAR, AIRCRAFT SHOCK ABSORBER (AIR-OIL TYPE), Department of Defense, Washington, D. C., 19 November 1965.



$$\eta_E \% = \frac{A}{L_M X_M} \times 100$$

A = ENERGY ABSORBED (AREA UNDER LOAD STROKE CURVE)

L_M = MAXIMUM LOAD OBTAINED DURING STROKE, LB

X_M = MAXIMUM STROKE, FT

η_E = ENERGY ABSORPTION EFFICIENCY

Figure 8. Load Stroke Curve.

Shock absorber efficiency based on length and stroke is a method of comparing the absorber length needed for a required stroke. The shock absorber length has a significant impact on the landing gear weight but a small effect on the fuselage weight, since a high stroke efficiency minimizes the length of the shock strut. The method of calculating the stroke efficiency is:

$$\eta_S \% = \left(\frac{L_E - L_C}{L_E} \right) \times 100$$

where

η_S = stroke efficiency

L_E = length fully extended, ft

L_C = length fully compressed, ft

The specific energy absorbed by a shock absorber is the measure of its ability to absorb energy as compared to its own weight. A practical comparison between absorbers can be achieved by dividing the total weight of the absorber into the maximum amount of energy absorbed. This gives the number of foot-pounds absorbed per pound of absorber.

The hydraulic or oil-orifice type absorber, through its wide usage, has been the work horse of industry for landing gears. However, the honeycomb-constructed absorber has been used and is comparable to the oil-orifice type absorber in attenuating large loads. The honeycomb design has crush strengths in the order of 10,000 psi, allowing reasonable diameters and lengths. Some of the other shock absorber designs listed in Table 3 are promising candidates for landing gear use. However, experience data regarding their capabilities is limited. It was therefore decided to drop these candidates from consideration for an advanced landing gear. The present state of the art in designing shock absorbers leaves two types, air-oil and honeycomb, either singly or in combination, that would best satisfy the advanced landing gear requirements.

TABLE 3. SHOCK ABSORBER EVALUATION

Device Description	Energy Absorption Process	η_E percent		η_S percent		Specific Energy Absorbed, ft-lb/lb		Reference
		ACT	EST	ACT	EST	ACT	EST	
HH YAH-64 Shock Strut	Oil through an orifice		75 to 90	30			2,564	6
Sikorsky S61L Shock Strut	Crushing of honeycomb	95		34		3,341		2
Tube Inversion	Hoop tension bending compression	96		73		7,500*		6,7,8
Boeing Vertol Tube Flaring	Hoop tension friction bending	67 to 81		56**		711		9
Arde's Bar Thru Die	Torsion	60 to 68		30**		518		9
MRI Rolling Torus	Cyclic bending shear	70		30**		1,090		9
All-American Co. Wire Thru Platen	Bending friction	81		30**		591		9
Ara's Tor-Shok Rolling Torus	Cyclic bending shear	81		30**		1,453		9
Fragmenting Tube	Hoop tension bending	56		56**		31,000*		8,10

*Would be reduced somewhat in a practical design by attachment weight, etc.

**Approximated for a landing gear application.

η_E = energy absorption efficiency

η_S = stroke efficiency

DESIGN CRITERIA

The design criteria were formulated by evaluating the criteria used for the main gear of the YAH-64 helicopter against the following results of the data search:

- MIL-STD-1290 (Reference 8) was the latest specification covering landing gear crashworthiness design.
- MIL-S-8698 (Reference 9) was the latest specification covering gear loads other than crash.
- The landing gear should increase the energy available to arrest autorotational landings by approximately 30 percent.
- The shock strut could be designed using honeycomb crushing and/or oil through an orifice to absorb energy.

The YAH-64 as baseline is equipped with a nonretractable landing gear consisting of two main wheel units and a single tail wheel meeting the requirements of MIL-S-8698. The landing gear shown in Figure 9 provides the ground stability necessary for taxi, takeoff, and landing at the basic structural design gross weight on terrain with slopes up to 12 degrees, and for landing sideways on a 15-degree slope under zero wind conditions. The landing gear conforms to MIL-STD-1290 by minimizing the possibility of structural components entangling brush, landing mats, and other obstructions. The gear subsystem is located so as to eliminate the possibility of a part of the gear or support structure being driven into an occupiable section of the helicopter or into a region containing a flammable fluid tank or line, for any accident falling in the survivable category as defined in TR 71-22 (Reference 4). An analytical and configuration analysis showed that the failure of the landing gear would not result in a failure of any crew restraint system or restraint system tiedown. Analysis also showed that the ground contact velocity at which the fuselage just touched the surface was 31 feet per second. The gear flotation capability allowed the aircraft to be towed at design gross weight on soil with a California Bearing Ratio (CBR) of 2.5 by vehicles normally assigned to Army aviation units. The landing gear provides kneeling capability and dimensional limits that permits expeditious handling and transport via C-130 and C-141 aircraft. The gear was designed for running landings and takeoffs at 45 knots. The limit drop was 10 feet per second and the reserve energy drop was 12.5 feet per second. The critical design conditions were a three-point crash landing with side load and a two-point landing with drag.

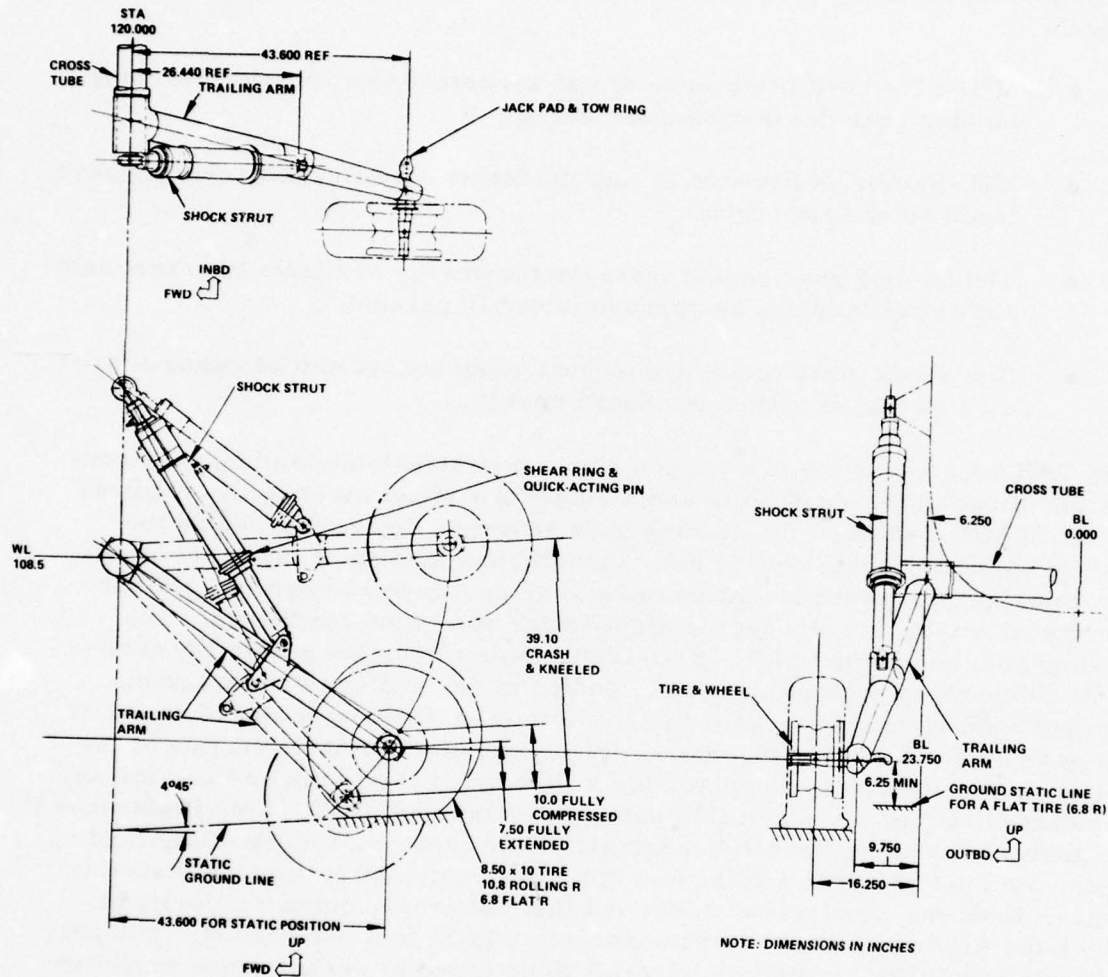


Figure 9. Three-View of Baseline Main Gear.

The baseline main gear also minimizes hard landing damage by utilizing a large deflection at a low load factor of 5 to attenuate 57 percent of the helicopter crash energy at 42 feet per second. Another important feature is that gear loads and moments are reacted across the width of the fuselage through a cross tube connecting the left- and right-hand gears. This characteristic ensures support of the fuselage throughout the crash impulse and not fail due to local rotation of the attachment fittings. The gear also improves autorotation safety for the baseline helicopter by adding 25 percent more energy to arrest vertical descent.

The major components of the baseline main gear, shown in Figure 9, are the cross tube, shock strut, and trailing arm with wheels, tires, and brakes. The trailing arms rotate on each side of the fuselage using the free floating cross tube as a pivot, stroking the shock strut, and absorbing the ground loads from the tires. The gear is capable of deflecting 10 inches for normal landings and 39 inches for crash landings. Kneeling capabilities are attained by hydraulically shortening the shock strut, and raising the gear 39 inches. This allows the helicopter to be transported by C-130 or C-141 aircraft. The tire is an 8.50-10 tubeless 10-ply using a 24- by 7.7-inch wheel. The brakes are hydraulic, with a single floating disc, and are manually operated with power assist. The shock strut is a combination standard air-oil oleo with a 3.63-inch stroke for normal operation and an in-line oil load limiter with an additional 11.16-inch stroke for crash landings. All components of the gear are easily removed by using a fuselage jack and disconnecting the required assembly.

MIL-STD-1290 EVALUATION

The primary design loads for the YAH-64 landing gear were derived from the crash requirements outlined in MIL-STD-1290 (Reference 8). The single exception was the two-point landing condition with drag from MIL-S-8698 (Reference 9) which dictated the design of the shock strut and its attachments. The portions of MIL-STD-1290 affecting the landing gear are as follows:

- The landing gear must be capable of decelerating the aircraft at normal gross weight from an impact velocity of 20 feet per second onto a level rigid surface without allowing the fuselage to contact the ground. This contract required that an impact velocity of 35 feet per second also be evaluated. The limit sink speed was 10 feet per second.
- The aircraft structure, except the rotor blades, shall be flight-worthy after the preceding impacts.

- The aircraft shall be capable of meeting the impact requirements in accidents, including a simultaneous fuselage angular alignment of ± 10 degrees in pitch or roll.
- The landing gear shall be capable of absorbing as much of the crash energy as practical, resulting from a vertical impact of 42 feet per second.

The design of an attack helicopter encompasses many variations of the fuselage, gear, gun, rocket pod, and main rotor locations. The YAH-64, due to the location and ground clearance needed for the 30mm gun, is able to have a 39-inch total vertical travel of the landing gear. The maximum normal travel of the gear is 10 inches, giving for a three-point landing a 3g ground load factor at limit drop and 4.5g at reserve energy drop. Table 4 summarizes the vertical impact capabilities for the baseline gear. The 39-inch gear travel allows the load limiter portion of the shock strut to be set at a low 5g load factor. The gear attenuates 57 percent of the helicopter energy resulting from a 42-feet-per-second vertical crash.

FUSELAGE IMPACT

The baseline gear decelerates the helicopter at normal gross weight from a vertical impact of 31 feet per second without allowing the fuselage to touch the ground. If this impact velocity was increased to 35 feet per second, either the ground load factor or fuselage ground clearance would have to be increased. Higher load factors would require additional fuselage strength; more fuselage clearance would require a longer landing gear. In both cases additional weight must be added to the helicopter. The resultant vertical load factor for a 35-feet-per-second impact, assuming no change in fuselage clearance and a 1g rotor lift is

$$\begin{aligned}
 N_Z &= \left(\frac{WV_c^2}{2g} - E_T \right) \frac{1}{W \eta_G S_G} \\
 &= \left(\frac{13,950 (35)^2}{64.4} - 10,374 \right) \left(\frac{1}{13,950 \times 0.9 \times \frac{39}{12}} \right) \\
 &= 6.25g
 \end{aligned}$$

TABLE 4. BASELINE VERTICAL IMPACT CAPABILITIES

Item	Impact Condition	Reference Requirement	Vertical Velocity (fps)	Rotor Lift Factor (g)	Maximum Ground Load Factor (g)	Required Vertical Axle Travel (in.)			Remarks	
						Due to Orifice Action	Due to Blowing or Yielding	Total		
①	Limit (ultimate = 1.5 x limit)	MIL-S-8698 (See Remarks)	10	0.67	3.0 (3-wheel) 2.8 (2-wheel)	10	0	10	0.75	Impact absorbed by normal oleo action plus tire - i. e., no yielding or blowoff
②	Reserve Energy	MIL-S-8698 (See Remarks)	12.5	0.67	4.5 (3-wheel) 4.2 (2-wheel)	10	2	12	0.85	Impact absorbed by normal oleo action plus blowoff (or yielding) to the extent shown
③	Design Maximum (at which fuselage or boom just contacts ground)	MIL-STD-1290	31	1.0	5.0 (3-wheel) 4.67 (2-wheel)	10	29	39	0.90	Maximum impact capability without fuselage/boom damage - blowoff (or yielding) deformation absorbs 50 to 75 percent of total impact energy
④	Crashworthiness Requirement	MIL-STD-1290	42	1.0	5.0 (3-wheel) (5.55 for ultimate strength)	10	29	39	0.75	Landing gear meeting this criterion, ①, ②, ③, and ④ will absorb 57 percent of total impact energy for the design 42 fps vertical velocity

where

N_Z = load factor, g

W = helicopter weight, lb

V = contact velocity, ft/sec

E_T = energy absorbed by tire, ft-lb

η_G = gear efficiency (energy absorbed)

S_G = gear vertical movement, ft

This represents a load factor increase of 25 percent. The estimated total weight of the baseline fuselage and main and tail landing gear affected was 816 pounds. The helicopter weight load factor varies in direct proportion and accordingly, the result is a 204-pound weight increase. This is 1.46 percent of gross weight.

$$\begin{aligned}\Delta W &= \frac{816 \times 0.25}{13,950} \times 100 \\ &= 1.46 \text{ percent}\end{aligned}$$

The required fuselage clearance using a 5g load factor, assuming a 1g rotor lift and a ground impact of 35 feet per second is

$$\begin{aligned}S_G &= \left(\frac{WV_c^2}{2g} - 10,374 \right) \frac{12}{WN_Z\eta_G} \\ &= \left(\frac{13,950 (35)^2}{64.4} - 10,374 \right) \frac{12}{13,950 \times 5 \times 0.9} \\ &= 48.74 \text{ inches}\end{aligned}$$

It was necessary to increase the length of the main gear trailing arm to provide for this clearance. This necessitated alteration of the forward fuselage because the cross tube had to be moved forward in order to keep the same pitching tipover angle. The estimated weight increase for these configuration changes was 152 pounds or 1.09 percent of the fuselage gross weight.

In summation, if the maximum impact velocity for no fuselage contact was changed to 35 feet per second, the fuselage weight would necessarily increase. However, this gives the gear more energy absorption capabilities, and allows the helicopter to attenuate a 45-feet-per-second vertical crash velocity. This exceeds the requirement of MIL-STD-1290 by 3 feet per second. Since weight and cost penalties caused by exceeding specifications were not cost-effective, an impact velocity of 35 feet per second could not be justified and was not used for the gear design criteria. It became obvious at this point that the 42-feet-per-second vertical crash requirements for the complete helicopter establishes the maximum impact velocity at which the fuselage will not touch the landing surface. Increasing the fuselage impact velocity to 35 feet per second gave unacceptable penalties and decreasing the velocity to 20 feet per second gave up hard landing capability. Therefore, an impact velocity of 31 feet per second was determined to be the optimum and was used as the criteria for the advanced landing gear.

The vertical crash requirements of 42 feet per second increased the ground load factor for the baseline helicopter from 4.5g to 5.55g. This was approximately a 25-percent load factor increase and, as previously determined, would increase fuselage weight approximately 1.46 percent of gross weight. This weight increase is considered acceptable in relation to the possible cost savings that will accrue due to the increase in helicopter crashworthiness.

AIRFRAME DAMAGE

Fuselage damage at the landing gear attachments due to loads resulting from a vertical ground impact of 31 feet per second was confined to local yielding because failure of the fuselage fittings due to rotation was eliminated by the cross tube method of gear attachment. Also, even though the fuselage structure was designed for 5.55g, the shock strut limited the load applied to the fuselage to 5g. This 10-percent failure margin permitted the local skin panels and fittings to yield and buckle but not rupture.

MAIN ROTOR BLADE

The main rotor blades can withstand the forces resulting from a high landing gear ground impact if it is assumed they do not strike the landing surface due

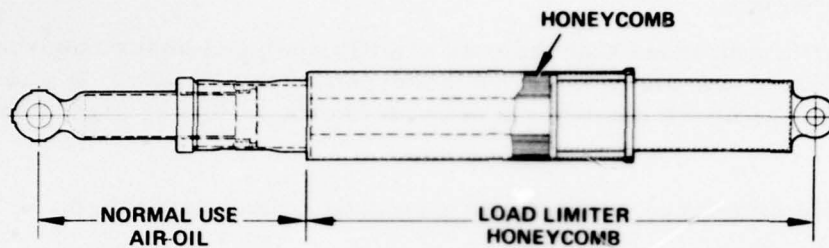
SHOCK ABSORBER

The data search concluded that the only readily designed shock absorbers were the standard air-oil type and the honeycomb load limiter. It was also concluded that the shock absorber must provide the following mandatory features:

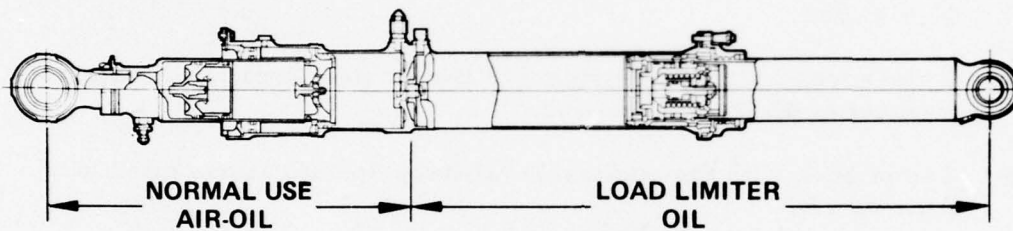
- A damping force sufficient to attenuate ground resonance.
- Shock attenuation during ground roll.
- Kneeling capabilities by shortening the static helicopter height 31.5 inches.
- Fifty-seven percent absorption of the vertical energy due to crash impacts at 42 feet per second.
- Compliance with the applicable Military Specifications cited in Appendix B.

The shock struts shown in Figure 10 were sized for the baseline gear and satisfy the preceding requirements, except that a separate kneeling capability would have to be provided for a helicopter with the honeycomb strut. The normal air-oil operating portion was common to both struts. It used air pressure as a return spring and oil flowing through an orifice for energy absorption. The honeycomb load limiter was made 95 percent efficient by precrushing the honeycomb 5 percent to reduce the initial peak in the load-stroke curve. The stroke of both shock struts was the same and met baseline requirements.

The struts are compared in Table 5. The air-oil type used on the baseline gear was the most efficient overall. Its load-stroke efficiency had been developed to values comparable to the honeycomb type. The length was 5.7 inches shorter, giving a high length efficiency. This strut reduced the helicopter maintenance and acquisition costs by providing integral kneeling capabilities and being reusable after full stroking. The potential hazard of spraying fluid during a crash is alleviated by containing the oil inside the strut. Both struts have rebound capabilities due to the air pressure in the small end. The air-oil shock strut weighs less, is the most efficient, eliminates customer logistic problems, and is therefore the most cost effective. This shock strut, therefore, was selected for use with the advanced landing gear.



a. Air-Oil and Honeycomb



b. Air-Oil (Baseline)

Figure 10. Shock Struts.

TABLE 5. ABSORBER COMPARISON

	Air-Oil	Air-Oil and Honeycomb
Length Efficiency, percent	30	27
Load Stroke Efficiency, percent	75 to 90	95
Specific Energy Absorbed, ft-lb/lb	2564	2205
Weight, lb	42	48.4
Rebound Capability	Yes	Yes
Kneeling Capability	Yes	No
Reusable	Yes	No
Fluid Hazard	No	No

DESIGN CRITERIA SUMMATION

The completion of the data search and evaluation of the latest military requirements found in MIL-STD-1290 (Reference 8) were completed. The results were used to formulate the following criteria for the advanced landing gear.

- The requirements of MIL-S-8698 (Reference 9) for a Class I helicopter must be met. This covers ground handling, and normal and obstructed landing loads. The limit drop shall be 10 feet per second. The reserve energy drop shall be 12.5 feet per second.
- The requirements of MIL-STD-1290 covering rotary-wing crashworthiness must be met or exceeded.
- The vertical velocity at which the fuselage will just touch the landing surface shall be 31 feet per second.
- Pitch and roll alignment at a ground impact of 31 feet per second shall be ± 12 and ± 15 degrees, respectively.
- The blades and fuselage shall be flightworthy after a vertical ground impact of 31 feet per second, assuming 0.38g rotor lift.
- The landing gear must minimize the possibility of entanglement with brush, landing mats, and other obstructions.
- The gear shall be located so as to eliminate the possibility of part of the gear or support structure being driven into the occupiable section or the flammable fluid tank or line of the helicopter during any survivable accident defined in AAMRDL Technical Report 71-22 (Reference 4).
- The helicopter shall be capable of being towed by assigned Army vehicles at design gross weight on soil with a California Bearing Ratio (CBR) of 2.5.
- The landing gear shall be wheeled and capable of 45-knot running landings and takeoffs.
- A fail-safe brake system with parking locks and capable of securing the helicopter on a 12-degree slope must be incorporated.

- The shock strut shall be an air-oil type, limiting the helicopter vertical ground load factor to 5g. Integral kneeling capabilities must be included.
- The gear shall attenuate 57 percent of the helicopter crash energy due to a vertical impact at 42 feet per second.
- The landing gear shall improve safety during autorotation landings by increasing the helicopter vertical arresting capabilities by 25 percent.

MATERIAL INVESTIGATION

The materials investigation task identified, for further evaluation, three advanced structural materials that had been established by industry and could be applied to landing gear design and fabrication. The gear on the baseline helicopter had been fabricated from 300m maraging steel conforming to MIL-S-8844 (Reference 13). This well-known steel retains high impact strength and toughness at the 280,000-psi strength level required on the baseline helicopter. The baseline gear was fabricated using established production machining methods and, therefore, had reliable cost data. This design approach was the most cost effective for the 1977 time frame.

Composite materials technology has been rapidly expanding in the field of structural materials. They have specific strengths three to four times that of metal, as shown in Figure 11. Improved fabrication methods such as wet-filament-winding (WFW) and pultrusion (Reference 14) are replacing costly hand layup techniques. A comparison of the relative fabrication costs between graphite and steel is shown in Figure 12.

The costs were determined for the baseline trailing arm. It was assumed graphite would reduce the weight of the metal arm 10 percent, and that \$100 would be the value of a pound saved. A WFW trailing arm was estimated on a pound basis to be five times more costly than composite blade fabrication. Hughes Helicopters had predicted fabrication costs for WFW main rotor blades to be in the order of \$14 per pound (Reference 15). This gave an

¹³ Military Specification MIL-S-8844, STEEL BAR, REFORGING STOCK, AND MECHANICAL TUBING, LOW ALLOY, PREMIUM QUALITY, Department of Defense, Washington, D.C., 25 May 1971.

¹⁴ Jones, B.H. and Jakway, W., MM&T - PULTRUDED COMPOSITE STRUCTURAL ELEMENTS, Goldsworthy Engineering, Inc.; USAAMRDL Technical Report 76-5, Eustis Directorate, U.S. Army Air Mobility Research and Development Laboratory, Fort Eustis, Virginia, December 1976, AD A035217.

¹⁵ Head, R.E., FLIGHT TEST OF A MULTI-TUBULAR SPAR MAIN ROTOR BLADE ON THE AH-1G HELICOPTER, VOLUME VI - PRODUCTION COST ASSESSMENT, Hughes Helicopters, Division of Summa Corporation; USAAMRDL Draft Technical Report, Eustis Directorate, U.S. Army Air Mobility Research and Development Laboratory, Fort Eustis, Virginia (to be published).

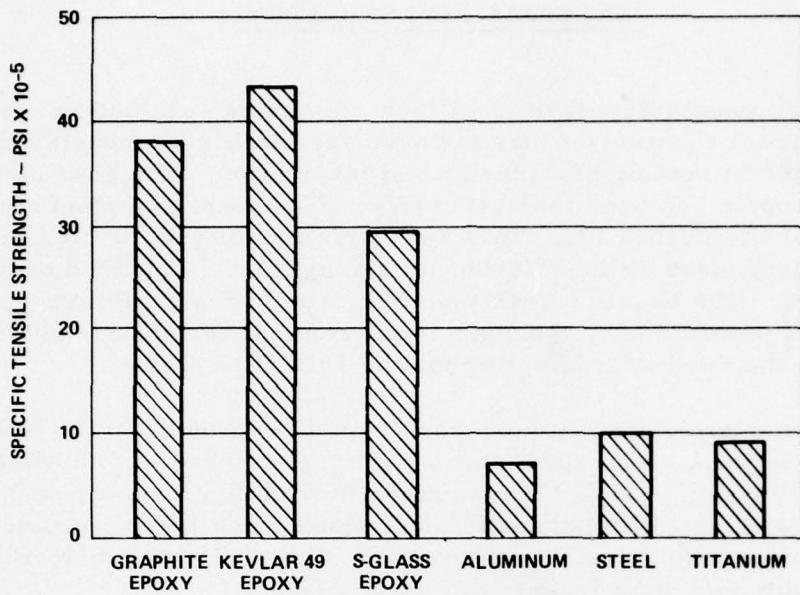


Figure 11. Materials Strength Comparison.

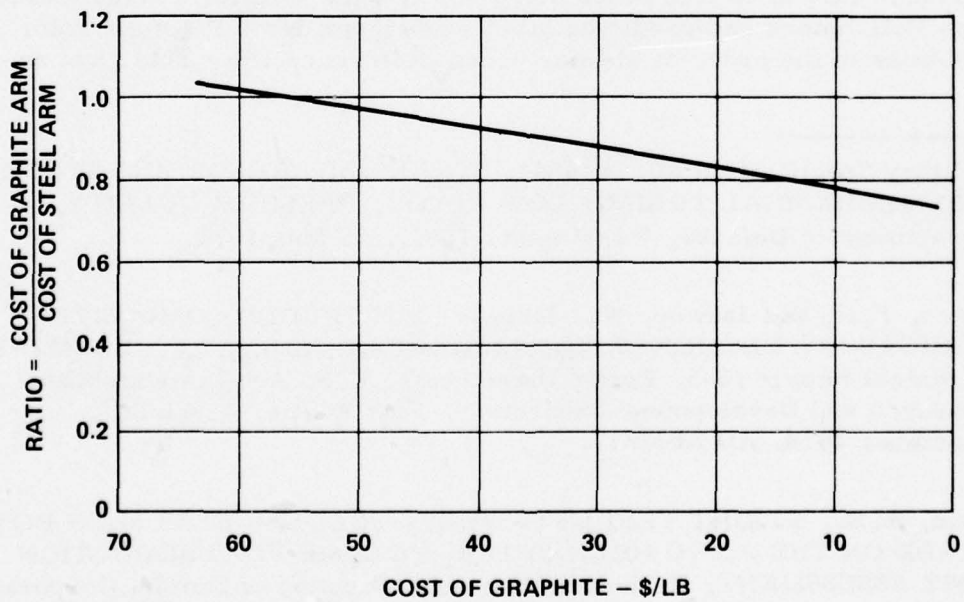


Figure 12. Graphite Versus Steel Cost Comparison.

estimated fabrication cost of \$70 per pound for the trailing arm. Figure 12 shows that graphite composite materials at the 1975 price of \$38 per pound competed successfully costwise with steel for trailing arm fabrication. Therefore, it was apparent that the most effective industry-established fiber, such as graphite, should be selected and used to design and fabricate a landing gear component in order to demonstrate the application and effectiveness of an advanced material for such a component.

COMPOSITE FABRICATION

The ever-present need to increase productivity has necessitated constant striving to improve the cost of fabrication by replacing hand methods with the repeatability and quickness of machines. Techniques such as the automatic tape layup, pultrusion, tape winding, and WFW are continuously being improved, giving steady increases in productivity. WFW is a relatively inexpensive method of fabricating various circular, elliptical, or rectangular parts by unwinding fibers from a storage spool, wetting them with resin, and winding them onto a rotating mandrel. The winding angle is the same as the fiber angle and is obtained by synchronizing the rotational speed of the mandrel with the traversing speed of the winding machine. The mandrel is relatively inexpensive and can be fabricated using a variety of materials such as plastic, air supported bladders, and shaped rubber.

Adding the resin during the winding process saves preimpregnation (prepreg) costs. The tension created in the filaments during WFW improves tensile and compressive strengths by keeping the fibers straight and aligned. The winding angle can be infinitely varied, producing the preferred orientation of the fiber. Preheating the filaments causes a dramatic improvement in interlaminar shear strength. Tests have shown that mechanical properties of WFW parts correlate closely with theoretical values determined by the rule of mixtures. The WFW fabrication process has been successfully used in several structural applications such as main rotor blades (Reference 15) and aft fuselage sections (Reference 16). The technique has provided low cost with excellent results; therefore, this process was selected for fabricating the advanced landing gear.

¹⁶ Needham, J. F., DESIGN, FABRICATION, AND TESTING OF AN ADVANCED COMPOSITE AH-1G TAIL SECTION (TAIL BOOM/VERTICAL FIN), Hughes Helicopters, Division of Summa Corporation; USAAMRDL Technical Report 76-24, Eustis Directorate, U. S. Army Air Mobility Research and Development Laboratory, Fort Eustis, Virginia, November 1976, AD A034457.

ENVIRONMENTAL DEGRADATION OF COMPOSITES

The data search found many reports concerned with the environmental degradation of composite materials. The most common problems were the craze cracking and powdering of the resin caused by ultraviolet light and the reduction of interlaminar shear strengths caused by the permeation of moisture into the resin. Many reports outline ongoing research efforts oriented to the understanding and solution of these problems. The many composite components in use certainly attest to the fact that these materials can effectively exist in the service environment.

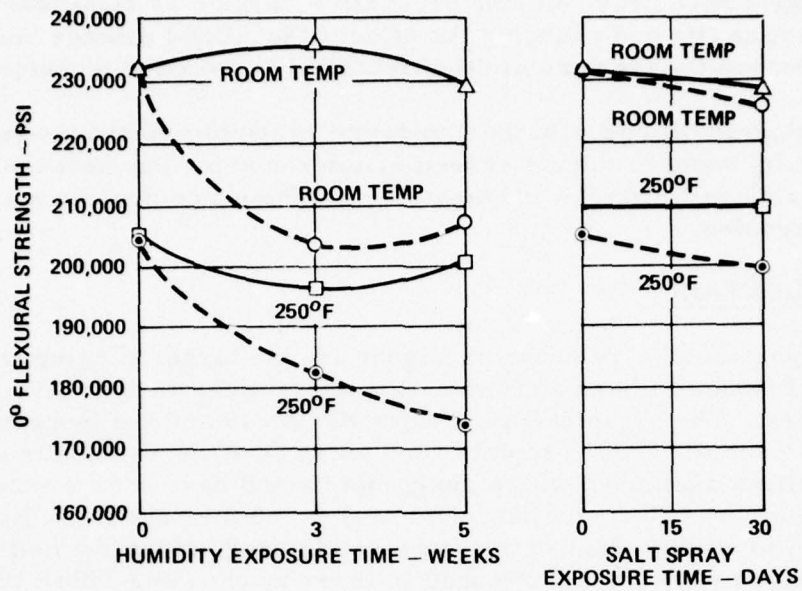
Some effective methods used to alleviate environmental problems are:

- Choose resins that exhibit reduced moisture permeation, such as the aromatic amine cured systems.
- Seal all cut edges and holes.
- Use a moisture barrier such as paint or a deposited coating over all exposed surfaces.
- Use curing methods that produce dense void-free laminates.

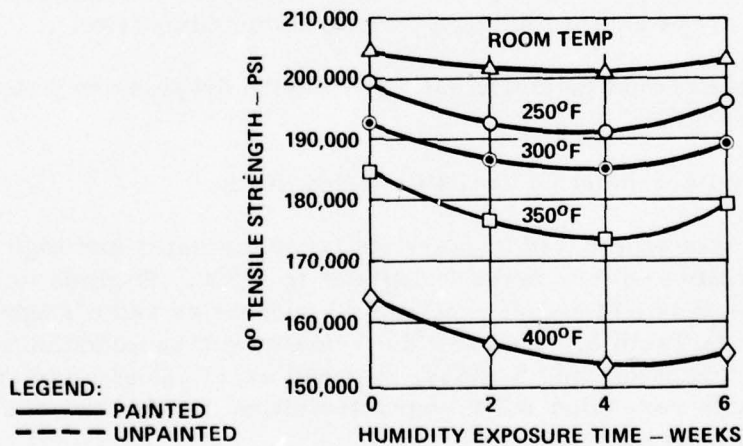
An excellent summary of environmental problems with corrective measures is given in the Advanced Composites Design Guide (Reference 17). Figure 13 was reproduced from this guide to show how severe moisture problems can be dramatically improved with a barrier coating such as polyurethane paint.

The long-term effects of ultraviolet light and moisture on composite materials is being assessed by many U. S. Government and industry programs. One program administered by Boeing for NASA monitors the in-service experience of a graphite 737 spoiler, using periodic strength tests checked against protected control samples. This program is one of many that will continue for a number of years, supplying information that will keep improving the methods used to protect not only composite but metal parts as well.

¹⁷ ADVANCED COMPOSITES DESIGN GUIDE, Advanced Development Division, Air Force Materials Laboratory, Air Force Systems Command, Wright-Patterson Air Force Base, Ohio.



a. 0° Flexural Strength of Boron/Epoxy Laminates After 100 Percent Humidity Exposure or 30-Day 5 Percent Salt Spray Exposure



b. 0° Tensile Strength of Boron/Epoxy Laminates After 100 Percent Humidity Exposure

Figure 13. Moisture Effects on Composite Materials.

Composite parts have provided long dependable service by significantly improving fatigue life and reducing the effect of localized damage because of the inherent multi-layer and multi-directional fabrication techniques.

Co-curing integral fittings with the composite assembly increases reliability by reducing alignment problems caused by tolerance buildup between parts. Composite parts will virtually eliminate the maintenance problems associated with corrosion.

FIBER EVALUATION

The field of possible fibers shown in Figure 14 was large, ranging from the centuries-old organic fibers such as cotton to the more recent Kevlar and graphite fibers. The organic aramid fiber Kevlar 49 and the inorganic man-made fibers made of boron, graphite, and glass have shown excellent structural capabilities when used with a resin matrix and have been developed and used extensively by industry. Sufficient design and fabrication information was available to qualify them as industry-established structural materials. These candidates were further reduced to three by choosing fibers that exhibit these WFW characteristics:

- The fiber* tow must be capable of withstanding the tension produced by the rotating mandrel.
- The fiber must be easily moistened with resin that adheres, allowing no dry areas and producing a homogeneous composite.
- The fiber should be sufficiently flexible to drape around the part being wound.
- The dry fiber must be available in tow form.

The boron fiber was eliminated because its large diameter and high modulus gave poor flexibility and thus made it difficult to WFW. E-glass was eliminated because S-glass had higher mechanical properties and a slightly lower weight as shown in Table 6. This left the remaining three candidates, Kevlar 49, Thornel 300 graphite, and S-glass, that had excellent strength-to-weight ratios coupled with very good WFW characteristics, for further evaluation in the design analysis section.

*A tow contains a large number of fiber filaments. This program used both a 3000- and 6000-filament tow.

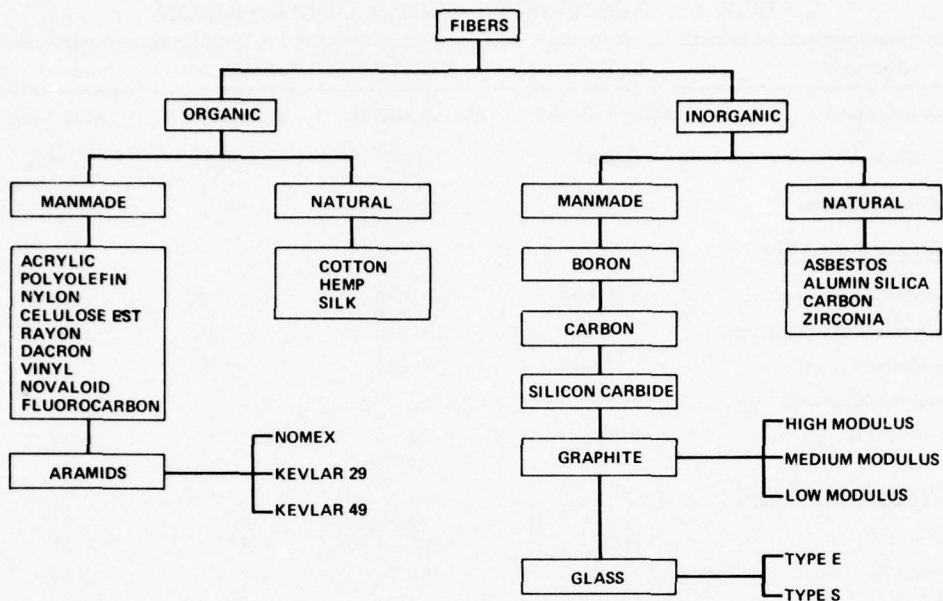


Figure 14. Fibers.

S-glass fibers are made from lime-alumina boro-silicate glass. They are continuously formed when molten glass flows through a specific number of metered orifices. These fibers, due to their abrasive nature, are given a surface coating to alleviate wear between the individual glass strands and to enhance resin adherence. The extensive usage of glass fiber goes back to the beginning of composite manufacture. It is the material with which the composite industry started and grew. Consequently, a high availability at a low cost is envisioned for the future. It has been successfully used in a wide range of applications, both structural and nonstructural. Thus, S-glass easily qualifies as a candidate material.

Kevlar 49 is a relatively new fiber with a high tensile strength-to-weight ratio and excellent adaptability to WFW. The manufacture of this synthetic fiber is accomplished by spinning specific polyamides in an inert atmosphere. This fiber also has many uses such as tire cord, rope, flywheels, and aircraft structure, thus assuring continual availability at competitive prices.

Medium modulus Thornel 300 was selected from the graphite fibers because of the excellent performance it has displayed in filament-wound structural parts. It was chosen over the high- or ultra-high-modulus graphite due to its higher strength-to-weight ratio and better impact strength. The graphite

TABLE 6. COMPOSITE FIBER COMPARISON

Filament	E-Glass	S-Glass	Kevlar 49	Thornel 300
Fiber Specification	MIL-R-60346	MIL-R-60346	AMS 3901	AMS 5892
Density, lb/in. ³	0.0666	0.0656	0.0468	0.0524
Fiber volume fraction	0.50	0.50	0.50	0.50
<u>Unidirectional Properties</u>				
Tension strength, psi	138,000	163,000	163,000	163,000
Compression strength, psi	92,500	107,500	35,000	107,500
Shear strength, psi	9,330	9,800	1,400	4,000
Tension modulus, 10 ⁶ psi	5.5	6.5	9.7	17.2
Shear modulus, 10 ⁶ psi	0.52	0.53	0.23	0.51
<u>Specific Strength x 10⁻⁶ inch</u>				
Tension, psi	2.07	2.48	3.48	3.11
Compression, psi	1.39	1.64	0.75	2.05
<u>Crossply (±15°) Properties</u>				
Tension strength, psi	116,000	133,000	92,000	101,000
Compression strength, psi	81,000	94,000	29,000	87,000
<u>Specific Strength x 10⁻⁶ inch</u>				
Tension, psi	1.74	2.03	1.97	1.93
Compression, psi	1.22	1.43	0.61	1.66
Price, dollars/lb	0.35	6.10	8.50	38.00

fiber is made from carbonaceous fibrous raw material that pyrolyzes to char, will not melt, and leaves a high carbon residue. If the fibers are restrained from shrinking during the pyrolysis step, a high degree of preferred orientation of the graphite layers parallel to the fiber axis results. This fiber is the most expensive of the three candidates chosen; however, its growing commercial and aerospace applications assure a continual supply at a steady reduction in price.

RESIN SYSTEMS

A brief overview of available resin systems is presented in Figure 15. The conventional and modified tooling resins are well established in industry. The two-phase or bimodal systems are relatively new. They incorporate

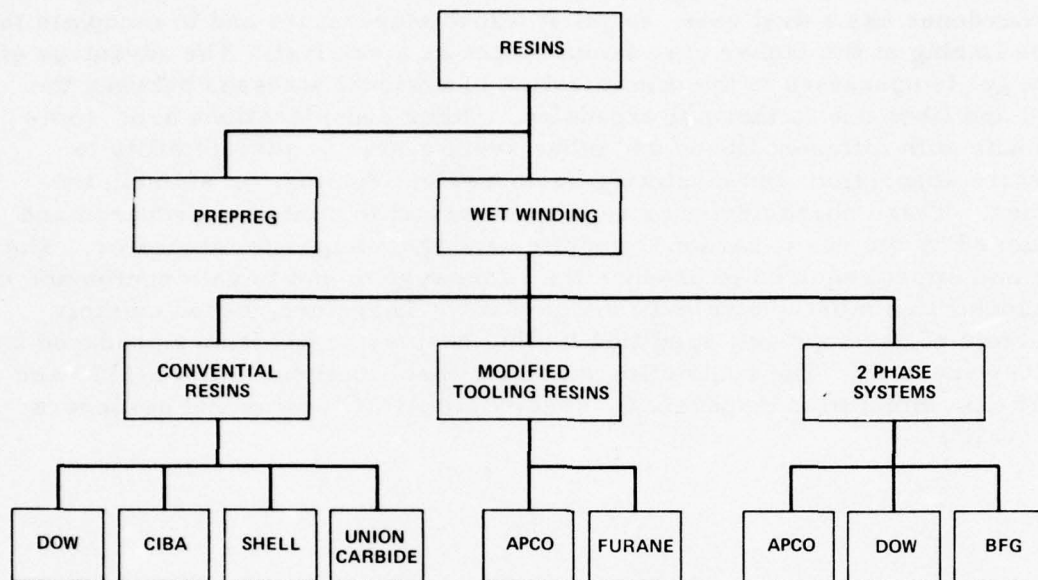


Figure 15. Resin.

generally 6 to 15 percent of an elastomeric resin in an epoxy system so as to improve:

- Fatigue life
- Thermal strength
- Fracture toughness
- Transverse properties
- Thermal shock resistance

The bimodal systems show great promise for future composite application. However, they have not been established in the filament-winding field, and therefore, were dropped from consideration.

Resins and hardeners used for WFW have special requirements because of the nature of the winding technique. The fiber is pulled through a resin at a fast rate, requiring the resin to have excellent fiber-wetting and low viscosity characteristics. If the fabricated part is large, a long pot life for the resin

is mandatory, while keeping good rub-out (removal of excess resin) capability. The hardener has a dual role: to gel at a low temperature and to complete the cross linking at the higher cure temperature as a catalyst. The advantage of a low gel temperature is the minimization of residual stresses between the resin and fiber due to thermal expansion. Other considerations are: compatibility with different fibers and other resin systems; susceptibility to moisture absorption; and exhibiting no corrosive, fuming, or staining tendencies. These characteristics require a special formulation prepared and developed by the resin-hardener supplier and the composite fabricator. The time and effort required to produce the resin system and to gain confidence in its capabilities must evolve over many years. Therefore, based on their high state of development, modified tooling resins and hardeners produced by APCO were used. The controlling material specifications HMS 16-1115 and HP 15-53, included in Appendix C, specify the APCO resins and hardeners that qualify.

DESIGN ANALYSIS

The design analysis task evaluated the three fibers, graphite, Kevlar 49, and S-glass, and selected one as the most cost-effective for landing gear fabrication. Analyses were also included for various landing gear configurations, leading to choosing the component and concept that was used to demonstrate the effectiveness of the advanced material selected.

FIBER SELECTION

A weight and cost study comparing the three candidate fibers was performed using the baseline cross tube as a basis for comparison. This component was common to most anticipated gear configurations. Its size, shape, and loading was similar to the trailing arm and therefore it was well suited to be used for fiber comparisons. The weights of the composite cross tube, sized by using the three candidate fibers, are presented in Figure 16. The assumed winding angle was 15 degrees with a fiber volume of 50 percent. The Kevlar 49 tube, compared with graphite and S-glass, had excessive weight and size due to its low compressive strength and was eliminated from further consideration. The graphite tube was 18 percent lighter than S-glass when comparing optimum diameters, but S-glass has lower material costs. Both materials had fabrication, handling, and maintenance costs that were essentially the same. The most cost-effective fiber was found by trading the low weight of graphite at its high material cost against the high weight and low cost of S-glass.

This cost comparison, presented in Figure 17, assumed that a pound of weight saved from a modern helicopter was worth \$100. The cost used per pound for S-glass was \$6.10. The graph plots that dollar value per pound where graphite and S-glass are determined to be equal in value; this is done by taking into consideration the differences in fiber cost and weight determined for the cross tube. Graphite was shown to be the most cost-effective when its cost was less than \$25 per pound.

Graphite manufacturing costs are gradually decreasing due to improved fabrication methods using pitch precursors. Information supplied by Union Carbide and plotted in Figure 18, show graphite costs in the 1980 time frame at levels well below the break-even cost with S-glass. Graphite, therefore, proved to be the most cost-effective material and was used for the design and fabrication of the advanced landing gear.

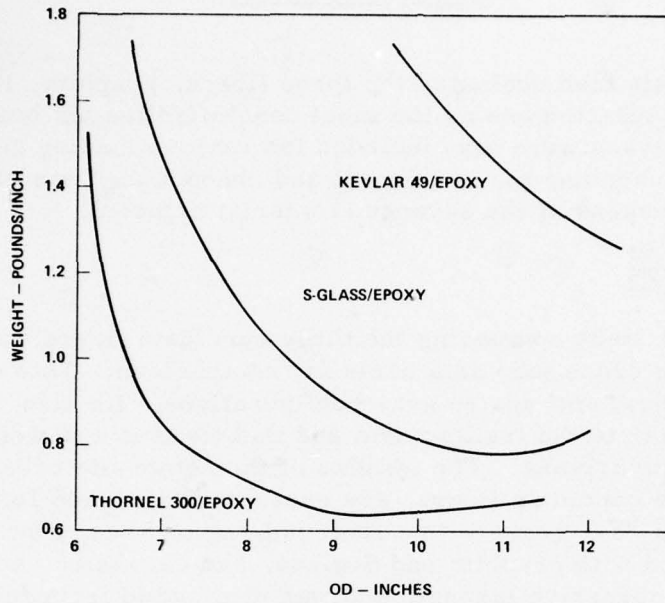


Figure 16. Materials Weight Comparison.

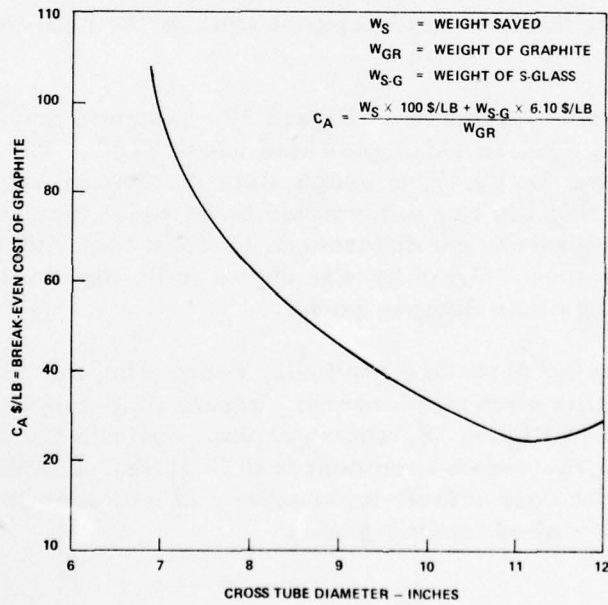


Figure 17. Graphite Versus S-Glass Cost Comparison.

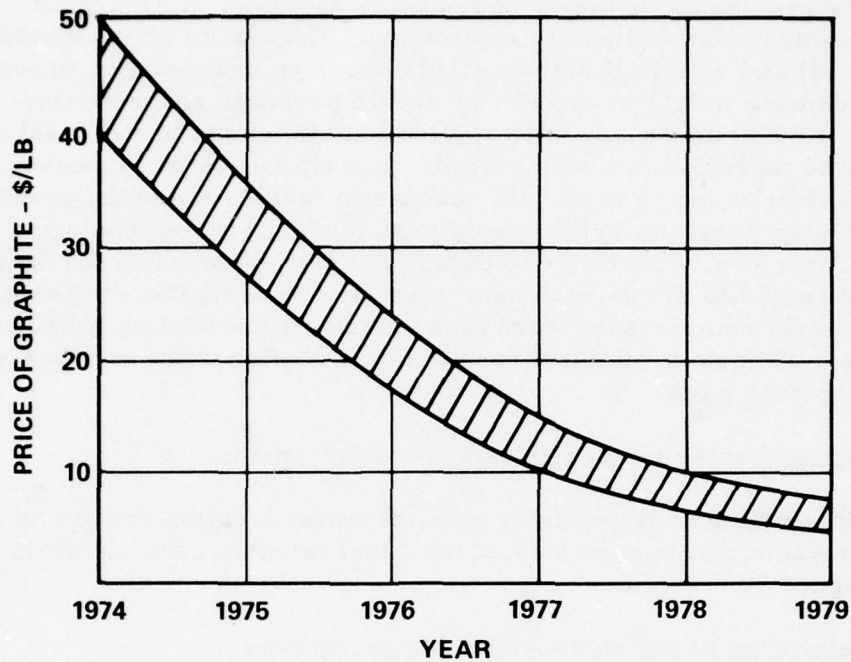


Figure 18. Price of Graphite.

CONCEPT EVALUATIONS

Composite design too often in the past had merely replaced the metal counterpart with fiber because of constraints such as the aerodynamic shape and the surrounding structure. This design effort strived to use the unique characteristics of the composite material to drive the configuration, by eliminating bonded metal parts and maximizing the use of graphite epoxy. Variations in size and location of members were allowed. However, for this study the established criterion was held, giving a firm basis for comparison between the baseline gear and the new gear concepts.

The baseline gear has four major components as shown in Figure 19. Each is a good candidate for composite application. Composite shock struts (Reference 18) and wheels (Reference 19) have been evaluated on previous programs showing weight savings of 10 and 16 percent, respectively. The cross tube, an excellent composite application, is unique to the baseline helicopter and therefore not widely used. The trailing arm, however, is found on many helicopters and, with successful fabrication using graphite fiber as the structural material, would push landing gear technology a step forward. Therefore, with this reasoning, the major emphasis for this program was directed to the development of an all composite trailing arm. However, weight comparisons were made using all the landing gear major components. This gave realistic results since configuration changes affected these landing gear parts.

The basic ground rules for design were established as:

- The trailing arm geometry with the wheel location and travel was the same as the geometry of the baseline main gear shown in Figure 20.
- Relocation of the shock strut was permissible.
- The cross tube was sized using graphite epoxy.
- The baseline test fixtures were used with minor alterations.
- The weights estimated for the shock strut, cross tube, and wheel maximized the replacement of metals with composites.

¹⁸ FILAMENT COMPOSITE MATERIALS LANDING GEAR PROGRAM, The Bendix Corporation, Energy Controls Division; AFFDL Technical Report 72-78, Air Force Flight Dynamics Laboratory, Air Force Systems Command, Wright-Patterson Air Force Base, Ohio.

¹⁹ Price, A.L., FILAMENT COMPOSITE WHEEL DEVELOPMENT FOR MILITARY AIRCRAFT, Whittaker Corporation; AFFDL Technical Report 71-144, Air Force Flight Dynamics Laboratory, Air Force Systems Command, Wright-Patterson Air Force Base, Ohio, October 1971.

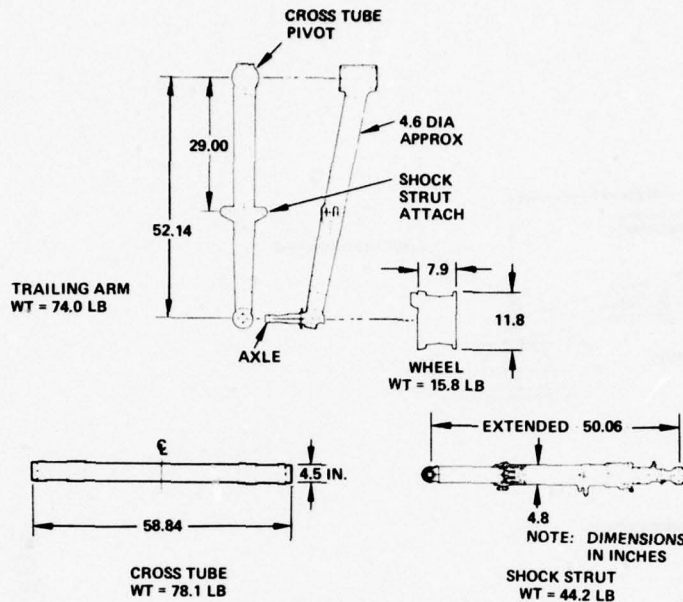


Figure 19. Baseline Gear Components.

The trailing-arm geometry and wheel travel was maintained in order to keep the same load factors and helicopter landing stability in pitch and roll. The deviations allowed from baseline geometry was the length and location of the shock strut and the necessary increase in size of the trailing arm and cross tube. The diameter of the composite cross tube was approximately twice that of the baseline tube. This increased the size and weight of the fuselage attachment fittings as well as the size of the trailing-arm attachment. Comparisons between different concepts were conducted using composite wheels and shock struts with weight reductions of 16 and 10 percent respectively, under the metal baseline parts.

The baseline trailing arm, cross tube, and shock strut are made of steel tensile properties 280,000 to 300,000 psi. The wheel is aluminum and is used with a tubeless 8:50-10, 10-ply tire. The composite trailing arm must hold the 52.14-inch length of the baseline arm, but can vary the location of the shock strut as well as the arm diameter. The baseline design loads given in Appendix A were used for the advanced landing gear concept designs and evaluation. Condition 5, a two-wheel landing with drag obstruction, was critical for the shock strut; whereas Condition 8, the crashworthiness ultimate failure load, was critical for the remaining components.

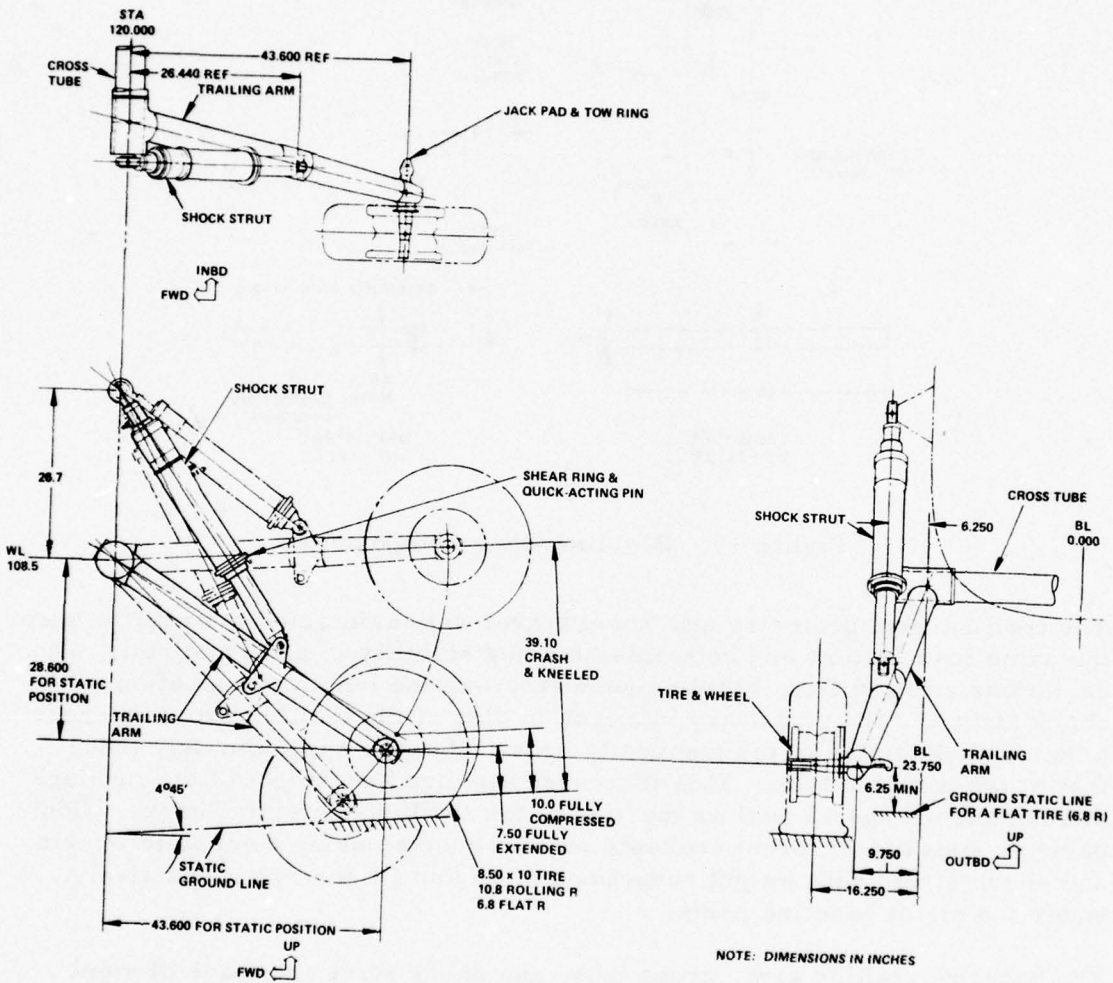


Figure 20. Geometry of Baseline Main Gear.

Ten concepts using three basic approaches were designed and are reviewed in Figure 21. Concepts 1 and 2 used the baseline geometry shown in Figure 20 and have essentially replaced the metal tube of the trailing arm with graphite. Steel fittings were added for attaching the cross tube, shock strut, and wheel. Concept 5 used the geometry shown in Figure 22. Here the cross tube and arm were combined to form a continuous curved tube with localized fittings for attaching the wheel, shock strut, and fuselage. The final approach, Concepts 3, 4, and 6, used Figure 22 geometry and disposed of the large steel cross tube attachment fittings of Configuration 1 by using an arm with a wider square or elliptical cross section. The loads in the trailing arm were transferred to the cross tube by bearing on the edges of the holes in the arm. The axle and shock strut attachments were fittings bolted through the composite arm. The detailed drawings for each concept can be found in Appendix E.

The following rationale outlines why Configurations 1, 5, and 6 were chosen for a more detailed evaluation. The trailing arm in Configuration 1 eliminated the differential expansion problems of the bonded steel fittings used in Configuration 1A and 1B and weighed less than Configuration 2. Configuration 1 used a steel tee fitting bolted to the trailing arm for attachment to the cross tube. Torsion loads were transferred from the graphite arm to the tee fitting by bolt bearing and bending loads, through socket action. The shock strut and axle attachments were single fittings bolted to the graphite arm. The circular cross section of the arm minimized aerodynamic drag and facilitated fabrication by the WFW process.

The curved shape of Configuration 5 used a graphite circular cross section. This was a more innovative approach that combined the cross tube with the trailing arm into a single curved tube. The shock strut was relocated to be closer to the axle. The axle attachment was similar to Configuration 1 and used an internal spacer and nut. The fuselage fittings were simply bolted to the tube and attached by a single bolt to a corresponding fitting in the fuselage. The tube could be fabricated as twins by winding an elliptical toroid, which when cut in halves would give tubes for two landing gears. Toroid winding is within current technology, requiring only the development of a new filament-winding machine. This approach reduced the size and complexity of the fuselage attachment fittings, eliminated the cross tube attachment, and used longer, more optimized members. This configuration was found to be an excellent application for composites and was chosen for further evaluation.

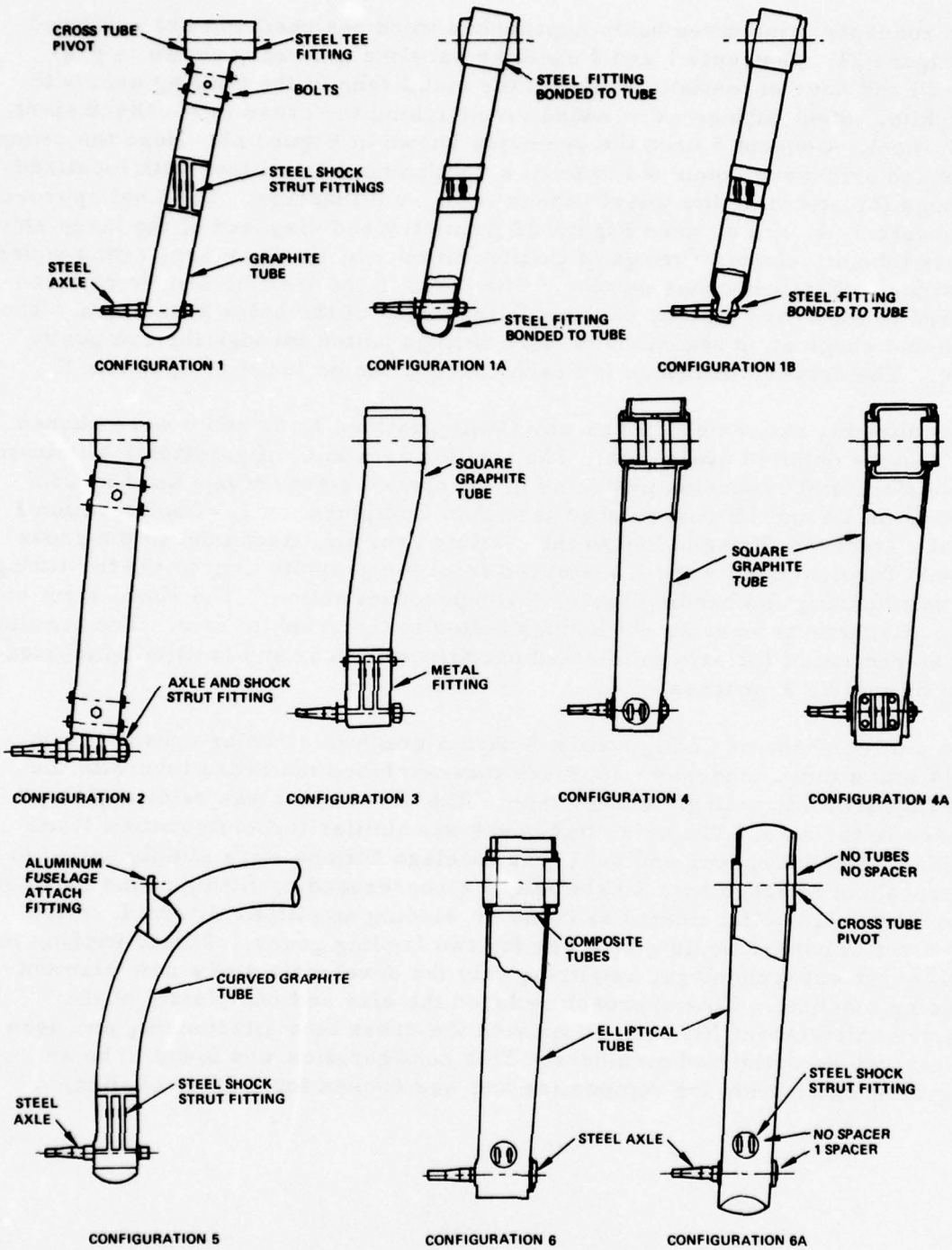


Figure 21. Trailing Arm Configuration Review.

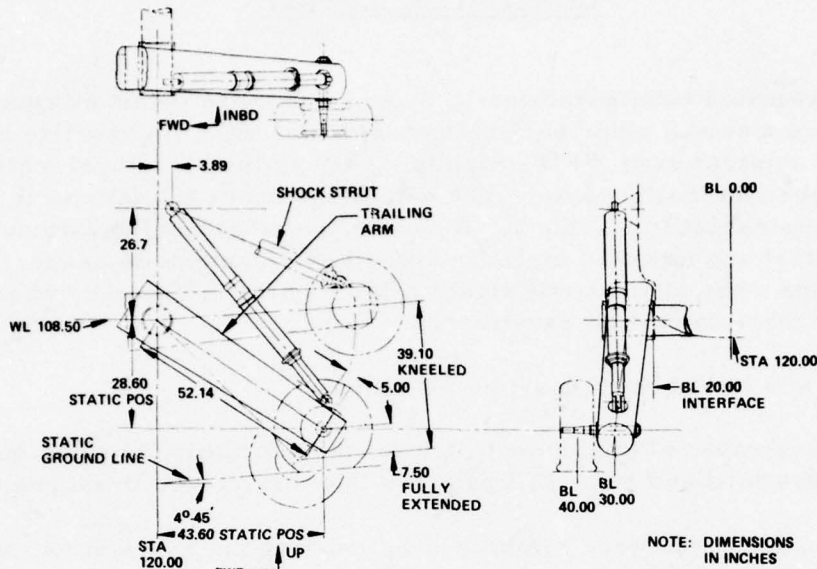


Figure 22. Geometry of Configurations 3, 5, and 6.

The remaining Configurations (3, 4, and 6) were attempts to maximize graphite usage while using existing winding machines. The shock strut was relocated and its length, as compared to the baseline strut, was increased. These concepts used either a rectangular or an elliptical cross section that made a larger trailing arm. The increase in size gave the section properties needed to resist the torsion and bending loads transferred from the axle and shock strut. The steel cross tube attachment fitting used in Configuration 1 was eliminated and the shock strut attachment was simplified. The fabrication cost for these configurations was minimized by using current equipment to WFW the arm as a twin. Configuration 6 was chosen for further evaluation because of its lower weight resulting from simplification of the cross tube, shock strut, and axle attachments.

CONCEPT SELECTION

This task evaluated Configurations 1, 5, and 6 in more detail by comparing weight differences and other pertinent parameters with the baseline metal gear. Each concept used WFW graphite-epoxy as the structural material for the cross tube and trailing arm. The detailed weight calculations in Appendix F are summarized in Table 7. It can be seen that Configurations 5 and 6 are the lightest and have the highest percentage of composite usage. These configurations were also quantitatively rated highest in Table 8, when compared using other important parameters.

Configuration 5 had several desired features:

- The number of attachment fittings were minimized by combining the cross tube and both trailing arms into one curved U-shaped tube.
- Bending loads were minimized by locating the shock strut attachment near the wheel.
- It had the lowest weight among the compared configurations.
- The tubular shape minimized aerodynamic drag.
- Costs could be minimized by simultaneously winding the two gears as twins.

The following disadvantages were also present:

- The total gear, being of one part, would have to be scrapped if one side was extensively damaged.
- The development of a special winding machine was required.
- New test fixtures were required.




This promising concept was eliminated as a contender due to the additional costs needed for a new winding machine and test fixtures.

TABLE 7. CONCEPT WEIGHT COMPARISON

Components		Baseline	Configuration		
			1	5	6A
Trailing Arm (2)	Weight (lb)	148.0	162.6	140.2**	137.4
	% Composite	0	47	71	81
Cross Tube (1)		78.1	55.4	**	51.6
Shock Strut (2)		88.0	80.4	96.7	95.4
Wheel (2)		31.6	26.9	26.9	26.9
Miscellaneous (lb)*		-	22.9	-8.0	16.0
Total Gear	Weight (lb)	345.7	348.2	255.8	327.3
	Ratio ***	-	1.01	0.74	0.95

*Weight Adjustments for changes to fuselage attachment.
 **Combines left and right trailing arms with cross tube.
 ***Ratio of total configuration weight to total baseline weight.

TABLE 8. CONFIGURATION EVALUATION

Configuration	Weight	Cost		Ease of Fabrication	Simplicity	Risk	Composite Application	M&R	Total
		Recur	Non R						
 1	1	2	3	2	1	3	1	3	16
 5	4	4	1	5	4	1	4	4	27
 6	3	4	4	4	3	3	4	4	29

1 Very poor 3 Fair 5 Excellent
 2 Poor 4 Good

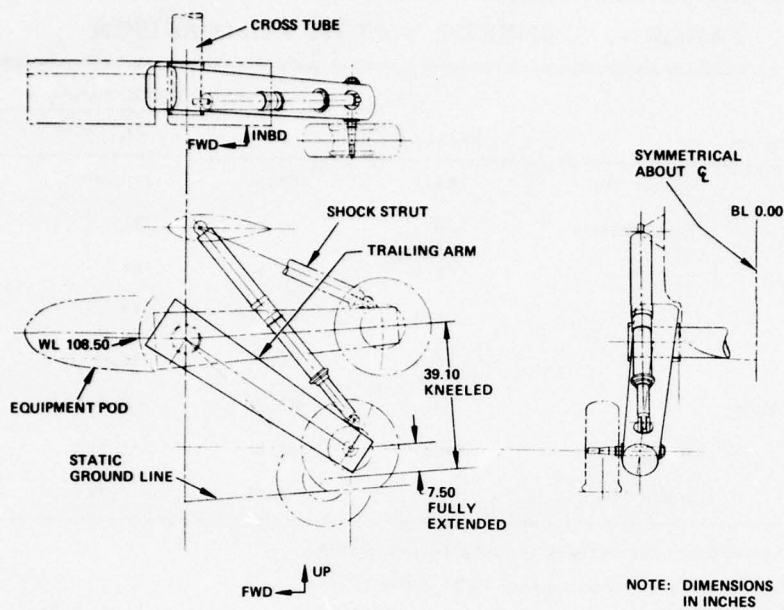


Figure 23. Three-View of Configuration 6.

Configuration 6, shown in Figure 23, was the composite gear that best satisfied the program requirements. The trailing arm of this concept was chosen for fabrication because present winding equipment could be used to minimize costs. Production versions could be fabricated as twins. The weight was less than baseline and composite usage was maximized.

The aerodynamic drag associated with the trailing arm size could be satisfactorily reduced by retracting the arm behind the forward equipment pods. The baseline dynamic test fixtures were used with minor modification and the new static test fixtures were relatively inexpensive since their costs were within the scope of the program. It was anticipated that the data from testing would give important information concerning the impact capabilities of a graphite-epoxy gear and would validate calculated allowable bearing, bending, and torsion stresses.

DESIGN

The first task of Phase 2 began with customer approval of Concept 6A and the advanced criteria based on the 15,000-pound class YAH-64 baseline helicopter. The geometry for the approved concept was similar to baseline except for component size and the location of the shock strut. There was a weight advantage in having the axle and shock strut attachment at the same end of the arm. The drawing of the trailing arm is in Appendix E and shows an elliptical cross section with inner and outer WFW graphite skins, honeycomb stabilized. The skins intermesh with graphite doublers and brooms to form fittings at each end. The upper fitting used graphite brooms and doublers around the cross tube pivot hole, with bosses and coated aluminum bearing surfaces for accurate cross tube interface. In the same manner, the lower fitting had doublers and bosses around the holes for the shock strut and wheel axle attachment fittings. The axle hole was supported with a graphite tube bonded to the internal surfaces of the arm. The ground loads from the wheel loaded the arm through the axle and were in turn reacted by the shock strut and cross tube. The critical stresses in the graphite arm were bending and torsion in the skins and bearing in the attachment holes.

The following ground rules for the design of the trailing arm were added to those established during the concept evaluations, because the fabrication of one arm necessitated a more conservative approach to meet program objectives. For instance, it was important to test the arm dynamically and statically for bending and torsion loads without premature failure of the graphite holes in bearing. Consequently, a means of clamping the hole edges to increase bearing strength was provided by the spacers and nuts shown in Figure 24 and in Drawing 416-100 in Appendix E. This capability was to be used if yielding due to bearing stresses in the holes became a problem. The bosses were increased in size to reduce the risk of adverse tolerance buildup. The shock strut and axle fittings were used solely to transfer loads to the graphite trailing arm and were not optimized for minimum weight. The cost of these metal parts was substantially reduced by machining only areas that were necessary to interface with the holes in the arm. The preceding changes were minor and had no effect on the strength of the composite arm. The weight differences were easily determined and the objective to assess the capabilities of a graphite-epoxy gear was assured. The expense of developing a new shock strut to meet the optimized geometry of the advanced gear was not warranted since the efficiencies and strength of air-oil absorbers are wellknown. The gear was dynamically tested using a combination of drop heights and weights to give ground load values comparable to the advanced criteria and baseline gear. The amount of energy attenuation required was

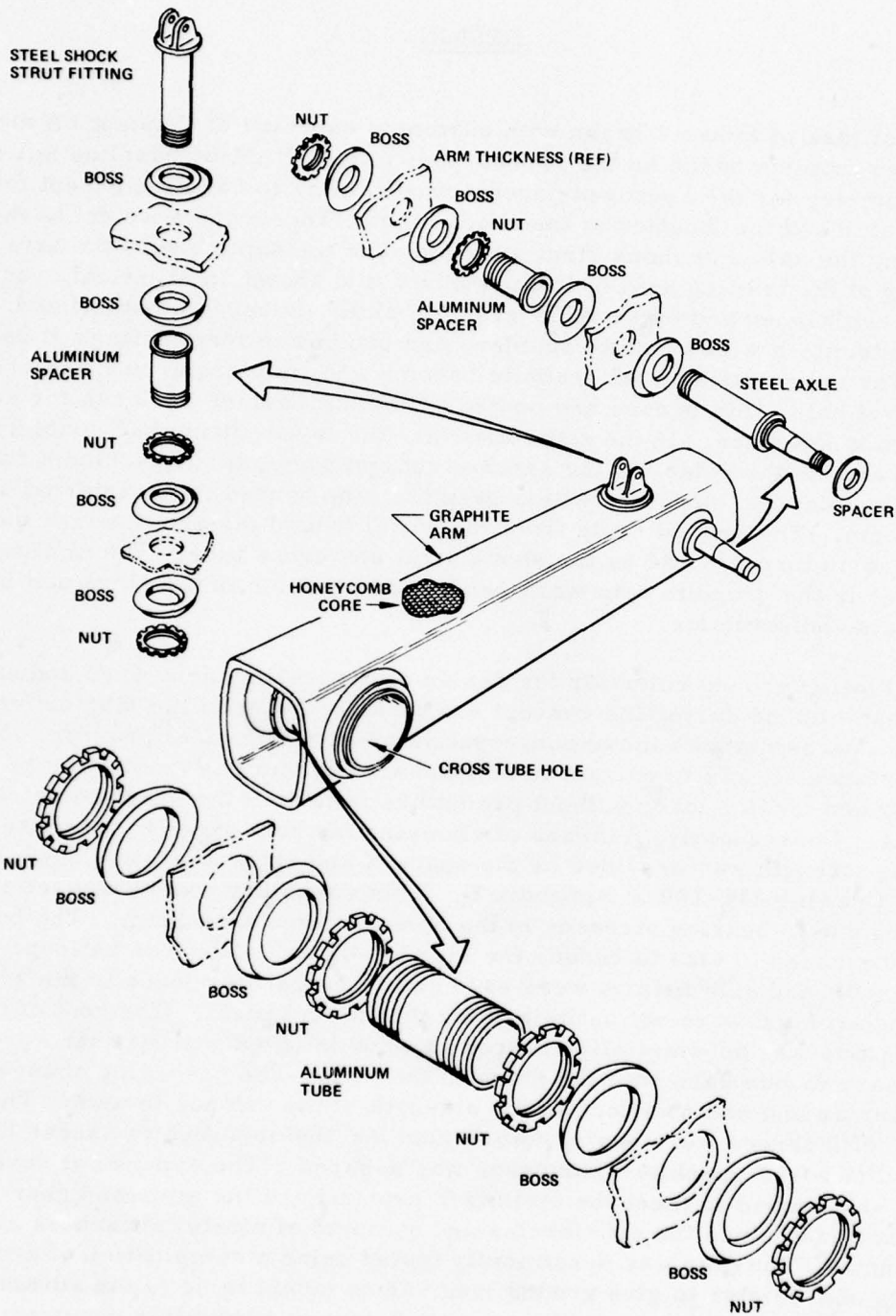
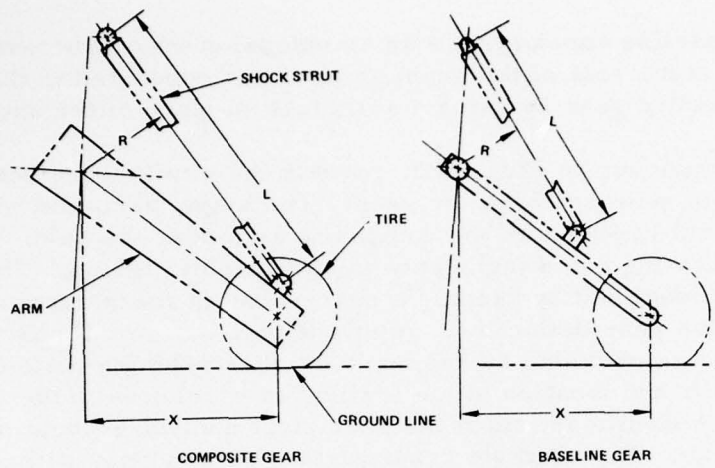


Figure 24. Composite Arm.

provided by the baseline shock strut with an extension added for test fixture attachment. The static test of the graphite arm was conducted in the same manner as the baseline gear by using a solid tube in place of the shock strut.

The geometry comparison in Figure 25, reveals the similarities between the advanced composite gear and baseline gear. The major variation was lengthening the shock strut to join with the composite arm near the axle. This saved weight by locating two attachments in one graphite fitting. The shock strut location was idealized by keeping a near-constant mechanical advantage (X/R) throughout the gear deflection. Ample length for the internal design of the shock strut was provided by keeping a stroke-to-length ratio of 0.31. Minor differences in the location of the trailing arm relative to the fuselage and wheel were not significant since the gear pivot and wheel locations were identical to baseline. The ultimate crashworthiness condition with an outboard side load was critical for the design of the trailing arm except for the shock strut attachment which was critical for a two-wheel landing with drag. The schematic in Figure 26 shows the composition of the arm, and Appendix D contains the critical design loads and stress analysis substantiating the design. Whereas the bending and torsion stresses established the sizing for the skins and honeycomb, the designs of the upper and lower fittings were determined by the bearing loads on the holes. The ply orientation and winding sequence are given on Drawing 416-100 in Appendix E. The graphite tow used in the winding of the arm contained 6,000 filaments and made the basic ply thickness for the skins and doublers 0.0164 inch. The skins were wound by using a two-ply layer thickness at the pivot hole of 0.0328 inch. This thickness increased linearly to 0.0458 inch at the axle centerline.

Each inner and outer skin as shown in Figure 26 contained two layers at a 15-degree winding angle, one layer at 45 degrees, and a half-ply layer at 90 degrees. The upper graphite fitting including the skin layers had six layers at 90 degrees, four layers containing brooms with doublers, four layers at 15 degrees, and four layers at 45 degrees, making a total of 18 layers. The lower graphite epoxy fitting had a total of 23 layers. The fitting contained nine layers at 90 degrees, 12 layers at 15 degrees, and two at 45 degrees. The fiberglass bosses completed the composite assembly. The metal attachment fittings are shown in Drawing 416-100 in Appendix E. They were designed to clamp the hole edges as well as to carry the landing loads.



POSITION	BASELINE GEAR		COMPOSITE GEAR	
	X/R	L (IN.)	X/R	L (IN.)
EXTENDED	2.71	50.06	1.82	67.04
STATIC	2.75	47.34	1.91	63.04
COMPRESSED	2.75	46.43	1.92	61.73
CRASHED	2.40	35.27	1.82	46.45

Figure 25. Geometry Comparison.

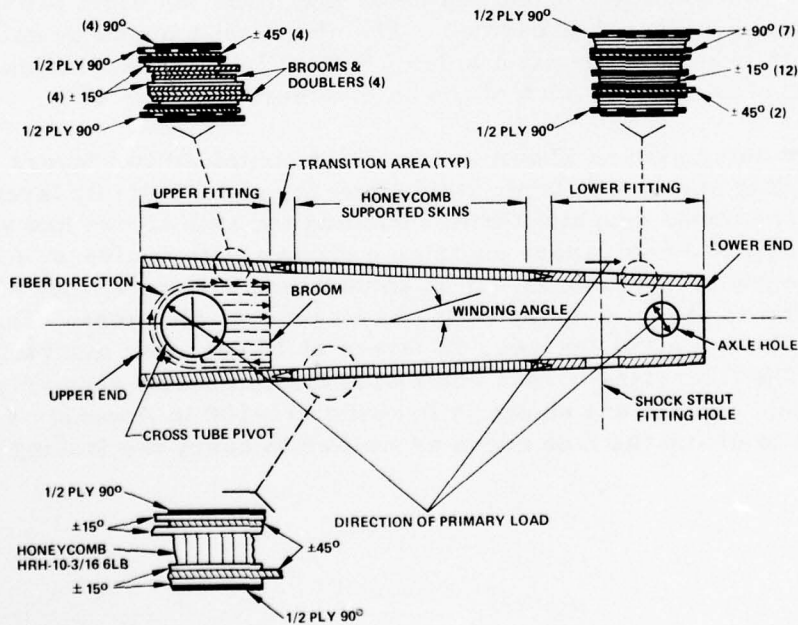


Figure 26. Construction Schematic of Trailing Arm.

FABRICATION

The complete trailing arm assembly, as described in the design section, consisted of a basic section made of graphite-epoxy with removable metal fittings and spacers. The tools required for the composite fabrication were a winding mandrel, various doubler trim templates, and shop aids for broom winding. The plaster winding mandrel shown in Figure 27 duplicated the inside surface of the arm. Turnaround areas were added for the winding process by extending the mandrel past both ends of the arm.

The elliptical tapered shape of the trailing arm was a deviation from the ideal geodesic path of cylindrical shapes predominately used for filament winding. This required close control of the winding machine in order to minimize slippage of the graphite tows as they were wound over the mandrel. The techniques for winding the tows so that they lay side by side without overlapping or gapping was developed during the fabrication process.

The trailing arm was fabricated to the process specifications in Appendix C. The sequence of operations are in Figure 28, and the doubler, broom, and honeycomb configurations are shown in Figure 29. The fabrication task began by heat-forming the nylon phenolic honeycomb to the arm contour.

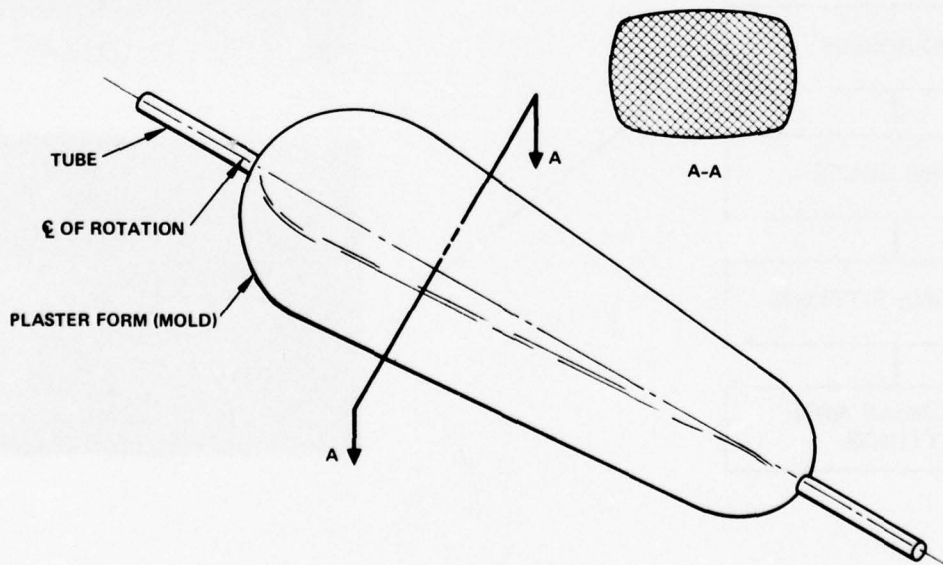


Figure 27. Winding Mandrel

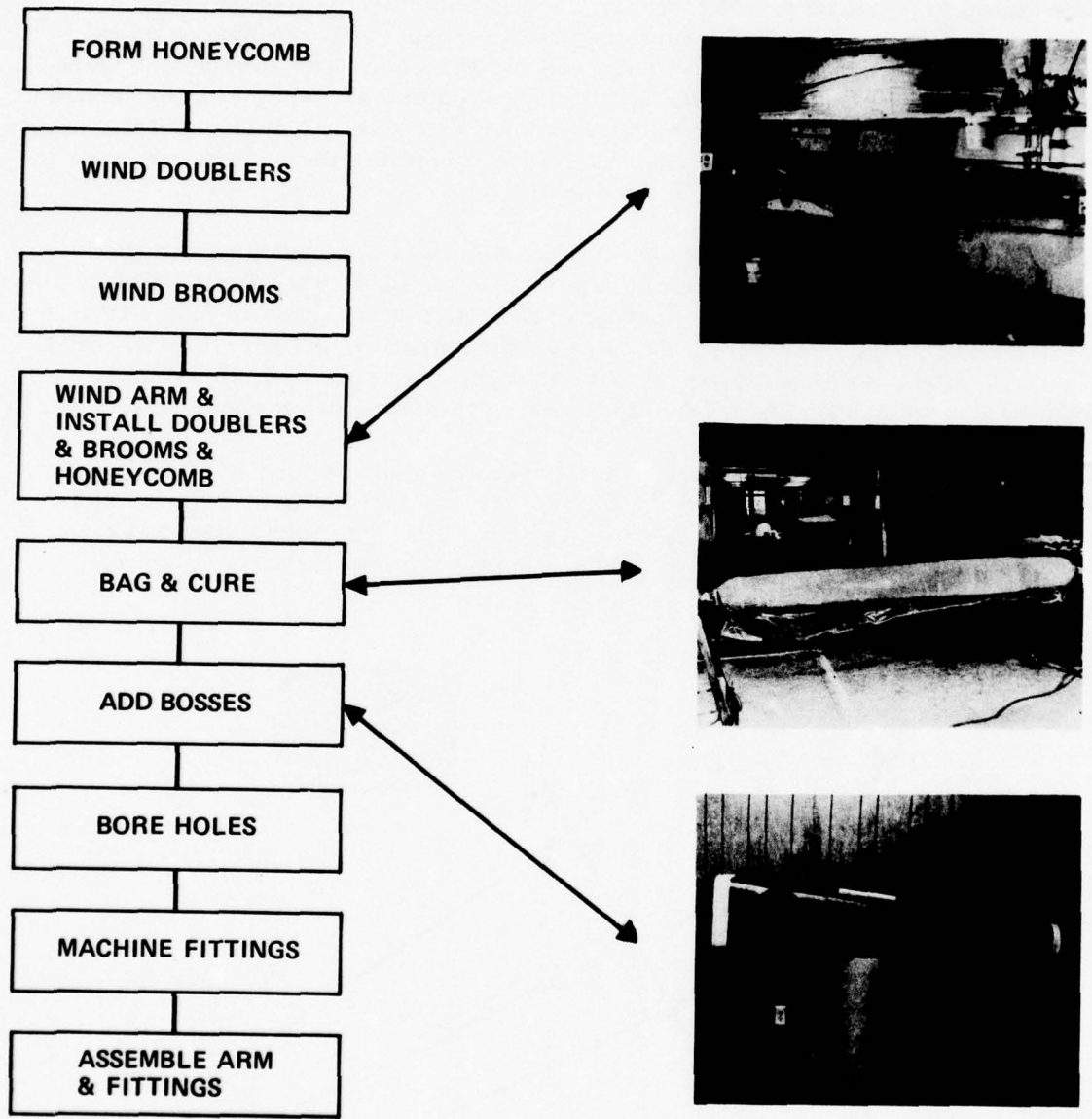
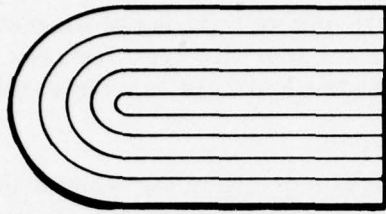
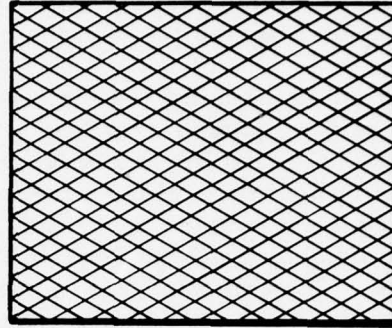


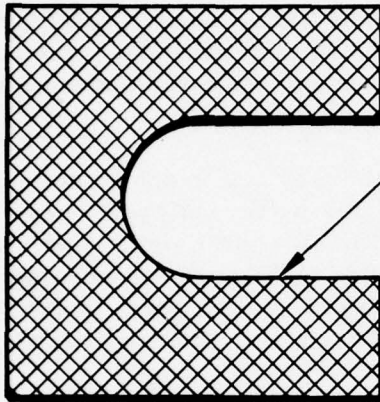
Figure 28. Fabrication Sequence.



BROOMS

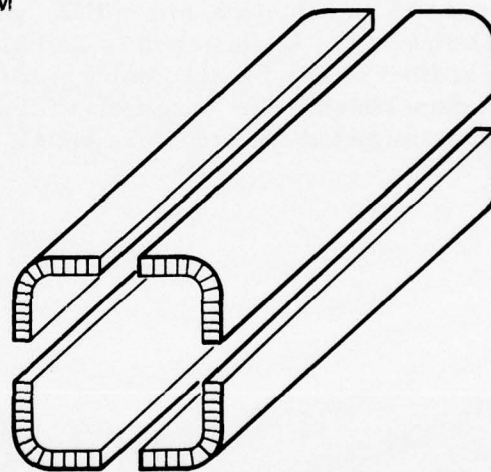


15° DOUBLERS

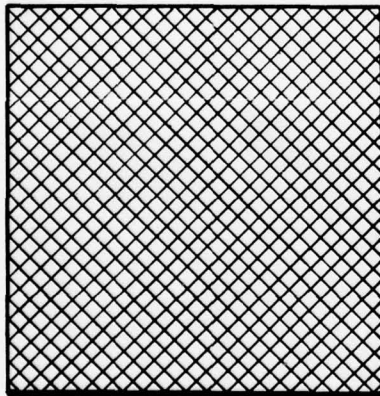


CUTOUT
FOR
BROOM

45° DOUBLERS
AT BROOMS



HONEYCOMB



45° DOUBLERS

Figure 29. Brooms and Doublers Configuration.

The doublers were fabricated by winding graphite/epoxy onto large diameter air-inflated mandrels. The brooms were wound on shop aid type fixtures. The doublers and brooms were then trimmed to size and held in refrigeration until needed during the winding of the arm.

The winding machine and the trailing arm mandrel were then set up and the WFW of the graphite arm began by using the sequence of operations shown on Drawing 416-100 (Appendix E) and the process specification (Appendix C). The first operation of the winding sequence was a short 90-degree (circumferential) wrap at the upper and lower ends. The winding process was completed by adding all the required doublers, brooms, and wound-in-place skin layers. The arm was then vacuum-bagged and cured, the mandrel removed, and the graphite arm rough-cut to length. The bosses were then added and the total composite assembly was finish cured.

The holes were then bored through the E-glass bosses and graphite arm. It was found that the cutting edge of a hard (C9) boring bar chipped away, necessitating the use of a softer (C2) bar to obtain straight holes. The inside of the holes in the E-glass had to be lightly sanded to remove the protruding edges of fiber. The finished holes were of excellent quality, both in accuracy and surface finish. The assembly of the steel attachment fittings, spacers, and nuts completed the structure shown in Figure 30.

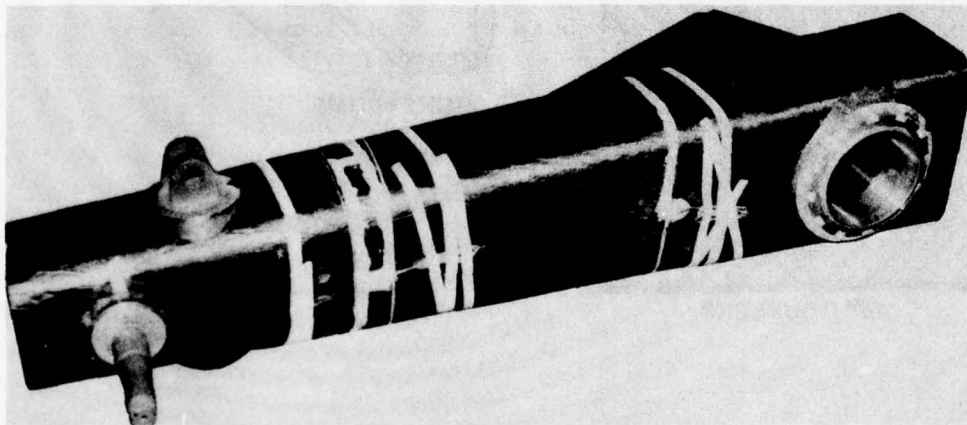


Figure 30. Trailing Arm Assembly.

TESTING

Dynamic and static testing of the advanced composite gear in accordance with the approved test plan in Appendix G was conducted at Menasco, Burbank, California. Menasco had tested the baseline gear and had dynamic fixtures that could be modified for use on this program. A new static test fixture was required because the graphite arm was larger than the baseline arm.

DYNAMIC TESTING

The dynamic testing was conducted as outlined in the test plan in Appendix G by varying drop height and weight until the ground loads for a 10-fps unit and 12.5-fps reserve energy drops were achieved. Dynamic testing was limited to 10 and 12.5 fps in order to preclude failing the trailing arm before static testing could be completed. The dynamic test fixture with the graphite arm installed is shown in Figure 31. The large diameter tube used as a pivot and arm attachment to the fixture is easily distinguished. The shock strut with its extension can also be seen. The wheel is in close proximity to the ground platform at the lower end of the arm assembly. Vertical ground reactions were measured using ring type load cells located between the floor and the platform. The locations of the bending and torsion strain gages, as well as the accelerometer, are illustrated in Figure 32.

Prior to testing, all the internal spacers were tightened to a snug fit with the internal bosses. The torque was set at 120 foot-pounds for the external nuts at the axle and shock strut fitting. One hundred fifty foot-pounds of torque was used for the external nuts at the pivot. These low torque values gave minimal clamping to the hole edges, and provided a snug fit between the nut and the bosses. The torque values were unchanged after dynamic testing, indicating no yielding of the composite materials. The dynamic test was completed using six impacts to give the loads and data presented in Table 9. The graphite arm resisted, without yielding or failure, the dynamic test loads which were 88 percent of the ultimate vertical three-point crash load of the advanced design criteria. The loads were limited to 88 percent in order to preclude failing the arm before static testing was conducted. The loads indicated by the bending and torsion strain gages, which were recorded for possible correlation with actual platform loads, gave poor results and were disregarded. The net result was that the graphite arm demonstrated its ability to withstand the high impacts associated with an advanced landing gear.

STATIC TESTING

Static testing was conducted in accordance with the test plan in Appendix G. The following data was recorded to determine the capabilities of the graphite trailing arm.



Figure 31. Dynamic Test Setup.

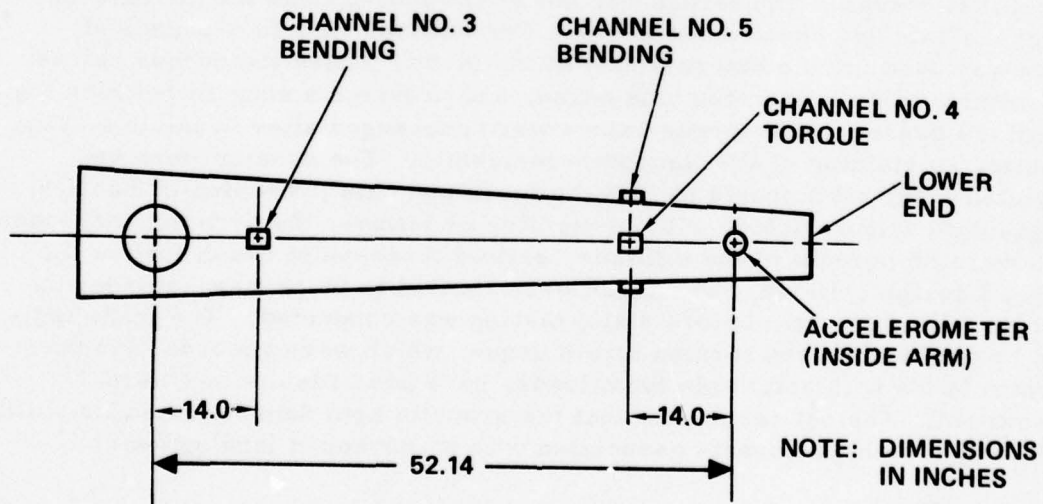


Figure 32. Location of Strain Gages and Accelerometer.

TABLE 9. DYNAMIC TEST DATA

	Menasco Drop Number	
	4	6
Aircraft Weight, lb	13,950	13,950
Drop Weight, lb (Actual/Calculated)	5,110/5,250	5,610/5,460
Aircraft Attitude	3-Point	3-Point
Tire Pressure, psig	105	105
Strut Pressure, psig	757	757
Wheel Speed	Zero	Zero
Jig Velocity, fps	9.1	10.9
Vertical Platform Load, lb	21,000	34,800
Accelerometer, g	7.2	9.8
Upper Strut Stroke, in.	2.31	2.56
Mass Displacement, in.	9.90	11.75
Bending - Upper, lb (Channel 3)*	19,100	27,500
Torque, lb (Channel 4)*	33,200	50,200
Bending - Lower, lb (Channel 5)*	22,200	33,500

*Maximum indicated loads applied at the wheel as calculated from static load calibrations.

- Incremental loads and deflections
- Permanent set at limit load
- Ultimate strength and mode of failure

The test setup in Figure 33 shows the trailing arm and shock strut lying on one side. The pivot and the strut are attached to a test fitting bolted to the test frame. Vertical loads, P_V , and lateral loads, P_S , were applied as located in Figure D-1, Appendix D, by two hydraulic jacks. Hydraulic pressure was supplied to the jacks by an electric pump. The locations of the deflection measurements associated with these loads are also shown. Prior to loading the arm, the torque for each nut was set at the values used for dynamic testing. The gear was tested for a two-wheel landing condition with an outboard side load. The deflections were measured relative to the axle and wheel center line with the arm in the fully extended position. The loads were applied in two tests. The first static test was to limit load and return to 10 percent load for permanent set readings. The permanent set readings were made at 10 percent load rather than zero in order to eliminate slight movements due to looseness in the bolted joints. The data showed no permanent set at a limit load.

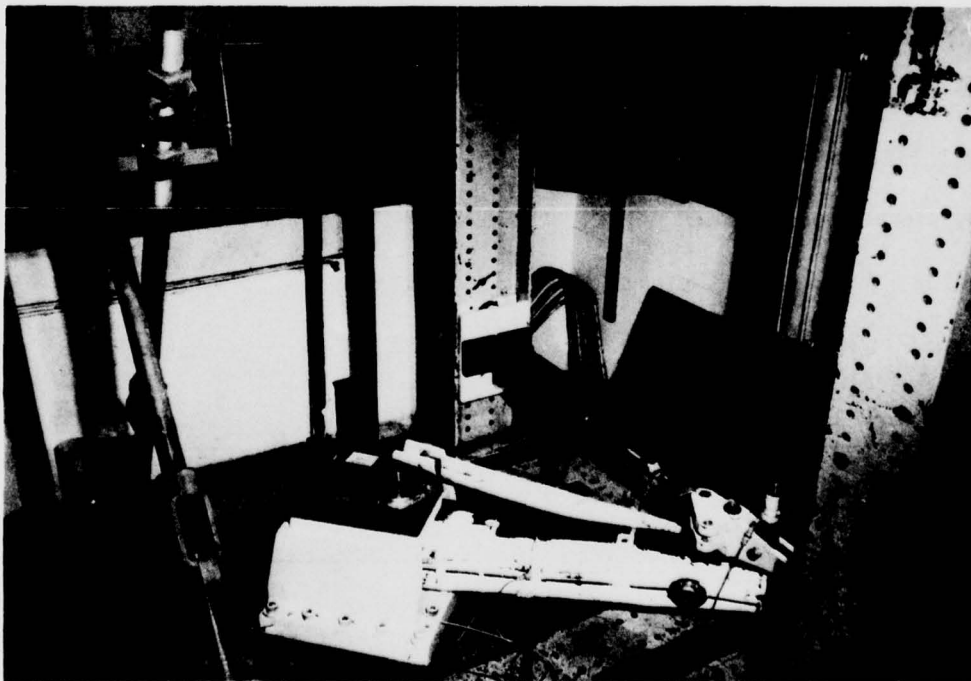


Figure 33. Static Test Setup.

The second test took the arm incrementally to failure which occurred just prior to recording the strains and deflections at 2.1 times limit load. The failed arm shown in Figure 34 had primarily a compressive failure with torsion in the skins located 14 inches below the pivot. The straight line load deflection curve plotted in Appendix G shows no yielding up to failure. The graphite holes with minimal clamping of the edges showed no yielding or cracking when examined after the test. However, the boss that provided a flat surface for the shock strut had a crack extending through the resin and chopped fiber, but it did not extend to the graphite arm. This was considered a secondary type failure that did not affect the strength of the graphite arm and could be alleviated by designing a smaller boss using woven material with a higher fiber volume.

Subsequent to the test, the arm was cut in half lengthwise as shown in Figure 35. This allowed thickness, specific gravity, and fiber volume samples to be taken at the failed section. Visually, the inner skins appeared thicker than the outer skins. The general appearance showed a structure completely cured with no additional unbonded or failed areas.

The loads applied to the trailing arm during the static test at the locations in Figure D-1 are compared with the critical design loads in Table D-1. The arm was generally designed for a three-point crash landing with an outboard side load. The shock strut attachment, the only exception, was critical for a two-point landing condition with drag. The statically applied loads and the design loads at the failed section in Figure 36 are compared in Table 10. The inner skin was 23 percent thicker than drawing requirements. This was due to the overlapping of the graphite tows when they were wound onto the mandrel. The shape and taper of the arm accentuates this problem by causing difficulty in matching the edges of each tow. However, improvement was made during fabrication in that the last skin wound, the outer skin, was only 7 percent over drawing requirements for thickness. It normally takes more than one part to completely solve these problems, thus the next skin would be closer to the requirements. This small deviation did not adversely affect the program results. The fiber content at 55 percent was 5 percent higher than anticipated. The specific gravity of 1.46 showed a dense composite with 1.3 percent voids.

Further evaluation of the static test, taking into account the extra load capabilities due to the increased skin thickness and fiber volume, showed the arm had an adjusted margin of 11.4 percent. The initial design of the failed section at point "a" in Figure 36 had a compressive stress

$$f_c = \frac{892,000 \times 5.2}{139.1} - \frac{39,770}{9.14} = 28,995 \text{ psi}$$

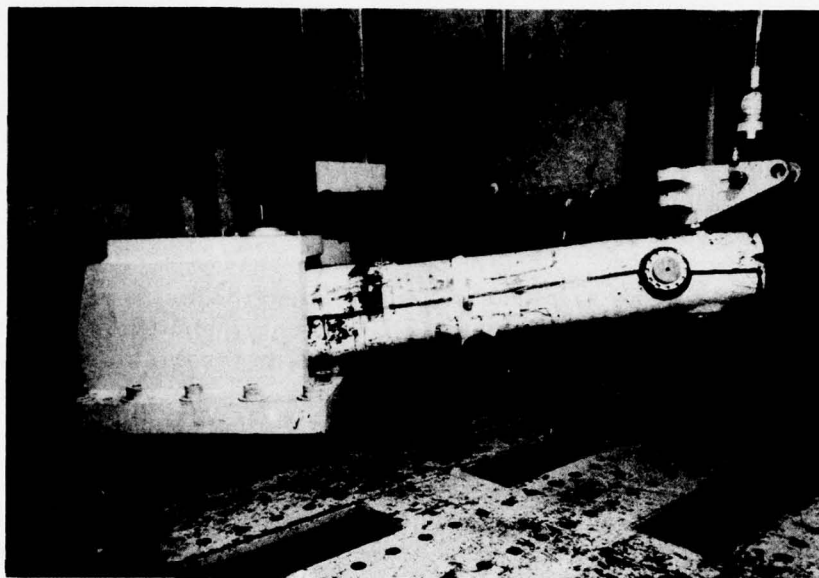


Figure 34. Static Failure.

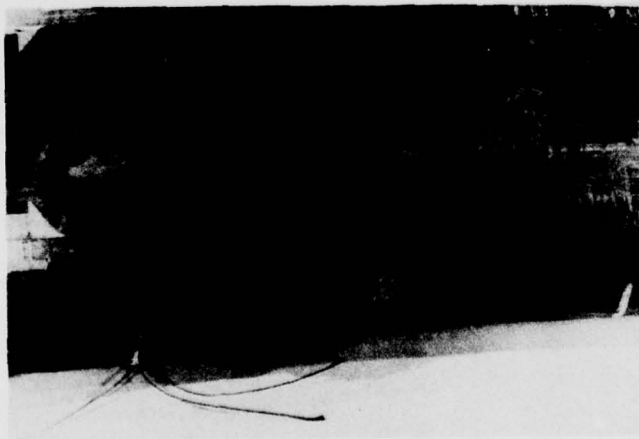
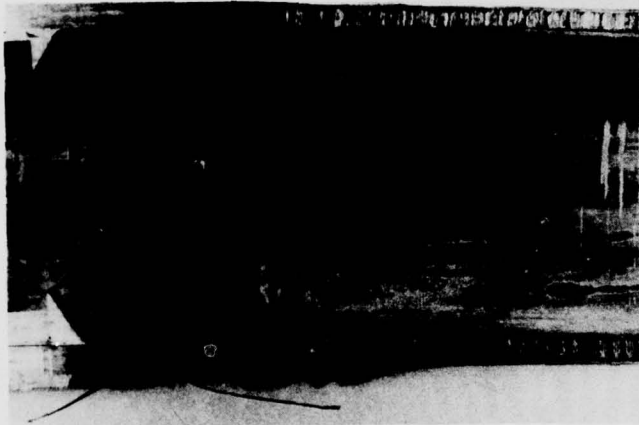


Figure 35. Trailing Arm Sections.

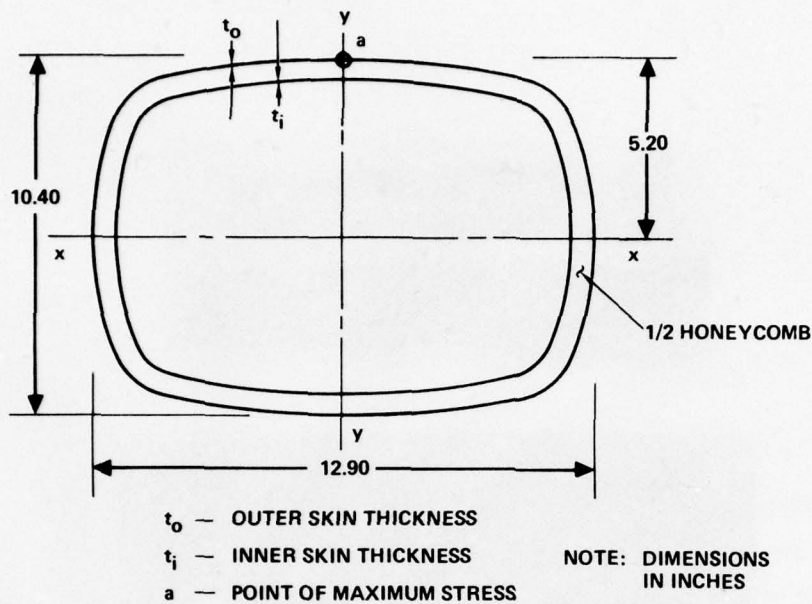


Figure 36. Section at Failure Location.

TABLE 10. APPLIED VERSUS DESIGN LOADS AT FAILED SECTION		
	Applied	Design
ULT Axial, P_A	55,940 lb	39,770 lb
ULT Lateral Moment, M_x	1,146,000 in. -lb	892,000 in. -lb
ULT Vertical Moment, M_y	146,200 in. -lb	115,800 in. -lb
ULT Torque, T	550,000 in. -lb	368,400 in. -lb
Skin Thickness, t_o	0.126 in.	0.1174 in.
Skin Thickness, t_i	0.145 in.	0.1174 in.
Skin Area	10.51 in. ²	9.14 in. ²
I_{xx}	158.5 in. ⁴	139.1 in. ⁴
I_{yy}	226.5 in. ⁴	198.3 in. ⁴
J	348.0 in. ⁴	305.0 in. ⁴
Fiber Volume, Percent	55	50

The tested design had a compressive stress

$$f_c = \frac{1,146,000 \times 5.2}{158.5} - \frac{55,940}{10.51} = 32,300 \text{ psi}$$

The trailing arm as designed, had an excessive strength of

$$M_S = \frac{32,300}{29,000} - 1 \times 100 = 11.4 \text{ percent}$$

The thickness of the graphite skins and end fittings could therefore be reduced 11.4 percent. The maximum bearing stress experienced was due to a resultant load on the shock strut and equaled

$$f_{b_r} = \frac{107,000}{3 \times 0.78} = 45,700 \text{ psi}$$

The vertical stiffness or spring rate of the graphite arm was 2.4 times that of the baseline gear. This allowed more fuselage deflection to stroke the shock strut rather than to deflect the arm. This made a more efficient energy-absorbing gear.

A redesign of the trailing arm was conducted using the information gained from testing. The thickness of the upper graphite fitting was reduced to 0.60 on the sides with the hole and to 0.45 on the other sides. The skins were reduced 11 percent in thickness and the ends were chamfered in eight places. The final design is shown in Figure 37 and the weight calculations are presented in Appendix F. The final weight summary in Table 11, when compared to baseline weights and Configuration 6A weights in Table 7, shows an overall 7-percent weight decrease for the gear with an 11-percent decrease for the trailing arm. The weights for the shock strut, cross tube, and wheel were those used during the concept comparisons.

Subsequent to testing, a cost analysis resulted in showing the WFW process to be cost-effective for fabricating the prototype composite landing gear arm since the \$25,000 cost of the composite arm was 63 percent less than the cost of its metal counterpart.

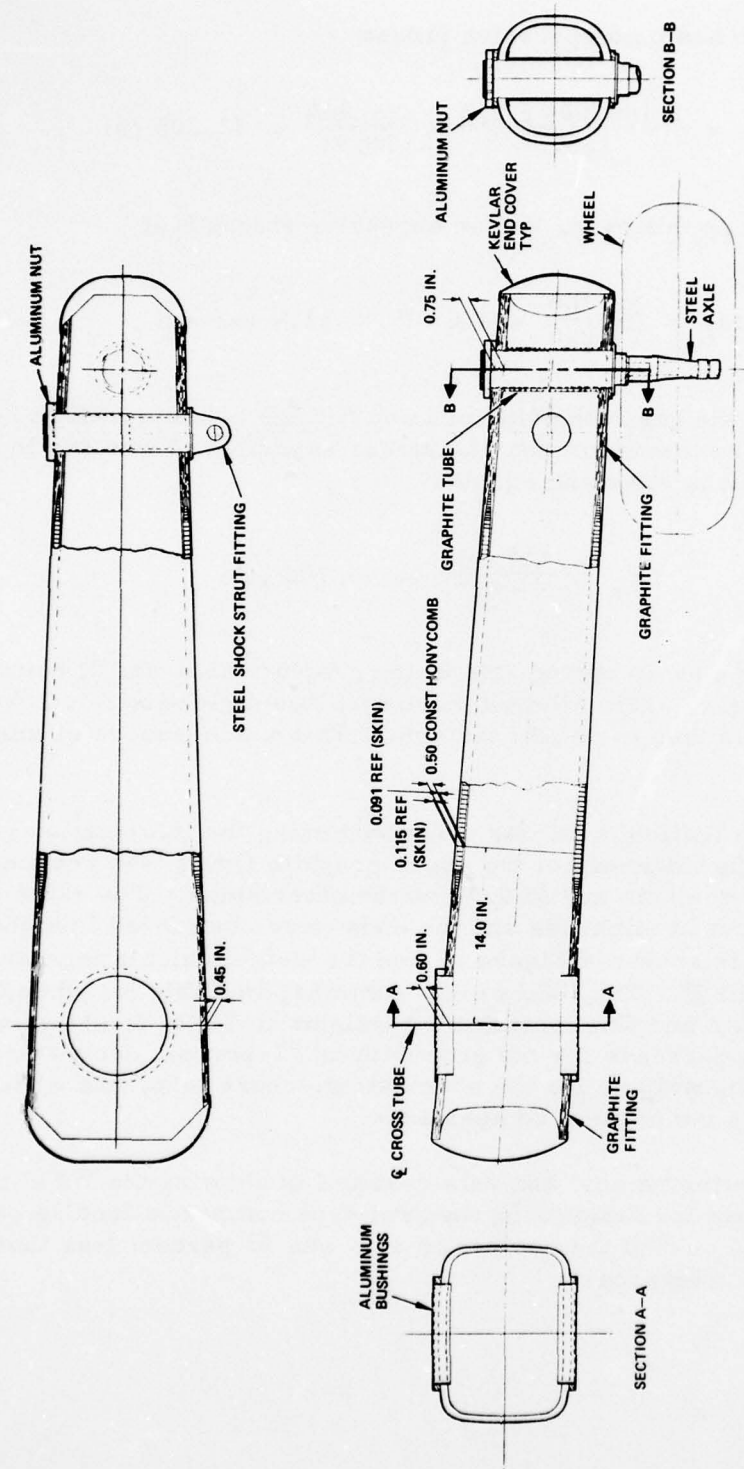


Figure 37. Trailing Arm Final Design.

TABLE 11. WEIGHT SUMMARY

Component	Baseline Weight (lb)	Configuration 6A Weight (lb)	Final Design Weight (lb)
Trailing Arm (2)	148.0	137.4	132.8
Cross Tube (1)	78.1	51.6	51.6
Shock Strut (2)	88.0	95.4	95.4
Wheel (2)	31.6	26.9	26.9
Miscellaneous*	-	16.0	16.0
Total Gear	345.7	327.3	322.7

*Weight adjustment for changes to fuselage attachments.

CONCLUSIONS

Based on the results of this effort, it is concluded that:

1. The primary objectives of the program were satisfied.
 - a. The design criteria for a high-energy-absorbing landing gear were established.
 - b. An advanced structural material and design techniques to satisfy the structural and functional requirements for this gear were selected.
 - c. A wheel-type helicopter landing gear was designed, fabricated, and laboratory tested.
 - d. The test results were evaluated against the design criteria.
2. A composite gear is lighter than the baseline steel gear; by 7 percent using present WFW equipment and by an estimated 26 percent if a toroidal winding machine were developed and used for fabrication.
3. Graphite epoxy is a practical landing gear structural material, with capabilities amply demonstrated by withstanding the dynamic and static loads associated with an advanced high-energy-absorbing gear.
4. Thornel 300 graphite is a more cost-effective landing gear material than steel. It will be more cost effective than other industry-established fibers when graphite costs are reduced.
5. WFW can be used to cost effectively fabricate tapered landing gear components with noncircular cross sections.
6. A stiffer gear can be designed using composites. This improves the energy absorption of the gear by allowing more fuselage deflection to actuate the shock strut versus deflecting the trailing arm.
7. Graphite epoxy structures have linear load-deflection curves showing virtually no yielding prior to failure.
8. The MIL-STD-1290 vertical crash landing requirement of 42 feet per second increases fuselage weight by approximately 1.46 percent of gross weight. This weight increase is considered to be acceptable in relation to the possible cost savings due to increased crashworthiness.

9. The landing gear in general can improve autorotation safety by making available 25 percent more energy attenuation to arrest vertical descent.
10. The ability of the landing gear to absorb energy inherently increases as helicopter gross weight increases, since ground clearances increase concordantly with aircraft size. Therefore, helicopter vertical ground contact velocities for crash should increase as gross weight increases.
11. WFW, a composite trailing arm for prototype fabrication, proved to be more cost effective than machining a steel gear. The composite arm cost 63 percent less than the metal arm.

RECOMMENDATIONS

It is recommended that:

1. A design study be initiated to investigate the practicality of developing a toroid winding machine capable of fabricating large landing gear components in order to realize weight savings in the order of 26 percent.
2. A graphite epoxy high-energy-absorbing landing gear be designed, fabricated, and installed on 10 airframes of an advanced helicopter in order to demonstrate composite capabilities under service conditions.
3. MIL-STD-1290 crash criteria be reviewed with regard to varying vertical crash velocities relative to helicopter gross weight, in order to make use of the greater ground clearances inherently associated with the larger helicopter.
4. MIL-STD-1290 criteria be reviewed with regard to requiring the main rotor blades as well as the fuselage to be flightworthy at 20 feet per second or higher ground contact velocities.

REFERENCES

1. EXPERIMENTAL RESEARCH, CH-21 HELICOPTER AIRFRAME DEFORMATION UNDER A DYNAMIC CRASH CONDITION, Aviation Safety Engineering and Research; TRECOTM Technical Report 63-77, U.S. Army Transportation Research Command, Fort Eustis, Virginia, January 1964.
2. Avery, James P., and Reed, William H., PRINCIPLES FOR IMPROVING STRUCTURAL CRASHWORTHINESS FOR STOL AND CTOL AIRCRAFT, Aviation Safety Engineering and Research; USAAVLABS Technical Report 66-39, U.S. Army Aviation Materiel Laboratories, Fort Eustis, Virginia, June 1966, AD 637133.
3. Drummond, John K., Gatlin, Clifford I., Goebel, Donald E., and Larsen, Stuart E., ANALYSIS OF HELICOPTER STRUCTURAL CRASHWORTHINESS, VOLUMES I-II, Dynamic Science; USAAVLABS Technical Reports 70-71A and 70-71B, U.S. Army Air Mobility Research and Development Laboratory, Fort Eustis, Virginia, January 1971, AD 880680/880678.
4. Turnbow, J. W., et al, CRASH SURVIVAL DESIGN GUIDE, Dynamic Science; USAAMRDL Technical Report 71-22, U. S. Army Air Mobility Research and Development Laboratory, Fort Eustis, Virginia, October 1971, AD 733358.
5. Carr, Richard W., Phillips, Norman S., and Scranton, Richard S., CRASHWORTHY LANDING GEAR STUDY, Beta Industries, Inc.; USAAMRDL Technical Report 72-61, U.S. Army Air Mobility Research and Development Laboratory, Fort Eustis, Virginia, April 1973, AD 765489.
6. Singley, George T. III, FULL SCALE CRASH TESTING OF A CH-47C HELICOPTER, Paper presented to the 32nd National V/STOL Forum of the American Helicopter Society, Washington, D.C., May 1976.
7. Rich, M. J., AN ENERGY ABSORPTION SAFETY ALIGHTING GEAR FOR HELICOPTER AND VTOL AIRCRAFT, Sikorsky Aircraft; IAS (AIAA) 62-16, American Institute of Aeronautics and Astronautics, New York, New York, January 1962.
8. Military Standard - 1290 (AV), LIGHT FIXED- AND ROTARY-WING AIRCRAFT CRASHWORTHINESS, Department of Defense, Washington, D. C., 25 January 1974.

9. Military Specification MIL-S-8698(ASG), STRUCTURAL DESIGN REQUIREMENTS, HELICOPTERS, Department of Defense, Washington, D.C., 1 July 1954, with Amendment 1, 28 February 1958.
10. Kimball, K.A., et al, ARMY AUTOROTATION ACCIDENTS, FISCAL YEARS 1970-1972, AARU Report 74-2, U.S. Army Aeromedical Research Unit, Fort Rucker, Alabama, August 1973.
11. Haley, J. T., ANALYSIS OF U.S. ARMY HELICOPTER ACCIDENTS TO DEFINE INJURY PROBLEMS, AGARD Conference Preprint 88-71, U.S. Army Board for Aviation Accident Research, Fort Rucker, Alabama, June 1971.
12. Military Specification MIL-L-8552C, LANDING GEAR, AIRCRAFT SHOCK ABSORBER (AIR-OIL TYPE), Department of Defense, Washington, D.C., 19 November 1965.
13. Military Specification MIL-S-8844, STEEL BAR, REFORGING STOCK, AND MECHANICAL TUBING, LOW ALLOY, PREMIUM QUALITY, Department of Defense, Washington, D.C., 25 May 1971.
14. Jones, B.H. and Jakway, W., MM&T - PULTRUDED COMPOSITE STRUCTURAL ELEMENTS, Goldsworthy Engineering, Inc.; USAAMRDL Technical Report 76-5, Eustis Directorate, U.S. Army Air Mobility Research and Development Laboratory, Fort Eustis, Virginia, December 1976, AD A035217.
15. Head, R.E., FLIGHT TEST OF A MULTI-TUBULAR SPAR MAIN ROTOR BLADE ON THE AH-1G HELICOPTER, VOLUME VI - PRODUCTION COST ASSESSMENT, Hughes Helicopters, Division of Summa Corporation; USAAMRDL Draft Technical Report, Eustis Directorate, U.S. Army Air Mobility Research and Development Laboratory, Fort Eustis, Virginia (to be published).
16. Needham, J.F., DESIGN, FABRICATION, AND TESTING OF AN ADVANCED COMPOSITE AH-1G TAIL SECTION (TAIL BOOM/ VERTICAL FIN), Hughes Helicopters, Division of Summa Corporation; USAAMRDL Technical Report 76-24, Eustis Directorate, U.S. Army Air Mobility Research and Development Laboratory, Fort Eustis, Virginia, November 1976, AD A034457.
17. ADVANCED COMPOSITES DESIGN GUIDE, Advanced Development Division, Air Force Materiels Laboratory, Air Force Systems Command, Wright-Patterson Air Force Base, Ohio.

18. FILAMENT COMPOSITE MATERIALS LANDING GEAR PROGRAM, The Bendix Corporation, Energy Controls Division; AFFDL Technical Report 72-78, Air Force Flight Dynamics Laboratory, Air Force Systems Command, Wright-Patterson Air Force Base, Ohio.
19. Price, A. L., FILAMENT COMPOSITE WHEEL DEVELOPMENT FOR MILITARY AIRCRAFT, Whittaker Corporation; AFFDL Technical Report 71-144, Air Force Flight Dynamics Laboratory, Air Force Systems Command, Wright-Patterson Air Force Base, Ohio, October 1971.

BIBLIOGRAPHY

1. Drake, R., and Siebert, A., ELASTOMER-MODIFIED EPOXY SYSTEMS FOR STRUCTURAL APPLICATIONS, B.F. Goodrich Chemical Company, Cleveland, Ohio, April 1975.
2. Sandhu, R.S., et al, LAMINATE TUBULAR SPECIMENS SUBJECTED TO BIAXIAL STRESS STATES (GRAPHITE/EPOXY), AFFDL Technical Report 73-7, Air Force Flight Dynamics Laboratory, Air Force Systems Command, Wright-Patterson Air Force Base, Ohio, March 1975.
3. PLASMA SPRAYED COATINGS, Materials Engineering, 1975.
4. ORGANIC COATINGS AND FINISHES, Materials Selector, 1975.
5. FLUOROPOLYMERS, Rennwalt Corporation.
6. Metzger, R.F., et al, DEVELOPMENT OF A METHOD FOR THE ANALYSIS OF IMPROVED HELICOPTER DESIGN CRITERIA, Kaman Aerospace Corporation; USAAMRDL Technical Report 74-30, Eustis Directorate, U.S. Army Air Mobility Research and Development Laboratory, Fort Eustis, Virginia, July 1974, AD 783392.
7. Wittlin, G. and Park, K.C., DEVELOPMENT AND EXPERIMENTAL VERIFICATION OF PROCEDURES TO DETERMINE NONLINEAR LOAD-DEFLECTION CHARACTERISTICS OF HELICOPTER SUBSTRUCTURES SUBJECTED TO CRASH FORCES, Lockheed California; USAAMRDL Technical Reports 74-12A and 74-128, Volumes 1 and 2, Eustis Directorate, U.S. Army Air Mobility Research and Development Laboratory, Fort Eustis, Virginia, May 1974, AD 784191, AD 784192.
8. PROCEEDINGS OF THE CONFERENCE ON FIBROUS COMPOSITES IN FLIGHT VEHICLE DESIGN, held at Dayton, Ohio, AFFDL Technical Report 74-103, Air Force Flight Dynamics Laboratory, Air Force Systems Command, Wright-Patterson Air Force Base, Ohio, 22-24 May 1974.
9. Kincock, James C., ADHESIVELY RELEASABLE AND REUSABLE SHOCK LOAD ABSORBING SYSTEM, U.S. Patent 3,804,698, 16 April 1974.

10. Harruff, P.W., et al, MANUFACTURING METHODS FOR HIGH TEMPERATURE REINFORCED PLASTIC AIRCRAFT RADOMES, Brunswick Corporation; AFML Technical Report 73-15, Air Force Materials Laboratory, Air Force Systems Command, Wright-Patterson Air Force Base, Ohio, March 1974.
11. BONDED COMPOSITES TO METAL SCARF JOINT PERFORMANCES IN AN AIRCRAFT LANDING GEAR DRAG STRUT (747), Langley Research Center; NASA TM X-71995, National Aeronautics and Space Administration, Washington, D.C., 1974.
12. AVIONIC RADOME MATERIALS, Royal Radar Establishment, Malvern, United Kingdom; AGARD AR 75, Advisory Group for Aerospace Research and Development, 7 Rue Ancelle, 92200 Neuilly Sur Seine, France, 1974.
13. Bonk, Robert B., and Teetsel, Dorothy D., WEATHERING OF GLASS FILAMENT WOUND EPOXIES, PA Technical Report 2102, Addendum 10, Picatinny Arsenal, Dover, New Jersey, November 1973.
14. Mayerjak, Robert J., and Smyth, William A., INVESTIGATION OF ADVANCED STRUCTURAL CONCEPTS FOR FUSELAGE, Kaman Aerospace Corp.; USAAMRDL Technical Report 73-72, Eustis Directorate, U.S. Army Air Mobility Research and Development Laboratory, Fort Eustis, Virginia, October 1973, AD 773597.
15. Swatton, S., STUDY OF ADVANCED STRUCTURAL CONCEPTS FOR FUSELAGE, Boeing Vertol Company; USAAMRDL Technical Report 73-69, Eustis Directorate, U.S. Army Air Mobility Research and Development Laboratory, Fort Eustis, Virginia, October 1973, AD 772708.
16. Faiz, Robert L., A DESIGN ANALYSIS OF A CH-54B MAIN ROTOR HUB FABRICATED FROM COMPOSITE MATERIALS; Sikorsky Aircraft Division, United Aircraft Corporation; USAAMRDL Technical Report 73-49, Eustis Directorate, U.S. Army Air Mobility Research and Development Laboratory, Fort Eustis, Virginia, October 1973, AD 774270.
17. Lark, R.F., FILAMENT WOUND COMPOSITE VESSEL MATERIALS TECHNOLOGY, Lewis Research Center; NASA TM X-68196, National Aeronautics and Space Administration, Washington, D.C., October 1973.

18. Cook, T.N., et al, MAINTAINABILITY ANALYSIS OF MAJOR HELICOPTER COMPONENTS, Kaman Aerospace Corp.; USAAMRDL Technical Report 73-43, August 1973, AD 769941.
19. Rich, M.J., et al, APPLICATION OF COMPOSITES TO HELICOPTER AIRFRAME AND LANDING GEAR STRUCTURES, Sikorsky Aircraft Company; NASA CR-112333, National Aeronautics and Space Administration, Washington, D.C., June 1973.
20. Scheltes, R., INFLUENCE OF OUTDOOR WEATHERING ON THE MECHANICAL PROPERTIES AND QUALITY OF APPEARANCE OF SEVERAL GLASS CLOTH REINFORCED THERMOSETTING RESIN LAMINATES, RNAFF FOK R-1627, Fokker, VFW, 8.V., March 1973.
21. Bonk, Robert B., Levi, David W., and Maciejczyk, Joseph, WEATHERING OF COMPOSITES REVIEW OF EPOXIDE CONTAINING GLASS FILAMENT WOUND STRUCTURES, PA Technical Report 4467, Picatinny Arsenal, Dover, New Jersey, February 1973.
22. GRAPHITE COMPOSITE LANDING GEAR COMPONENTS - SIDE BRACE ASSEMBLY AND TORQUE LINK FOR A37-B AC, Hercules, Inc.; AFFDL Technical Report 73-69, Air Force Flight Dynamics Laboratory, Air Force Systems Command, Wright-Patterson Air Force Base, Ohio.
23. Kulkarni, S.V., et al, AN INVESTIGATION OF THE COMPRESSIVE STRENGTH OF PRD 49-111/EPOXY COMPOSITES, Materials Sciences Corporation; NASA CR-112334, National Aeronautics and Space Administration, Washington, D.C., 1973.
24. Chamis, C.C., et al, CRITERIA FOR SELECTING RESIN MATRICES FOR IMPROVED COMPOSITE STRENGTH, Lewis Research Center; NASA TM X-68166, National Aeronautics and Space Administration, Washington, D.C., 1973.
25. Rosen, B. Walter, COMPOSITE MATERIALS, AGARD LS 55, Advisory Group for Aerospace Research and Development, 7 Rue Ancelle, 92200 Neuilly Sur Seine, France, 1973.
26. Hofer, K.E., et al, DEVELOPMENT OF ENGINEERING DATA ON MECHANICAL AND PHYSICAL PROPERTIES OF ADVANCED COMPOSITES MATERIALS; ITT Research Institute; AFML Technical Report 72-205, Air Force Materials Laboratory, Air Force Systems Command, Wright-Patterson Air Force Base, Ohio, September 1972.

27. Fay, R.J., PROGRAM FOR THE EXPLOITATION OF UNUSED NASA PATENTS, University of Denver; NASA CR 128294, National Aeronautics and Space Administration, Washington, D.C., August 1972.
28. Clark, M.W., Krauss, W.K., and Ciecott, J.M., IDENTIFICATION AND ANALYSIS OF ARMY HELICOPTER RELIABILITY AND MAINTAINABILITY PROBLEMS AND DEFICIENCIES, Volumes I, II, and III, American Power Jet Co.; USAAMRDL Technical Reports 72-11A, 72-11B, and 72-11C, Eustis Directorate, U.S. Army Air Mobility Research and Development Laboratory, Fort Eustis, Virginia, April 1972, AD 901456L, AD 901457L, AD 901458L.
29. ANALYSIS OF TEST METHODS FOR HIGH MODULUS FIBERS AND COMPOSITES, A symposium held in San Antonio, Texas, ASTM STP-521, American Society for Testing Materials, San Antonio, Texas, 12-13 April 1972.
30. FILAMENT COMPOSITE MATERIALS LANDING GEAR PROGRAM, The Bendix Corporation, Energy Controls Division; AFFDL Technical Report 72-78, Air Force Flight Dynamics Laboratory, Air Force Systems Command, Wright-Patterson Air Force Base, Ohio.
31. IMPACT OF COMPOSITE MATERIALS ON AEROSPACE VEHICLES AND PROPULSION SYSTEMS, AGARD CP-112, Advisory Group for Aerospace Research and Development, 7 Rue Ancelle, 92200 Neuilly Sur Seine, France, 1972.
32. Fay, Richard J., and Wittrock, Edward P., METAL SHEARING ENERGY ABSORBER, Application No. 212977, December 28, 1971.
33. Bonk, Robert B., and Teetsel, Dorothy D., RESISTANCE OF PLASTICS TO OUTDOOR WEATHERING GLASS FILAMENT WOUND EPOXIES, PA Technical Report 2102, Addendum 9, Picatinny Arsenal, Dover, New Jersey, September 1971.
34. Bonk, Robert B., and Teetsel, Dorothy D., RESISTANCE OF PLASTICS TO OUTDOOR WEATHERING, PA Technical Report 2102, Addendum 8, Picatinny Arsenal, Dover, New Jersey, April 1971.
35. Gatlin, C.I., et al, ANALYSIS OF HELICOPTER STRUCTURAL CRASHWORTHINESS, VOLUME I - MATHEMATICAL SIMULATION AND EXPERIMENTAL VERIFICATION FOR HELICOPTER CRASHWORTHINESS, Dynamic Science; USAAVLABS Technical Report 70-71A, Eustis Directorate, U.S. Army Air Mobility Research and Development Laboratory, Fort Eustis, Virginia, January 1971, AD 880680.

36. Haley, Jr., J. L., HELICOPTER STRUCTURAL DESIGN FOR IMPACT SURVIVAL; USABAAR, Fort Rucker, Alabama; AIAA A71-15416, American Institute of Aeronautics and Astronautics, New York, N. Y., November 1970.
37. Swieskowski, Henry, SIDE SPREADING SPRINGS ABSORB HIGH-ENERGY IMPACT; AMSWE RE 70-137, Army Weapons Command, Rock Island, Illinois, March 1970.
38. Day, L. E., and Readdy, A. F., THE EFFECTS OF INDOOR STORAGE AND OUTDOOR WEATHERING ON NAVAL ORDNANCE LABORATORY NOL RING TEST SPECIMENS, PA Technical Report 3918, Picatinny Arsenal, Dover, New Jersey, March 1970.
39. Day, L. E., and Readdy, A. F., FEASIBILITY OF GLASS FILAMENT-WOUND PLASTICS FOR ARMY ROCKET MOTOR CASES, PA Technical Report 3918, Picatinny Arsenal, Dover, New Jersey, Final Progress Report, March 1970.
40. Mazza, L. T., Paxson, E. B., and Rodgers, R. L., MEASUREMENT OF DAMPING COEFFICIENTS AND DYNAMIC MODULUS OF FIBER COMPOSITES, USAAVLABS Technical Note 2, U. S. Army Aviation Materiel Laboratories, Fort Eustis, Virginia, February 1970, AD 869025.
41. Yurenka, S., INVESTIGATION OF ADVANCED FILAMENT WOUND AIRCRAFT LANDING GEAR, Douglas Aircraft Company; AFML Technical Report 69-229, Air Force Materials Laboratory, Air Force Systems Command, Wright-Patterson Air Force Base, Ohio, January 1970.
42. Carr, Richard W., and Phillips, Norman S., DESIGN CRITERIA FOR ENERGY ABSORPTION SYSTEMS, Beta Industries, Inc.; NADC AC-7010, Naval Air Development Center, Johnsville, Warminster, Pennsylvania.
43. THE SHOCK AND VIBRATION BULLETIN; Naval Research Laboratory, Washington, D. C., NRL Bulletin 38, Part 3, Naval Research Laboratory, Washington, D. C., November 1969.
44. DYNAMIC TESTING OF ENERGY ATTENUATING DEVICES, Foundation Research Project, NADC AC 6905, Naval Air Development Center, Johnsville, Warminster, Pennsylvania, October 1969.

45. THE EXPLOITATION OF THE UNUSED NASA PATENTS, University of Denver; NASA 1st Annual Report, NASA CR 106648, National Aeronautics and Space Administration, Washington, D.C., May 1969.
46. Balogh, Steve E., DESIGN PRINCIPLES FOR SHOCK LOAD PROTECTION THROUGH ENERGY ABSORPTION AND DISSIPATION METHODS, ASME 69-DE-37, American Society of Mechanical Engineers, May 1969.
47. Griffith, E.D., FEASIBILITY STUDY OF NON-NEWTONIAN GELLED FLUIDS, Western Company Research Div., USAAVLABS Technical Report 69-20, U.S. Army Aviation Materiel Laboratories, Fort Eustis, Virginia, April 1969, AD 858383.
48. Cutler, M.B., and Pinckney, R.L., STATIC AND FATIGUE TEST PROPERTIES FOR WOVEN AND NONWOVEN S-GLASS FIBERS, Boeing Vertol Company; USAAVLABS Technical Report 69-9, U.S. Army Aviation Materiel Laboratories, Fort Eustis, Virginia, April 1969, AD 688971.
49. THE SHOCK AND VIBRATION BULLETIN, Naval Research Laboratory; DOD BULL 39 PT-2, Director of Defense, Research and Engineering, Washington, D.C., February 1969.
50. Boller, K.H., EFFECT OF NOTCHES ON FATIGUE STRENGTH OF COMPOSITE MATERIALS, AFML Technical Report 69-6, Air Force Materials Laboratory, Air Force Systems Command, Wright-Patterson Air Force Base, Ohio.
51. Aston, J.E., Halpin, J.C., and Petit, P.H., PRIMER ON COMPOSITE MATERIALS ANALYSIS, Technomic Publishing Company, Inc., Stanford, Connecticut, 1969.
52. Chadsey, Earl E., et al, INVESTIGATION OF COMPOSITE STRUCTURES FABRICATION WITH ADVANCED HIGH-STRENGTH, HIGH-MODULUS REINFORCEMENT MATERIALS, Norton Research Corporation; USAAVLABS Technical Report 68-56, U.S. Army Aviation Materiel Laboratories, Fort Eustis, Virginia, August 1968, AD 678641.
53. Noyes, J.V., and Jones, B.H., CRAZING AND YIELDING OF REINFORCED COMPOSITES, McDonnell Douglas Corporation; AFML Technical Report 68-51, Air Force Materials Laboratory, Air Force Systems Command, Wright-Patterson Air Force Base, Ohio, March 1968.

AD-A048 891

HUGHES HELICOPTERS CULVER CITY CALIF
ADVANCED TECHNOLOGY HELICOPTER LANDING GEAR.(U)
OCT 77 R E GOODALL

F/G 1/3

UNCLASSIFIED

HH-77-41

USAAMRDL-TR-77-27

DAAJ02-75-C-0028
NL

2 of 2

ADAO48 891



END

DATE
FILMED
2-78

DDC

54. Rich, M.J., VULNERABILITY AND CRASHWORTHINESS IN THE DESIGN OF ROTARY WING VEHICLE STRUCTURES, SAE Paper 680673, Society of Automotive Engineers, Inc., New York, New York, 1968.
55. Smith, H.G., and McDermott, Jim, DESIGNING FOR CRASHWORTHINESS AND SURVIVABILITY, AHS No. 225, American Helicopter Society, 1968.
56. Holsten, Jr., A., et al, STABILITY OF FILAMENT WOUND CYLINDERS UNDER COMBINED LOADING, AFFDL Technical Report 67-55, Air Force Flight Dynamics Laboratory, Air Force Systems Command, Wright-Patterson Air Force Base, Ohio, May 1967.
57. Hall, H., SOME THEORETICAL STUDIES CONCERNING OLEO DAMPING CHARACTERISTICS FOR NASA, ARC CP-951, Aeronautical Research Council, London, England, 1967.
58. EXPLORATORY APPLICATION OF FILAMENT WOUND REINFORCED PLASTICS FOR AIRCRAFT LANDING GEAR, Bendix Corporation, Analytical Mechanics Department; AFML 66-309, Air Force Materiels Laboratory, Air Force Systems Command, Wright-Patterson Air Force Base, Ohio, December 1966.
59. Guist, L.R., Marble, D.R., PREDICTION OF THE INVERSION LOAD OF A CIRCULAR TUBE, NASA TN-D 3622, Ames Research Center, Moffett Field, California, September 1966.
60. Tsai, J., THE BUCKLING STRENGTH OF FILAMENT WOUND CYLINDER UNDER AXIAL COMPRESSION, Martin-Marietta Corp.; NASA CR-266, National Aeronautics and Space Administration, Washington, D.C., July 1966.
61. Turnbow, J.W., Robertson, S.H., Carron, D.F., and McWilliam, R.D., FULL SCALE DYNAMIC CRASH TEST OF A SMALL OBSERVATION-TYPE HELICOPTER, Aviation Safety and Research; USAAVLABS Technical Report 66-32, U.S. Army Aviation Materiel Laboratories, Fort Eustis, Virginia, May 1966, AD 483730L.
62. McGehee, J.R., EXPERIMENTAL INVESTIGATION OF PARAMETERS AND MATERIALS FOR FRAGMENTING TUBE ENERGY ABSORPTION PROCESS, Langley Research Center; NASA TN-D-3268, National Aeronautics and Space Administration, Washington, D.C., February 1966.

63. Anderson, Leon R., et al, REINFORCED PLASTIC GEAR FOR UH-1 HELICOPTER, Hayes International Corporation; USAAVLABS Technical Report 66-3, U. S. Army Aviation Materiel Laboratories, Fort Eustis, Virginia, January 1966, AD 628681.
64. Whitney, J.M., and Riley, M. B., ELASTIC PROPERTIES OF FIBER REINFORCED COMPOSITE MATERIALS, AIAA Journal, Vol. 4, American Institute of Aeronautics and Astronautics, New York, New York, 1966, p. 1537.
65. Fricker, W.W., DEVELOPMENT OF AIRCRAFT SHOCK ABSORBERS USING FRICTION AS THE ENERGY DISSIPATOR, Cleveland Pneumatic Tool Company; AFFDL Technical Report 65-96, Air Force Flight Dynamics Laboratory, Air Force Systems Command, Wright-Patterson Air Force Base, Ohio, October 1965.
66. ENERGY ABSORBING CHARACTERISTICS OF CRUSHABLE ALUMINUM STRUCTURES IN A SPACE ENVIRONMENT, Bendix Corporation; NASA CR-65096, National Aeronautics and Space Administration, Washington, D. C., July 1965.
67. HIGH ENERGY ABSORBER AND STRUCTURAL OVERLOAD DEVICES, Aerospace Research Associates; NASA CR-63602, National Aeronautics and Space Administration, Washington, D. C., June 1965.
68. MacNeal, R.H., and Loisch, J., ON THE USE OF FILAMENT WOUND TOROIDS AS PNEUMATIC SHOCK ABSORBERS, Astro Research Corporation; NASA CR-574, National Aeronautics and Space Administration, Washington, D. C., June 1965.
69. Dow, N.F., and Rosen, W. B., EVALUATIONS OF FILAMENT REINFORCED COMPOSITES FOR AEROSPACE STRUCTURAL APPLICATIONS, General Electric Company; NASA CR-207, National Aeronautics and Space Administration, Washington, D. C., April 1965.
70. Platus, D.L., et al, CONCEPTS OF MULTIPLE IMPACT STUDY OF ENERGY ABSORPTION, NASA CR-273, National Aeronautics and Space Administration, Washington, D. C., 1965.
71. BAND PASS SHOCK ABSORBER STUDIES, SH 64-1, Bendix Corporation, South Bend, Indiana.
72. Mitchell, B., DESIGN NOTES FOR THE DYNASORB ENERGY ABSORBER, LR 17201, Lockheed California, December 1963.

73. Blanchard, Ulysses J., LANDING CHARACTERISTICS OF A WINGED RE-ENTRY VEHICLE WITH ALL SKID LANDING GEAR HAVING YIELDING METAL SHOCK ABSORBERS, Langley Research Center; NASA TN-D-1496, National Aeronautics and Space Administration, Washington, D.C., December 1962.
74. McGehee, J.R., A PRELIMINARY EXPERIMENTAL INVESTIGATION OF AN ENERGY ABSORPTION PROCESS EMPLOYING FRANGIBLE METAL TUBING, Langley Research Center; NASA TN-D-1477, National Aeronautical and Space Administration, Washington, D.C., October 1962.
75. Fisher, Jr., L.J., LANDING IMPACT DISSIPATION SYSTEMS, Langley Research Center; NASA TN-D-975, National Aeronautics and Space Administration, Washington, D.C., December 1961.
76. Phillips, L.N., CARBON FIBER REINFORCED PLASTICS - AN INITIAL EVALUATION, RAE Technical Report 67088, Royal Aeronautical Establishment, England, 1957.
77. Mitchell, Bruce, SHOCK ABSORPTION WITH ONE-SHOT TUBES, LR 16869, Lockheed California, June 1953.
78. Readdy and Holman, RESISTANCE OF PLASTICS TO OUTDOOR WEATHERING, PA Technical Report 2102, Addendum 6, Picatinny Arsenal, Dover, New Jersey.
79. YAH-64 LANDING GEAR SPECIFICATION, Hughes Helicopters, Culver City, California PS 10-11014A, July 1974.
80. Kroell, C.K., A SIMPLE EFFICIENT ONE-SHOT ENERGY ABSORBER; General Motors Research Laboratory, Warren, Michigan, February 1962.

APPENDIX A

LANDING GEAR STRUCTURAL REQUIREMENTS

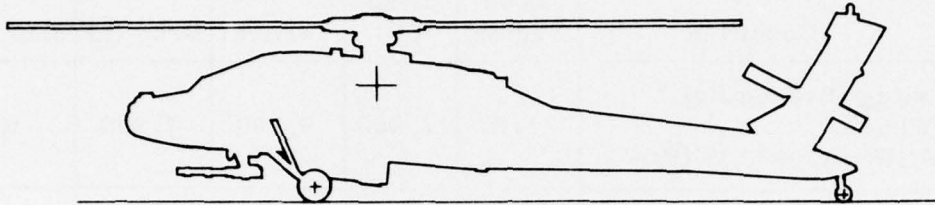


TABLE A-1. LANDING GEAR STRUCTURAL REQUIREMENTS

	Condition	Ground Load Factor	Total Ground Load (lb)	Load Per Main Wheel (lb)		
				Vertical	Drag (E)	Side (D)
1	3-Point Landing	3.0	41,850	21,305	0	0
1a	3-Point Landing With 25% Drag	3.0	41,850	22,080	5,520	0
2	Level 2-Wheel Landing	2.8	39,060	21,970	0	0
2a	Level 2-Wheel Landing With Drag	2.8	39,060	21,970	5,490	0
3 & 3a	One Main Wheel Landing With and Without Drag	-	-	Same as 2 and 2a respectively		
4	Tail Wheel First (A)	-	-	-	0	0
4a	Tail Wheel First With Obstruction (A)	-	-	-	0	0
5	Level 2-Wheel Landing With Obstruction	2.8	39,060	21,970	10,980 (B)	

TABLE A-1. LANDING GEAR STRUCTURAL REQUIREMENTS (CONT)

	Condition	Ground Load Factor	Total Ground Load (lb)	Load Per Main Wheel (lb)		
				Vertical	Drag (E)	Side (D)
6	Taxiing (Braked Roll) 2-Wheel; MAGW = 17,400 lb (F)	1.0	17,400	9,790	7,830	0
7	Taxiing, Reverse Braking, Static Oleo; MAGW = 17,400 lb (F)	1.0	17,400	7,930	-6,340 (C)	0
8	Crashworthiness Ultimate Failure Loads (G) (H) (K)	5.55 ULT	77,420	39,410	16,470 (B) (H)	

NOTES:

- (A) Condition 1 was used conservatively for vertical tail load since it was greater than the load obtained by using effective mass.
- (B) Load acts in any horizontal direction.
- (C) Positive drag load acts aft.
- (D) Apply side loads at ground.
- (E) Apply drag load at axle (with the exception of braking).
Apply drag brake load at the ground.
- (F) GW = 13,950 lb for all conditions except 6 and 7. For Conditions 6 and 7, GW = 17,400 (maximum alternate GW).
- (G) Ultimate loads for strength only (maximum impact loads not to exceed 90 percent of these values).
- (H) Vertical/drag load combinations will not produce a larger shock strut load than produced by a vertical wheel load at a ground load factor of 5.55.
- (K) Loads apply through entire stroke from fully extended to crash position. The relief valve located in the oleo is set to operate so that a maximum ground load factor of 5.00 is achieved. For the setting of this valve, the cg shall be assumed to be on the centerline of the aircraft.

APPENDIX B

LANDING GEAR SPECIFICATIONS

SPECIFICATIONS

Military

MIL-P-116E	Preservation, Method of
MIL-W-5013H	Wheel and Brake Assemblies, Aircraft
MIL-T-5041F	Tire, Pneumatic, Aircraft
MIL-W-5086	Wire, Electric, Hookup and Interconnecting Polyvinyl Chloride-Insulation, Nylon Jacket, Tin Coated Copper Conductor, 600 Volt, 150°C
MIL-B-5087B	Bonding, Electrical and Lightning Protection for Aerospace Systems
MIL-W-5088E	Wiring, Aircraft, Installation of
MIL-E-5400N	Electronic Equipment, Airborne, General Specification for
MIL-C-5503C	Cylinder, Aeronautical, Hydraulic Actuating, General Requirements for
MIL-H-5606C	Hydraulic Fluid, Petroleum Base; Aircraft, Missile, and Ordnance
MIL-E-6051D	Electromagnetic Compatibility Requirements Systems
MIL-E-7080B	Electrical Equipment, Aircraft, Selection and Installation of
MIL-I-8500C	Interchangeability and Replaceability of Component Parts for Aerospace Vehicles

MIL-L-8552C	Landing Gear, Aircraft, Shock Absorber (Air-Oil Type)
MIL-B-8584C	Brake Systems, Wheel Aircraft, Design of
MIL-P-8651B	Plates; Identification and Modification (for Aircraft), Installation of
MIL-S-8698	Structural Design Requirements, Helicopter
MIL-H-8775C	Hydraulic Systems Components, Aircraft and Missiles, General Specifications for
MIL-A-008862A	Airplane Strength and Rigidity, Landing and Ground Handling Loads
MIL-Q-9858A	Quality Program Requirements
MIL-W-16878D	Wire, Electrical, Insulated, High Tempera- ture
MIL-W-81044/4A	Wire, Electric Crosslinked Polyalkene Insulated Tin Coated Copper, Light Weight

STANDARDS

Military

MIL-STD-129E	Marking and Shipment for Storage
MIL-STD-130D	Identification Marking of U. S. Military Property
MIL-STD-143B	Standards and Specifications, Order of Pre- cedence for Selection of
MIL-STD-454C	Standard General Requirements for Electronic Equipment
MIL-STD-461A	Electromagnetic Interference Characteristics Requirements for Equipment, Subsystem and System

MIL-STD-704A	Electrical Power, Aircraft, Characteristics and Utilization of
MIL-STD-805	Towing Fittings and Provisions for Fixed Wing Aircraft Design, Requirements for
MIL-STD-809	Adapter, Aircraft, Jacking Point, Design and Installation of
MIL-STD-810B	Environmental Test Methods
MIL-STD-1367	Packaging, Handling, Store and Transportability Program Requirements for System and Equipment
MIL-STD-1290	Light Fixed and Rotary Wing Aircraft Crashworthiness
MIL-STD-1472A	Human Engineering Design Criteria for Military Systems, Equipment and Facilities

OTHER PUBLICATIONS

ADS-13	Material, Processes and Parts
AMCP 706-203	Engineering Design Handbook, Helicopters, Part III, Qualification Assurance
AR 70-38	Research, Development, Test and Evaluation of Material for Extreme Climatic Conditions
MIL-HDBK-5B	Metallic Materials and Elements for Aerospace Vehicle Structures
SC-5180-99-CL-A01	Tool Kit, Aircraft Mechanic's, General
TR 71-22, USAAMRDL	Crash Survival Design Guide

APPENDIX C

PROCESS SPECIFICATIONS

RESINS, EPOXY, FILAMENT WINDING, FOR STRUCTURAL APPLICATIONS

1. SCOPE

- 1.1 Scope. This specification covers the requirements for epoxy resins used in fabricating fiber based, structural composite parts by filament winding methods.
- 1.2 Classification. The resin shall be furnished in the following types and forms, as specified:
 - a. Type I. Liquid epoxy resin with a specified hardener, general purpose.
 - b. Type II. Modified liquid epoxy resin with a specified hardener, high impact strength.

2. APPLICABLE DOCUMENTS

- 2.1 The following documents form a part of this specification to the extent specified herein. In case of conflict between these documents and this specification, the requirements of this specification shall prevail. In case of conflict between the requirements of this specification and the requirements of applicable engineering drawings, the engineering drawing shall prevail.

Specifications

Federal

PPP-C-96 Cans, Metal, 28 Gage and Lighter

Military

MIL-H-5606 Hydraulic Fluid, Petroleum Base, Aircraft Missile and Ordnance

MIL-H-5624 Turbine Fuel, Aviation Grades JP-4 and JP-5

MIL-L-7808 Lubricating Oil, Aircraft Turbine Engine, Synthetic Base

MIL-C-9084 Cloth, Glass, Finished, for Polyester Resin Laminates

Standards

Federal

Fed Test Method
Std No. 406 (ASTM)

Plastic: Method of Testing

ASTM-D 785-65

Rockwell Hardness Measurement

ASTM-D 445-65

Kinematic Viscosity Measurement

Military

MIL-STD-129

Marking for Shipment and Storage by Attributes

Others

The Society of the
Plastics Industry, Inc.

Thermosetting Resin Formulators Division
(TRF)

3. REQUIREMENTS

3.1 Preproduction. The resin furnished under this specification shall be a product which has been subjected to and has passed the preproduction inspection specified herein and in Table I.

3.1.1 One-Year Weathering Data. As part of the qualification requirements, the supplier shall submit certified data to Materials, Processes and Standards Department of Hughes Helicopters, showing that a glass cloth based plastic laminate, fabricated as specified in 4.4.1 from the type of resin to be furnished under this specification, has been exposed to outdoor weathering in accordance with 4.5.5 for a period of one year and has subsequently met the requirements of Table II. The data shall identify the geographical location in which the outdoor weathering was accomplished.

3.2 Materials. The materials used in the manufacture of the resin shall be of high quality and as specified herein. Type I resin shall be an epoxy, thermosetting, low pressure laminating. Type II resin shall be a Carboxy Terminated Butadiene Acrylonitrile modification (CTBN) or equivalent of thermosetting epoxy resin. CTBN modification in the thermosetting epoxy resin shall be between 6 to 15 percent.

TABLE C-1. PHYSICAL AND REACTIVE PROPERTIES OF LIQUID RESINS/HARDENER SYSTEMS

Property	Requirements (Type I and Type II)	Fed-Std-406* Test Method
Viscosity in cps ($N5/m^2$) @ 75° ±5°F (24° ±3°C)	500 to 2000 (0.5 to 2)	TRF 1-74 ASTM-D 445- 65
Pot life - 1 lb (450 ±25 grams) of mixed resin with a specified hardener @ standard conditions - minimum	4 to 6 hours	TRF 13-74 Method A
Laminating life - 1 lb (450 ±25 grams) of mixed resin. Viscosity of resin mix to reach 5,000 to 10,000 (5 to $10 N5/m^2$)		
@ 30° to 40°F (0° to 5°C)	2 weeks	
@ 40° to 60°F (5° to 15°C)	1 week	
@ 60° to 90°F (15° to 32°C)	48 hours	
Wetting characteristics	Wets glass cloth or fiber to render it transparent	Visual
Gel time		
@ 150°F ±10°F (65° ±6°C) (No thermal stress)	1 to 2 hours	TRF 2-74
Gel time		
@ Ambient conditions, minimum	72 hours	TRF 2-74
Cure time		Manufacturer supplied information
@ 150° ±10°F (65° ±6°C)	4 to 6 hours	
@ 250° ±10°F (121° ±6°C)	4 to 6 hours	
@ 300° ±10°F (149° ±6°C)	2 to 3 hours	
Post cure @ 350-400°F (177 to 205°C)	4 hours to achieve maximum heat distortion and mechanical properties	
Physical Properties of Cured Resin With Appropriate Hardeners		
Tensile strength, psi (MPa), min	12,000 (83)	Fed-Std Method No. 1011
Flexural modulus, psi x 10 ⁶ , (MPa) min	0.5 (3447)	Fed-Std Method No. 1031
Elongation, %	2% (Type I) , 5% (Type II)	
Barcol hardness/shore D hardness	70 minimum/70	ASTM-D 785-65
Heat distortion temp	200°F minimum (90°C)	TRF 17-74

*Except as noted

TABLE C-2. MECHANICAL AND PHYSICAL PROPERTIES OF
GLASS CLOTH BASE LAMINATES - WET LAYUP

Property	Requirements (Type I and Type II)	Test Method Fed-Std Method No. 406 (Except As Noted)
Barcol hardness, min/shore D hardness	70/	ASTM-D 785-65
Tensile strength, min, psi and tensile modulus x 10 ⁶ , psi, min. (MPa)	48,000 (331) 3.2 (22064)	1011
Flexural strength, dry, min, psi (MPa)	75,000 (517)	1031
Flexural modulus of elasticity, min, 10 ⁶ , psi, (MPa)	3.2 (22064)	1031
Water absorption, 24 hours, immersion, % change in weight, tested wet (see 4.5.2)	0.5 max	7031
Flexural strength, wet, min, psi (MPa) (4.5.2)	65,000 (448)	1031
Flexural modulus, wet, min, 10 ⁶ , psi (Mpa) (4.5.2)	3.2 (22064)	1031
Tensile strength and tensile modulus x 10 ⁶ , min, psi (Mpa) wet (4.5.2)	45,000 and 3.0 (310 and 20685)	1011
Treated After Immersion in Chemical Fluids (See 4.5.4)		
MIL-H-5606 hydraulic fluid		
MIL-L-7808 lubricating fluid		
MIL-H-5624 jet fuels		
Percent change in weight (increase or decrease) after immersion in above fluids	0.2 max	7011
Flexural strength, min, psi, after immersion in above fluids	10% change max	1031
Tested at 160° ±5°F (71° ±3°C) After Exposure to 160° ±5°F (71° ±3°C) for 24 Hours (4.5.3)		
Flexural and tensile properties	10% max change from the original	1011 and 1031
Tested after 1 year of outdoor weathering (see 4.5.5). No more than 10% change mechanical and physical properties after 1 year outdoor weathering.		

- 3.2.1 Hardener. Type I and II resins shall be formulated with appropriate hardeners to achieve the maximum properties specified in Table I and Table II.
- 3.2.2 Mechanical and Physical Properties of the Laminate. For both Type I and Type II resins, the mechanical and physical properties of a glass cloth based plastic laminate, fabricated as specified in 4.4.1, shall conform to the requirements listed in Table II.
4. QUALITY ASSURANCE PROVISIONS
- 4.1 Responsibility for Inspection. Unless otherwise specified in the contract or purchase order, the supplier is responsible for the performance of all inspection requirements as specified herein. Except as otherwise specified, the supplier may utilize his own facilities or any commercial laboratory acceptable to the MP&S Department of Hughes Helicopters. HH reserves the right to perform any of the inspections set forth in the specification where such inspections are deemed necessary to assure supplies and services conform to prescribed requirements.
- 4.2 Classification of Tests. The tests performed under this specification shall be of the following classifications:
- a. Qualifications Tests
 - b. Acceptance Tests
- 4.2.1 Qualification Tests. The qualification tests shall consist of all the requirements of this specification.
- 4.2.2 Acceptance Tests. The acceptance tests are performed to assure the conformance of the material to the specification requirements and shall consist of the following tests:
- a. Viscosity
 - b. Pot life
 - c. Gel time and peak exotherm
 - d. Barcol hardness /shore hardness on neat resin
- 4.3 Sampling for Quality Conformance Inspection
- 4.3.1 Lot. A lot shall consist of all the resin of one code number manufactured in one continuous operation and subjected to all inspection at one time.

- 4.3.2 One gallon of liquid resin with appropriate hardener for each type shall be selected at random from each lot. An approved instruction sheet, preferably adherent to the container, with the following information shall be provided with all products.
- a. Type of resin and number of HH material specification
 - b. Mixing ratio of resin and hardener
 - c. Maximum usable storage life of the unactivated and activated resin and recommended storage conditions
- 4.4 Laminate Preparation for Mechanical Properties - Wet Lay Up
- 4.4.1 The laminate sample for mechanical and physical properties test shall be fabricated in the form of a sheet or sheets 0.125 \pm 0.010 inch in thickness, using the resin which is under test and 12 plies, laid up parallel, of 181 glass cloth conforming to MIL-C-9084 with a finish compatible with the resin being tested. The 181 glass fabric shall be impregnated by wet lay up with 40 \pm 5 percent test resin by weight. The sample shall be laminated at 30 to 50 psi pressure and shall be fully cured in accordance with the resin supplier's instruction sheet. The sample shall represent best quality workmanship and shall be tested to determine conformance to the mechanical and physical requirements of Table II.
- 4.4.2 Rejection Criteria. If any sample of liquid resin or laminated sample to represent the liquid resin fails to conform completely with the requirements of this specification, the lot of resin represented by the sample shall be rejected.
- 4.5 Test Conditions
- 4.5.1 Standard Conditions. Liquid resin and laminate samples shall be conditioned and tested at an air temperature of 75° \pm 5° F (24° \pm 3° C) and relative humidity of 40-60 percent. The conditioning period prior to test shall be 24 hours minimum.
- 4.5.2 Wet Conditions (for Mechanical and Physical Tests). Specimens shall be immersed for 18 to 24 hours in boiling distilled water by Procedure E of Method No. 7031, Fed Test Method Std No. 406. Specimens shall then be cooled in water at 75° \pm 5° F (24° \pm 3° C) and tested wet at that temperature immediately after removal from the water. In case of any question as to validity of the test results, specimens shall be soaked for 30 days in distilled water at 75° \pm 5° F and tested wet at that temperature immediately after removal from the water. Results obtained under the later conditioning shall be final.

- 4.5.3 Exposure to 160° ±5°F. Specimens shall be exposed for one-half hour to a temperature of 160° ±5°F (71° ±3°C) in a previously heated test chamber and shall then be tested immediately at the same temperature.
- 4.5.4 Immersion in Chemical Fluids. Specimens shall be immersed in chemical fluids specified in Table II. A separate set of specimens shall be used for each fluid. The immersion procedure shall be in accordance with Method 7011 of Fed Test Method Std No. 406, except that the immersion time shall be 24 hours at 75° ±5°F (24° ±3°C). The specimens shall be removed from the fluids at the close of exposure period and tested immediately.
- 4.5.5 One-Year Outdoor Weathering (for Supplier's Certified Test Data 3.1.1). The laminate shall be exposed to outdoor weathering for one year in the north temperature or south temperature zone on a land rack inclined 45 degrees to the horizontal, facing the equator. The laminate shall be turned over every 14 to 16 days. At the end of the weathering period, specimens shall be cut from the laminate, subjected to standard conditions for 96 hours and tested at standard conditions.
- 4.6 Test Methods
- 4.6.1 Viscosity. Viscosity of the mixed liquid epoxy resin shall be run with a Brookfield viscometer in accordance with TRF 1-74. For more precise viscosity measurement, Kinematic procedure of ASTM-D 445-65 may be followed.
- 4.6.2 Pot Life. Pot life of the mixed epoxy resin is defined as the time to double the original viscosity and is measured by Method A of TRF 13-74.
- 4.6.3 Laminate Life. Laminate life of the mixed epoxy resin is defined as time to reach the viscosity of 5,000 to 10,000 cps (5 to 10 NS/m²) and is measured by Method A of TRF 13-74.
- 4.6.4 Wetting Characteristics. This is a visual method. The glass fiber of MIL-C-9084 is wetted thoroughly by standard shop methods with the mixed resin system in test. The glass fiber will appear to be transparent when impregnated with the resin. Wetting characteristics of the resin partly depends on the type of finish used on the glass fiber.
- 4.6.5 Gel Time and Peak Exotherm. Gel time of the mixed resin is measured at 150° ±10°F (65° ±6°C) and also at ambient conditions in accordance with TRF 2-74.
- 4.6.6 Hardness for Cured Epoxy Compound. Hardness for cured epoxy compound is measured by Rockwell type hardness tester in accordance with ASTM-D 785-65 or by Barber-Coleman (Barcol) impression tester by direct reading.

- 4.6.7 Mechanical and Physical Properties of the Laminate. The mechanical and physical properties of the laminate shall be determined in accordance with the methods of Table II, using specimens prepared from the 0.125 inch thick laminate samples of 4.4.1.
- 4.7 Records
 - 4.7.1 Records pertinent to the testing of the product shall be maintained by the supplier for a minimum of 3 years. These records shall be made available to HH upon request.
- 5. PREPARATION FOR DELIVERY
 - 5.1 Liquid Resin and Hardener. The resin and the appropriate hardner shall be packaged as specified in the procurement documents, in 1, 5, or 55 gallon cans conforming to Type V, Class 2, of PPP-C-96. Cans in accordance with PPP-C-96 shall be rust resistant coated on the exterior in accordance with Plan B of that specification and the side seam shall be striped with a suitable corrosion resistant coating.
 - 5.2 Marking for Shipment
 - 5.2.1 In addition to any special marking required by contract or procuring documents, interior packages and exterior shipping containers shall be marked in accordance with MIL-STD-129. The nomenclature shall include:

RESIN, EPOXY, FILAMENT WINDING FOR
STRUCTURAL APPLICATIONS

Hughes Helicopters Material Specification No. HMS 16-1115 Type _____
 Manufacturer's Code No. Resin: _____ Hardener _____
 Hughes Helicopters Purchase Order No. _____
 Manufacturer _____
 Batch No.: _____ Date of Manufacture _____
 Shelf Life Expiration Date _____
 Warning _____ Hazardous Chemicals _____

- 6. APPROVED PRODUCT AND VENDOR
 - 6.1 Products acceptable under this specification are listed in Hughes Approved Vendors List 1115.

FILAMENT WOUND LANDING GEAR STRUT

1. APPLICATION

This specification defines materials and processes for fabrication of an advanced composite landing gear arm.

2. APPLICABLE DOCUMENTS

- 2.1 Arm assembly - main landing gear, Hughes Helicopter (HH) Drawing 416-100, Revision N.C.
- 2.2 Fiber Science drawing number 662-001. Winding Mandrel-Landing Gear.
- 2.3 Hughes Helicopters fabrication of composite parts by filament winding method HP-15-53.
- 2.4 Hughes Helicopters fabrication of reinforced plastics HP-15-42.

3. PROCESS MATERIALS

- 3.1 Thornel 300 (Grade WYP 15 1/0 6000 filament) graphite roving/ epoxy. Fiber ratio = 0.50 by volume (0.607 by weight).
- 3.2 Miller E-glass fibers mixed with APCO 2434/2340 epoxy resin/ hardener system. Fiber ratio = 0.50 by weight.
- 3.3 Syntactic Foam - Kurea A-200 carbon microballoons mixed with APCO 2434/2347 resin system. Mixing ratio to be 20 percent by weight (20 parts microballoons, 80 parts resin).
- 3.4 APCO 2434/2347 resin system, 7.5 ± 0.5 parts hardener per hundred parts of resin by weight (phr).
- 3.5 APCO 2434/2340 resin system, 27 ± 1.0 parts hardener per hundred parts of resin by weight (phr).
- 3.6 Honeycomb core, HRH-10-3/16-6# (1/2-inch thick) AMS-3711. (Heatformed)
- 3.7 Mold release, "Part-All #10", Rexco. Polyvinyl alcohol (PVA emulsion or equivalent).

- 3.8 Mold wax "Mirror Glaze" or equivalent.
- 3.9 Mold release mixture, "Plastilease 334" and "Ram 225", Ram Chemical Company.
- 3.10 HRH 10/0X-3/16-3# (1/2-inch thick) nomex. (Flexible)
- 3.11 Carbon microballon Kurea A-200.
- 3.12 Shop aid materials.
- 4. PURCHASED PARTS
 (None)
- 5. TOOLING
- 5.1 503-152 Mandrel, Spar Cap.
- 5.2 662-101 Winding Mandrel, Strut per Loft Line SK 12376.
- 5.3 503-156 Doubler Templates.
- 5.4 503-106 Resin Applicator.
- 5.5 503-165 Resin Impregnator.
- 5.6 503-167 Resin Squeeze Roll Assembly.
- 5.7 503-171 Longo Resin Bath.
- 6. STRUT MANDREL PREPARATION
- 6.1 Apply Mirror Glaze mold wax and buff.
- 6.2 Apply Ram 225/Plastilease 334 very slightly (blend equal parts by weight).
- 6.3 Spray mold with PVA and cure at room temperature until tack free.
- 6.4 Establish tooling points on mandrel per Drawing 662-101. Drill hole through plaster and metal tube of mandrel and emplace 1/8-inch diameter dowel pins at boss centers.

- 6.5 Establish reference station on large end of mandrel 30 inches from large end template. Make permanent mark on mandrel shaft.
7. HONEYCOMB CORE PREPARATION
- 7.1 Trim pieces on mandrel to fit strut mandrel per HH Drawing 416-100.
- 7.2 Using (3.10) Nomex honeycomb 1/2-inch thick, cut 3-inch wedge sections to provide taper at end of honeycomb per HH Drawing 416-100.
8. BROOM LONGO FABRICATION (8 required)
- 8.1 Mount broom longo fixture with release film in space groove area.
- 8.2 Weigh 40-foot lengths of dry filament and wet filament before beginning to wind part. Dry filament weight to wet filament weight ratio must be 0.607 ± 0.03 .
- 8.3 Wind the broom from graphite WYP 15-1/0 and APCO 2434/2347 resin. Maximum winding tension should be less than 10 pounds per band.
- 8.4 Wind with Thornel 300/epoxy (3.1) to fill the spaced groove on fixture.
- 8.5 Remove broom with release film from fixture.
- 8.6 Store in cold box per (10.7).
9. DOUBLER FABRICATION
- 9.1 Weigh 40-foot lengths of dry filament and wet filament before beginning to wind part. Dry filament to wet filament weight ratio should be 0.607 ± 0.03 .
- 9.2 Set up the skin winding mandrel (503-150) in winding machine #150-136. Tape on 1/4-inch thick x 1-inch wide wooden strips butted together at the trim line at both the top and bottom of mandrel. Wrap the mandrel with yellow backing film.
- 9.3 Wind according to the table below with Thornel 300 WYP 15 and APCO 2434/2347 resin.

No. Rovings	Winding Angle*	No. Circuits Per Pattern	No. Circuits Per Layer	Bandwidth** (Inches)	No. Layers	Length
15	±45°	5	70	0.63	1	Full Length
15	±75°	4	28	0.63	1	*** 96-Inch Part Length

*Tolerance = ±2°

**Tolerance = ±0.05 inches

***Separate from 45° winding with release film.

9.4 Remove winding from mandrel and trim as required (see below).

12 pieces ±45° Doublers - Per Template

8 pieces ±15° Doublers - Per Template

4 pieces ±15° Test Coupons - 5-inch x 8-inch rectangle

9.5 This part may be stored up to 48 hours at room temperature.

10. WINDING/LAYUP ASSEMBLY

10.1 For assembly record, Polaroid pictures should be made at appropriate assembly steps.

10.2 Prefabricated parts should be on hand.

10.3 Using spacers to represent the inner skin thickness, locate honeycomb on strut mandrel and final trim per HH Drawing 416-100.

10.4 Proceed through the winding/layup steps as per chart (Ref: HH 416-100) using Thornel 300 WYP 15 1/0, 15 rovings* at 0.63-inch BW allowing no gapping between bands at large end of mandrel.

NOTE: A single roving open hoop winding should be used to hold parts to mandrel during assembly.

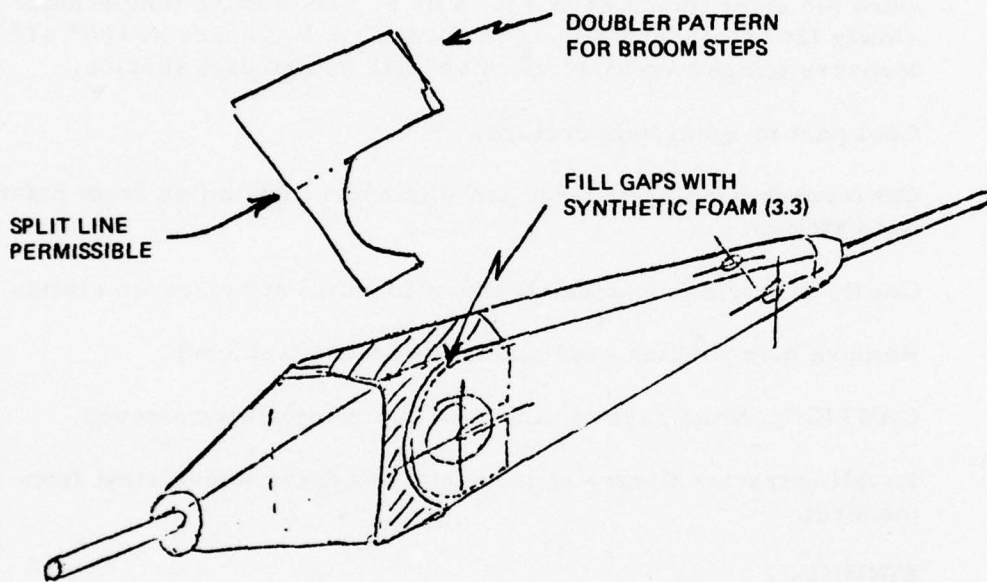
*Except steps 2 and 24 (see chart).

WINDING/LAYUP STEP CHART									
SEQUENCE	WINDING		REINFORCEMENT LAYUP				REMARKS		
	ANGLE	STATION	LARGE END BOSS	STATION	SMALL END BOSS	STATION			
			LAYER	STATION	ANGLE	LAYER	STATION		
1	90°	30-55						A	
2	90°	81.14-103						A	
3	90°	30-103	1	30-54	15°	1	82.14-103	A	
4	90°	30-53						A	
5	15°	Full length						A	
6			1 Broom	CL-52	15°	1	82.64-103.5	A	
7	90°	83.14-103	3	28-52				A	
8	45°	Full length						A	
9	90°	83.64-103	1 Broom	CL-51				A	
10			2	27-51	15°	1	84.14-105	A	
11	15°	Full length						A	
12								A	
13	90°	85.14-103	--- Add Honeycomb	---	15°	1	84.64-105.5	A/A/C/L	
14								A	
15	15°	Full length						A	
16								A	
17	90°	83.64-103	1 Broom	CL-51				A	
18	45°	Full length	2	27-51				A	
19	90°	83.14-103						A	
20			1 Broom	CL-52				A	
21	15°	Full length	3	28-52	15°	1	82.64-103.5	A	
22	90°	30-53						A	
23								A	
24	90°	30-103	1	30-54	15°	1	82.14-103	A	
								A	
25	90°	81.14-103						A	

This layer only -- 10 rovings at 0.8" BW.
 Stagger the circumferential butt joints of doublers (small end only) by 90°.

See Sketch "A".

Bond 4 quadrants of honeycomb using Hardman adhesive. Fill open cells of wedge honeycomb and any gaps with syntactic foam Para. 3.3a.
 2 Piles.



SKETCH A

- 10.5 After completion of winding steps above, wrap nylon peel ply over part and apply vacuum bag. Draw 20-inch HG vacuum over part.
- 10.6 Add thermocouples at small end of strut (beyond E. O. P.) approximately station 103 to 105. One on surface of mold and one in center of windings.
11. CURING/MANDREL REMOVAL
- 11.1 Place strut mandrel with wound assembly and test coupons* in oven. Cure for eight (8) hours at $130^{\circ} \pm 10^{\circ}\text{F}$. Then raise temperature slowly (20° to 25°F per hour) and cure for two hours at $180^{\circ} \pm 10^{\circ}\text{F}$. Measure temperatures at thermocouple on mandrel surface.
- 11.2 Cool part to room temperature.
- 11.3 Cut through winding at large end of mandrel 29-inches from reference station.
- 11.4 Cut through winding at small end of mandrel at reference station 103.
- 11.5 Remove both winding ends and tooling pins (6 places).
- CAUTION: Make sure tooling pins are completely removed.
- 11.6 Install extractor fixture at large end and drive wound strut from mandrel.
12. FINISHING
- 12.1 Remove peel ply from outside of strut.
- 12.2 Clean inside and outside strut surfaces with hot water to remove mold release.
- 12.3 Build up bosses centered on tooling pins, both inside and outside surface per dimensions on Drawing HH 416-100. Use (3.2) milled fiber/epoxy for boss material (room temperature set).

*Vacuum to flat plate.

- 12.4 Trim ends per HH 416-100 drawing dimensions*. Laminate end caps of two ply style 1581 glass cloth with 3.5 resin. Vacuum bag for curing. Use thermocouple located in part.
- 12.5 Perform final cure in oven for two hours at $130^{\circ} \pm 10^{\circ}\text{F}$ in horizontal position. Then raise oven temperature to $180^{\circ} \pm 10^{\circ}\text{F}$ for two hours. Then cure at $250^{\circ} \pm 10^{\circ}\text{F}$ for two hours.
- 12.6 Cool to room temperature. Remove all shop aids.
13. FINAL INSPECTION
- 13.1 Inspect strut dimensionally for conformance to Drawing HH 416-100 excluding machine surfaces and metal parts.
- 13.2 Measure and record Barcol hardness on a minimum of three locations on part. Hardness to be 55 minimum.
- 13.3 Weigh and record the strut weight.
- 13.4 Deliver material samples and test coupons with strut.

*Save cut ends for material samples (13.4) and post cure with strut.

APPENDIX D

TRAILING ARM STRESS ANALYSIS

DESIGN CALCULATIONS

This section of the report contains a summary of the structural analysis used to substantiate the design of the fabricated composite trailing arm.

The landing gear strut and trailing arm loads and reactions are shown in Figure D-1. The magnitude of the critical design loads and reactions are given in Table D-1. The test loads at which the trailing arm failed in static test are also given for comparison purposes.

BASIC ARM ANALYSIS

The critical section for the arm is located in Figure D-1, 14 inches below the cross tube pivot. The cross section is similar to Figure 36 and has the following properties:

$$\text{Cross Sectional Area, } A = 9.14 \text{ in.}^2$$

$$\text{Moment of Inertia, } I_{xx} = 129.1 \text{ in.}^4$$

$$\text{Distance from Neutral Axis, } c = 5.2 \text{ in.}$$

The compressive stress, $f_c = M_X C / I - P_A / A$, where M_X = lateral moment and P_A = axial load from Table 10.

$$f_c = \frac{892,000 \times 5.2}{129.1} - \frac{37,770}{9.14} = 29,000 \text{ psi}$$

The computed allowable stress = 30,300 psi

$$\therefore \text{Margin of Safety} = M_S = \frac{30,300}{29,000} - 1 = 0.04$$

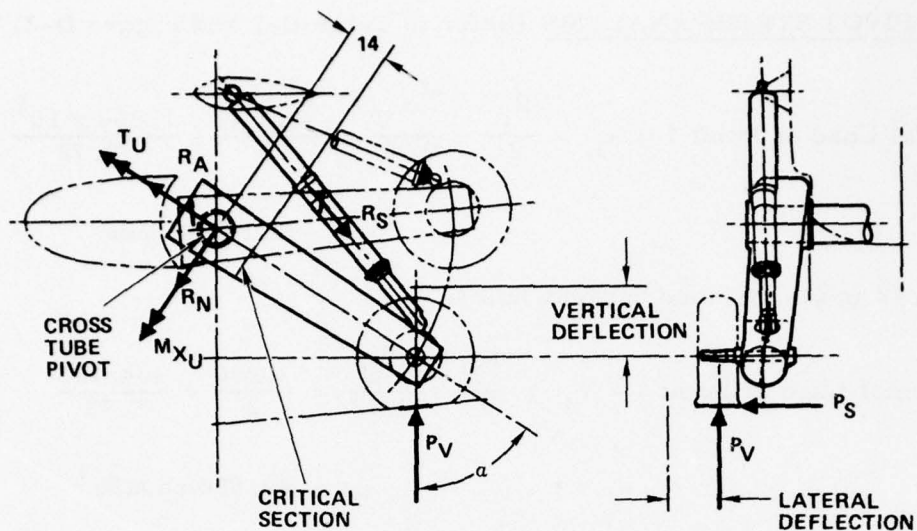


Figure D-1. Gear Loading.

TABLE D-1. TEST AND DESIGN LOADS			
Item		Test	Design Ultimate
α Arm Angle	- deg	45.36	40.60
Vertical load (P_V)	- lb	45,100	39,070
Lateral load (P_S)	- lb	23,100	16,480
Shock strut load (R_S)	- lb	90,270	71,520*
Axial arm load (R_A)	- lb	55,940	39,770
Normal arm load (R_N)	- lb	10,440	8,270
Arm lateral moment (M_{XU})	- in. -lb	1.398×10^6	1.069×10^6
Arm torque (T_U)	- in. -lb	575,700	444,700

*The maximum design ultimate load is 104,500 pounds for a two-point landing condition with drag load.

UPPER PIVOT STRESS ANALYSIS (Refer to Table D-1 and Figure D-2)

$$\begin{aligned} \text{Axial Load at Point 1} = H_1 &= \frac{R_A}{2} - \frac{M_{XU}}{9.72} = \frac{39,770}{2} - \frac{1.069 \times 10^6}{9.72} \\ &= -90,100 \text{ pounds} \end{aligned}$$

where 9.72 is the distance between holes.

$$\begin{aligned} \text{Normal Load at Point 1} = V_1 &= \frac{R_N}{2} + \frac{T_U}{9.72} = \frac{8,270}{2} + \frac{444,700}{9.72} \\ &= 49,900 \text{ pounds} \end{aligned}$$

Similarly:

$$\text{Axial Load at Point 2} = H_2 = 19,900 + 110,000 = 129,900 \text{ pounds}$$

$$\text{Normal Load at Point 2} = V_2 = 4,100 - 45,800 = -41,600 \text{ pounds}$$

Maximum bearing load is at Point 2:

$$P_{BR} = [H_2^2 + V_2^2]^{1/2}$$

$$P_{BR} = [(129,900)^2 + (-41,600)^2]^{1/2} = 136,400 \text{ pounds}$$

$$\text{The Bearing Stress} = \frac{P_{BR}}{Dt} = \frac{136,400}{8.27 \times 0.705} = 23,400 \text{ psi}$$

where D is the diameter of the hole and t is the thickness of the graphite.

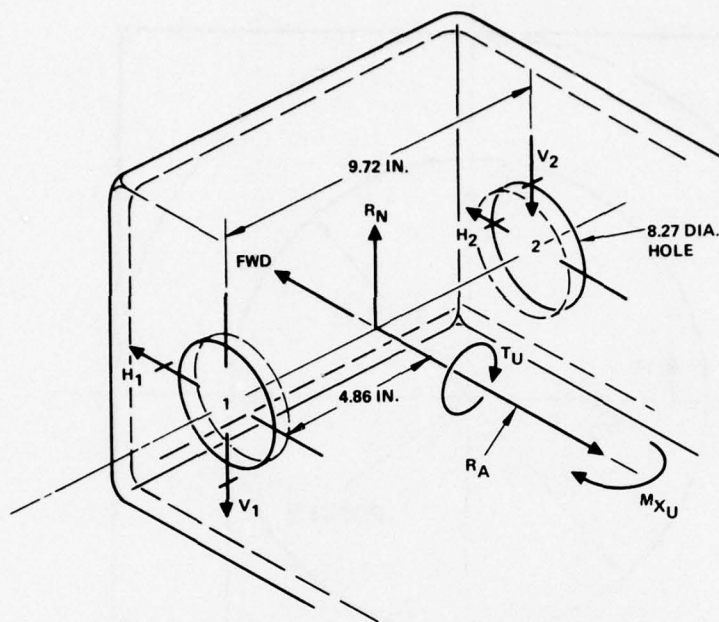


Figure D-2. Upper Pivot Loads and Reactions.

The margin of safety for bearing in the graphite is high when compared to an estimated bearing stress allowable of 85,000 psi (Reference D1).

PIVOT LUG ANALYSIS

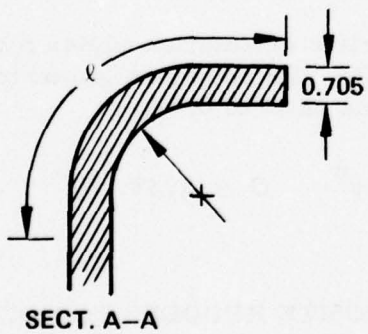
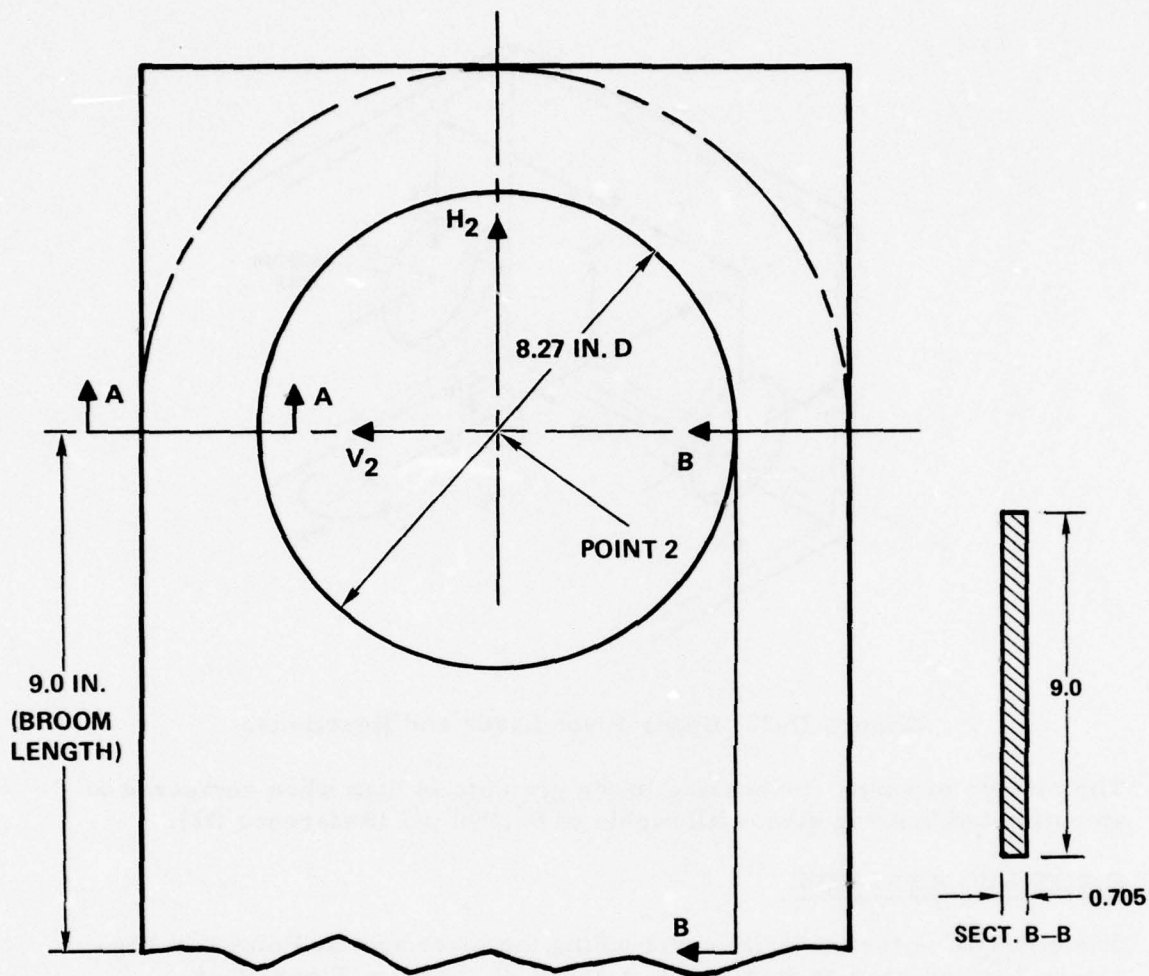
The strength of the material surrounding the pivot hole at Point 2 in Figure D-2 is analyzed at Sections A-A and B-B shown in Figure D-3.

Stress Analysis at Section A-A

The individual fiber properties at their respective orientation angles for a fiber volume ratio of 0.5 is found in Table D-2. The combined laminate properties for Section A-A using a fiber volume ratio of 0.5 are:

$$EX = 11.0 + 10^6 \quad EY = 5.05 \pm 10^6 \quad G = 1.45 + 10^6$$

D1 Techman, G.M., et al, ADVANCED COMPOSITE RUDDERS FOR DC-10 AIRCRAFT DESIGN, MANUFACTURING, AND GROUND TESTS, McDonald Douglas, Long Beach, California, NASA DR-145068.



l = assumed effective length of corner = 3.6 in.

The material fiber orientation and percent of total is:

0° (41.9), 90° (20.9),

±15° (18.6), ±45° (18.6)

Figure D-3. Pivot Hole.

TABLE D-2. FIBER PROPERTIES AT THEIR RESPECTIVE ORIENTATION ANGLES FOR A FIBER VOLUME RATIO OF 0.5

Fiber Angle	A Area in. ²	EX 10 ⁶ psi
0°	1.063	17.25
90°	0.530	0.90
±15°	0.472	13.79
±45°	0.472	1.93
Total	2.537	

where EX and EY are Young's moduli at 0-degree and 90-degree azimuth, respectively. G is the shear modulus. The laminate axial stiffness at Section A-A is AEX and is equal to

$$2.537 \times 11.0 \times 10^6 = 27.91 \times 10^6 \text{ pounds}$$

The maximum tension load = $H_2/2 + C_1 V_2$, where H_2 and V_2 are previously determined loads for Point 2 and C_1 is the coefficient to determine the tension load induced on Section A-A due to load V_2 (Reference D2, Table VIII, Case 27)

$$\therefore \text{Tension Load} = \frac{129,900}{2} + 0.318 (41,600) = 78,180 \text{ pounds}$$

$$\text{Gross Ultimate Stress} = \frac{78,180}{2.537} = 30,816 \text{ psi}$$

Maximum stress occurs in the 0-degree fibers;

$$f = \frac{78,180 (17.25 \times 10^6)}{27.91 \times 10^6} = 48,320 \text{ psi}$$

^{D2} Roark, R. J., FORMULAS FOR STRESS AND STRAIN, Second Edition, 1943.

Unnotched tension allowable of Thornel 300 graphite fibers at 0 degree with an epoxy matrix is equal to 162,500 psi.

∴ The lug notch factor would have to exceed $(162,500/48,320) = 3.36$ for failure.

The arm was acceptable structurally since the 3.36 allowable notch factor was judged adequate. Subsequent static testing substantiated this analysis.

Stress Analysis at Section B-B

The approximate shear load (P_{SB}) on Section B-B necessary to obtain a uniform strain in the side of the arm at 9 inches below the pivot with D the pivot hole diameter

$$P_{SB} \cong \left(\frac{H_2}{2}\right) \left(\frac{D}{D+2l}\right) \cong \left(\frac{129,900}{2}\right) \left(\frac{8.27}{8.27+2 \times 3.6}\right)$$
$$= 34,720 \text{ pounds}$$

$$\text{Shear Stress, } f_s = \frac{P_{SB}}{A} = \frac{34,720}{9.0 \times 0.705} = 5,470 \text{ psi}$$

where A is the area at Section B-B.

The allowable shear stress $\geq 15,000$ psi.

$$\text{The Margin of Safety, } M_S = \frac{15,000}{5,470} - 1 = 1.74$$

Design of lug is structurally acceptable.

ATTACHMENT OF AXLE TO TRAILING ARM ANALYSIS

Figure D-4 shows the vertical load P_V and the side load P_S both applied to the wheel. The magnitude of the applied loads and the resultant loads at the trailing arm axle are as follows:

$$\text{Vertical Load, } P_V = 39,070 \text{ pounds}$$

$$\text{Side Load, } P_S = 16,480 \text{ pounds}$$

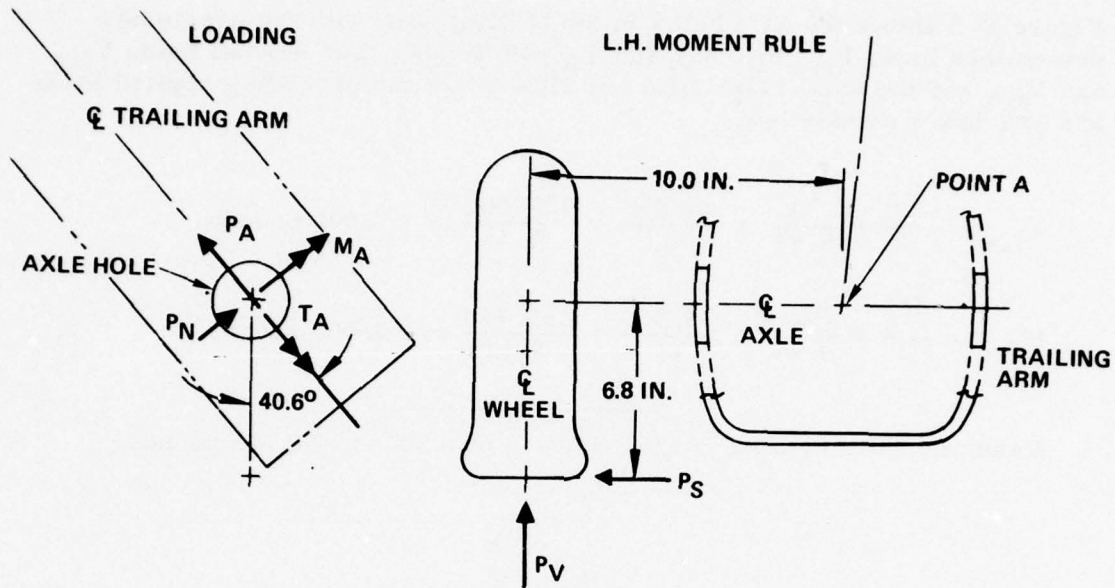


Figure D-4. Axle Loading.

$$\text{Axial Load, } P_A = 39,070 \cos 40.6 = 29,660 \text{ pounds}$$

$$\text{Normal Load, } P_N = 39,070 \sin 40.6 = 25,430 \text{ pounds}$$

$$\begin{aligned} \text{Lateral Moment, } M_A &= (39,070 \times 10 + 16,480 \times 6.8) \cos 40.6 \\ &= 381,734 \text{ inch-pounds} \end{aligned}$$

$$\text{Torque, } T_A = 502,764 \sin 40.6 \approx 327,185 \text{ inch-pounds}$$

Figure D-5 shows the axle holes in the trailing arm with the previously determined loads P_A , P_N , M_A and T_A positioned. The normal loads V_{LA} and V_{RA} and the axial loads H_{LA} and H_{RA} react the preceding applied loads and are determined below.

$$V_{LA} = \frac{P_N}{2} + \frac{T_A}{8.44} = \frac{25,430}{2} + \frac{327,200}{8.44} = 51,500 \text{ pounds}$$

$$H_{LA} = \frac{P_A}{2} + \frac{M_A}{8.44} = \frac{29,660}{2} + \frac{381,700}{8.44} = 60,000 \text{ pounds}$$

$$\text{Resultant bearing load} = \sqrt{51,500^2 + 60,000^2} = 79,100 \text{ pounds}$$

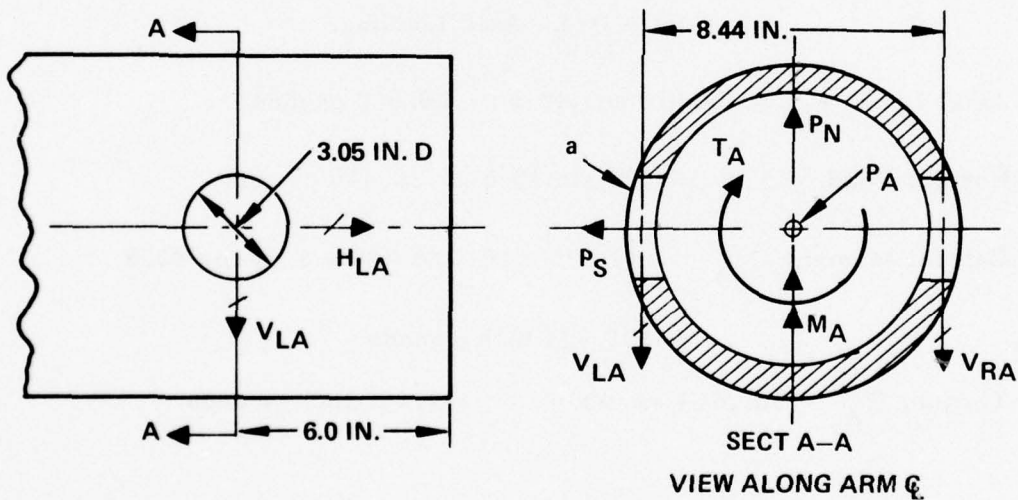


Figure D-5. Axle Hole.

The composite material thickness of the trailing arm is 0.783 inch. The material fiber orientation and percent of total thickness is

$$\pm 15^\circ (56.9), \pm 45^\circ (11.6), \text{ and } 90^\circ (31.5)$$

Composite properties are

$$EX = 9.36 \times 10^6 \quad EY = 6.51 \times 10^6 \quad G = 1.55 \times 10^6$$

The net section properties of arm at axle centerline are

$$\text{Cross Section Area} = 18.20 \text{ in.}^2$$

$$\text{Moment of Inertia, } I_{xx} = 146.3 \text{ in.}^4$$

$$\text{Effective Torque Area } (A_T) = 54.4 \text{ in.}^2$$

The distance from the x-x axis to point a in Figure D-5 is 4.5 inches.

The compressive and shear stresses at point a are

$$\text{Compressive stress, } f_c = \frac{29,660}{18.20} + \frac{381,734 \times 4.5}{146.3} = 13,371 \text{ psi}$$

$$\text{Shear stress, } f_{st} \cong \frac{327,185}{2 \times 54.4 \times 0.783} = 3,840 \text{ psi}$$

The estimated allowable compressive stress is 66,000 psi and shear stress is 25,000 psi.

∴ The margin of safety is high making the axle attachment structurally acceptable

ATTACHMENT OF STRUT TO TRAILING ARM

Figure D-6 shows the shock strut attachment to the trailing arm. As shown, it is located above the axle holes. The bearing stress in the strut attachment hole will be determined using the shock strut load R_S from Table D-1 as the applied load. R_U and R_L are reactive loads and are determined below. D is the diameter of the strut hole and t is the thickness of the graphite arm at the shock strut location.

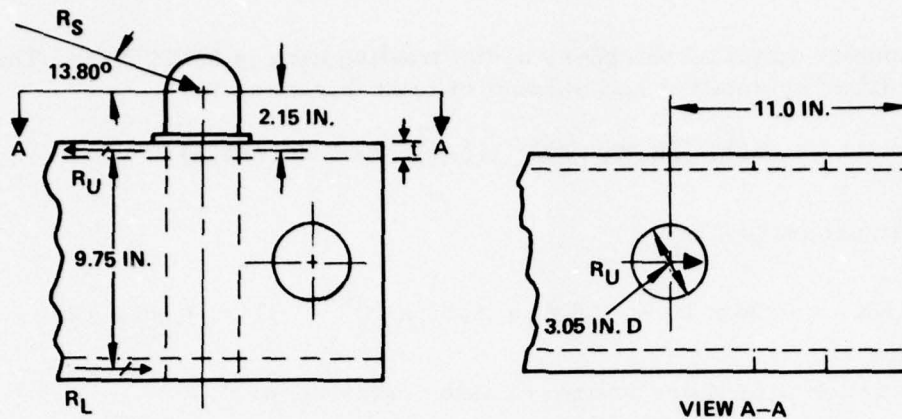


Figure D-6. Shock Strut Attachment.

$$R_S = 104,500 \text{ pounds}$$

Upper Reaction

$$R_U = \frac{(104,500 \cos 13.80^\circ) 11.90}{9.75} = 123,862 \text{ pounds}$$

Lower Reaction

$$R_L = 123,862 - 101,483 = 22,379 \text{ pounds}$$

$$\text{Bearing stress, } f_{br} = \frac{R_U}{Dt} = \frac{123,862}{3.05 \times 0.783} = 51,865 \text{ psi}$$

where D is hole dia and t is wall thickness

Estimated allowable bearing stress $\geq 85,000$ psi (Reference D1)

$$\text{Margin of safety} = \frac{85,000}{51,865} - 1 = 0.64$$

$$\begin{aligned} \text{Shearout stress, } f_{so} &\cong \frac{R_U}{2(11.0 - 0.5D)t} \\ &= \frac{123,862}{2(11.0 - 0.5 \times 3.05) 0.783} = 8348 \text{ psi} \\ &\quad \text{(conservative)} \end{aligned}$$

Estimated allowable shear stress = 25,000 psi.

$$\text{Margin of safety} = \frac{25,000}{8348} - 1 = 1.99$$

The shock strut attachment was declared structurally acceptable with the preceding margins.

APPENDIX E
LANDING GEAR DRAWINGS

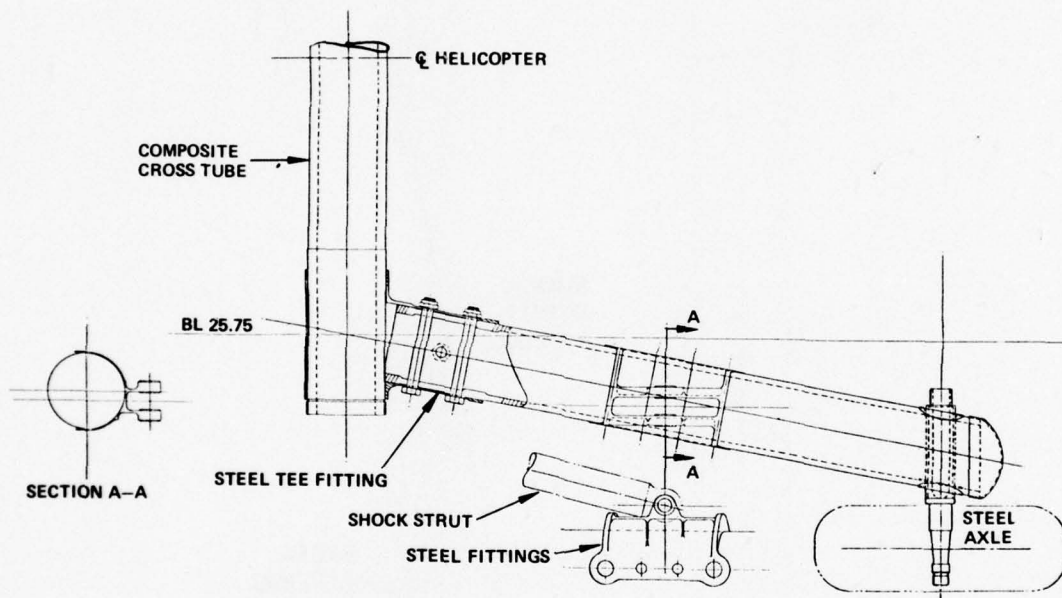


Figure E-1. Configuration 1.

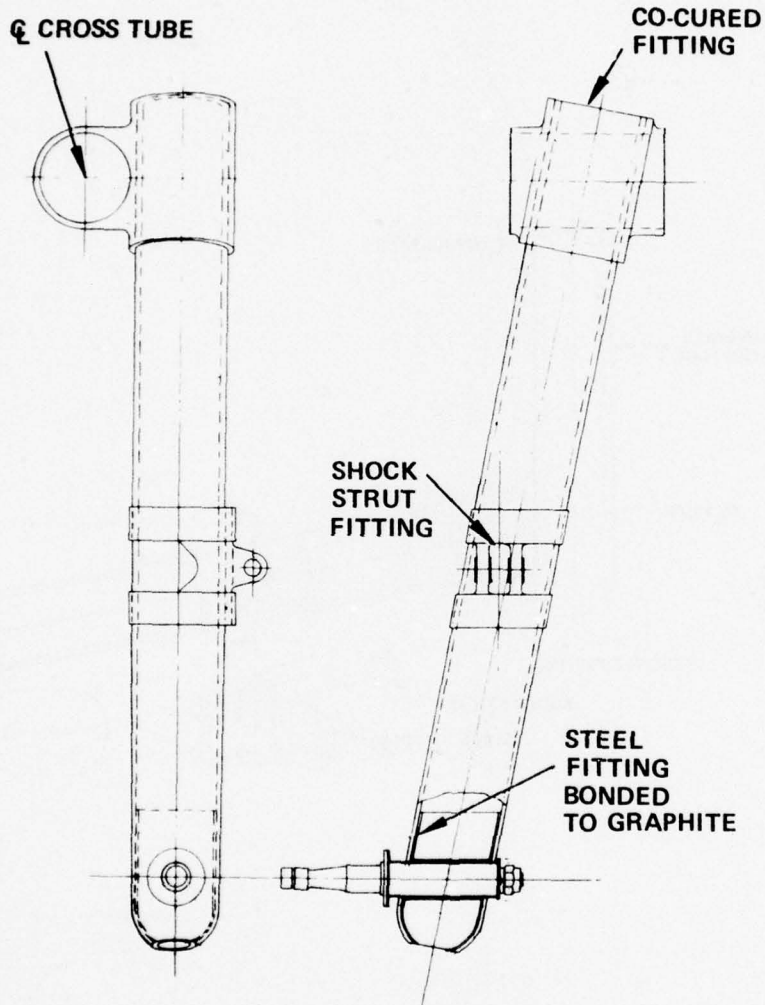


Figure E-2. Configuration IA.

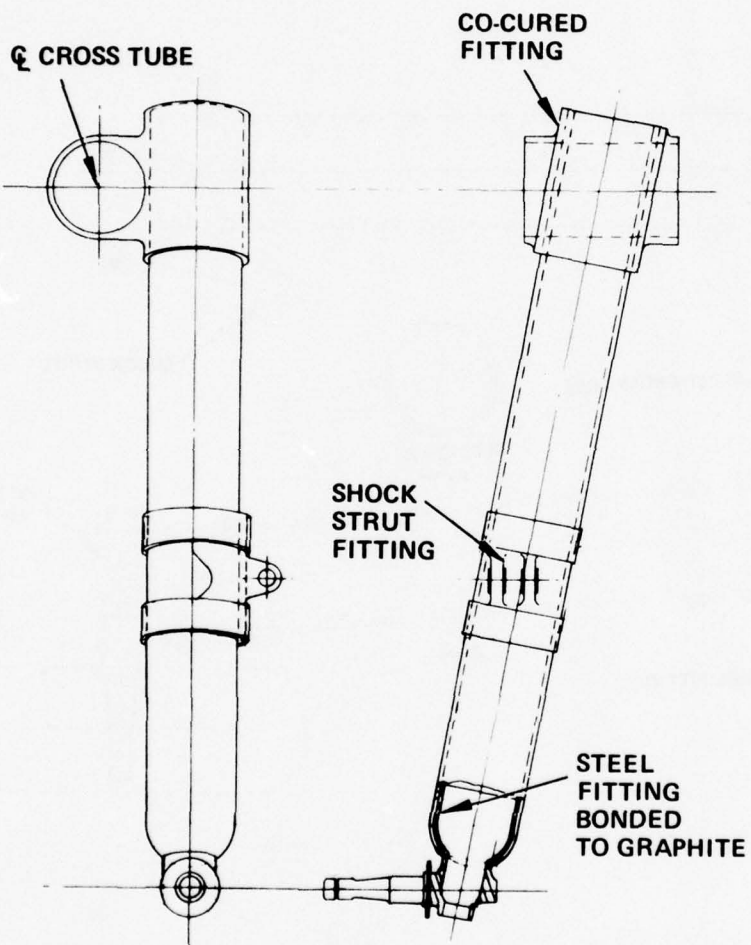


Figure E-3. Configuration 1B.

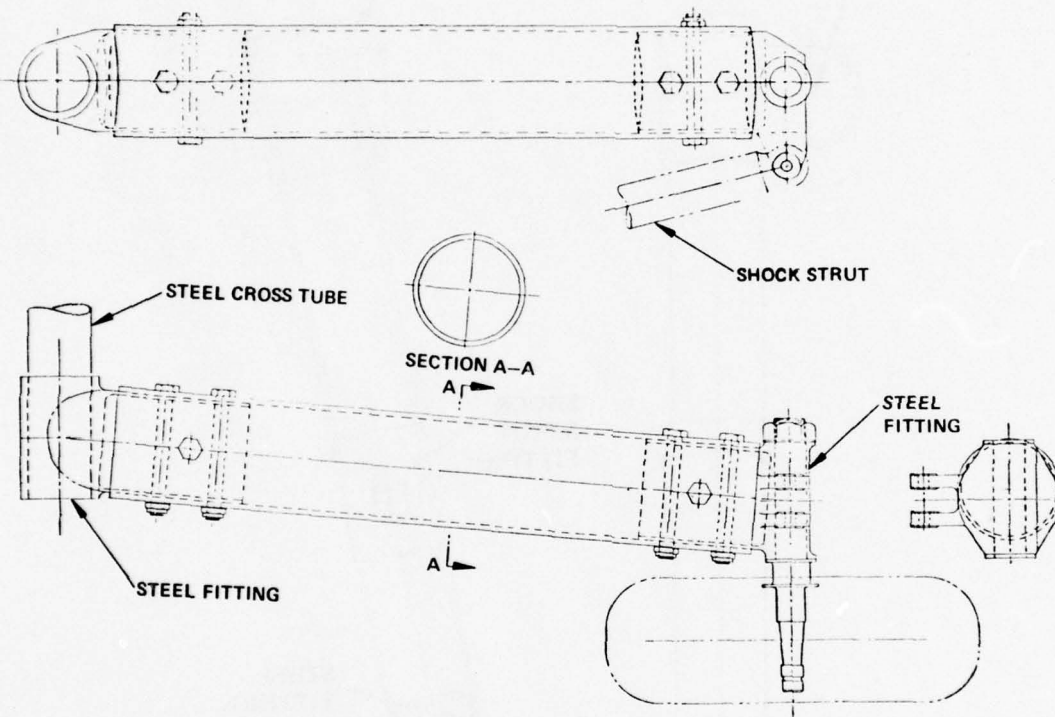


Figure E-4. Configuration 2.

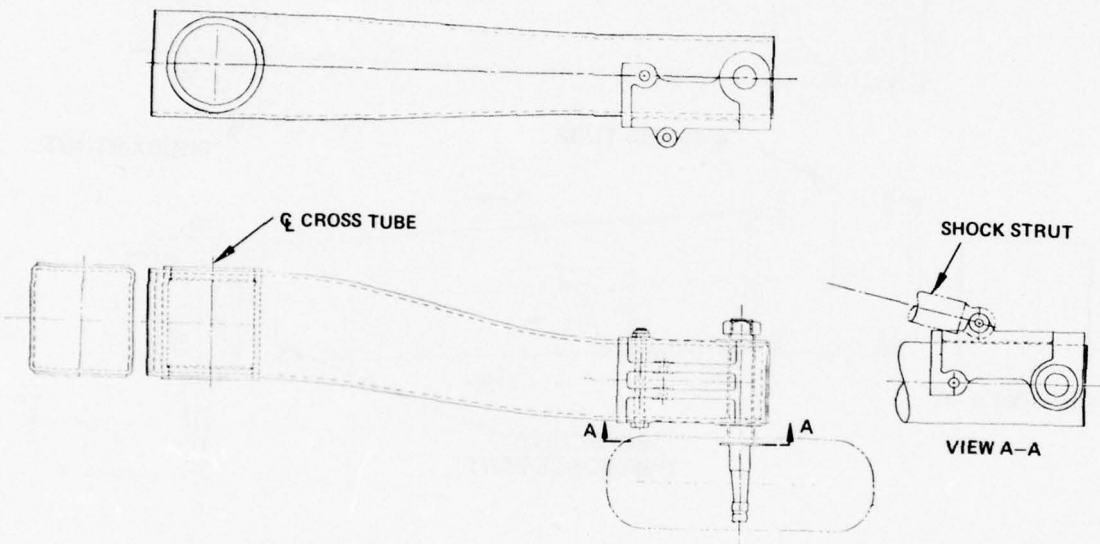


Figure E-5. Configuration 3.

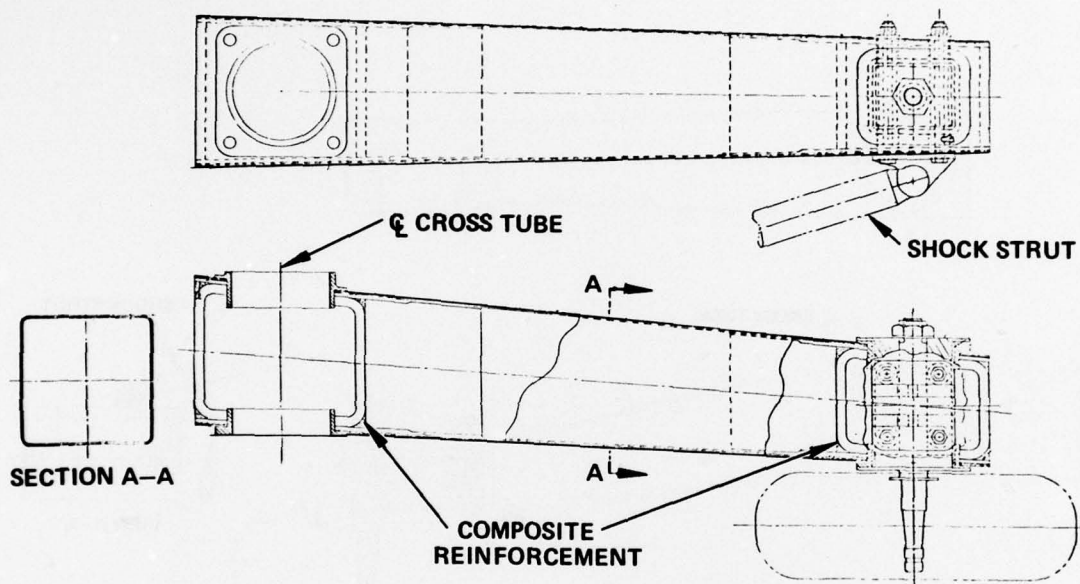


Figure E-6. Configuration 4.

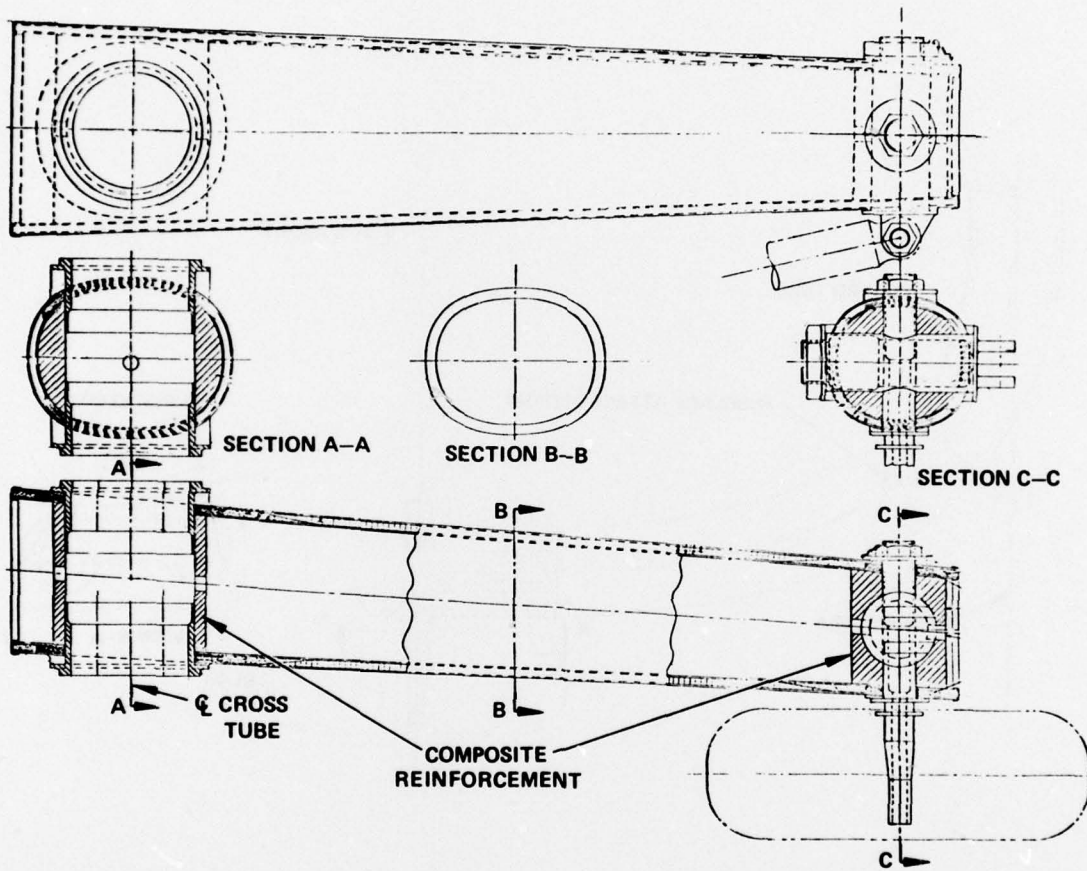


Figure E-7. Configuration 4A.

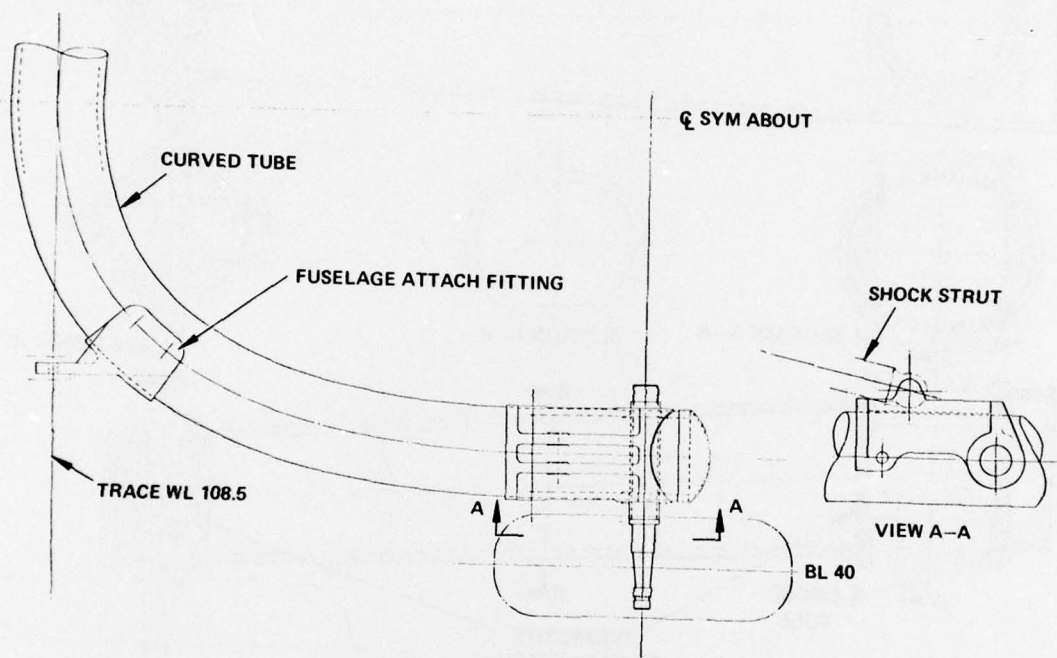


Figure E-8. Configuration 5.

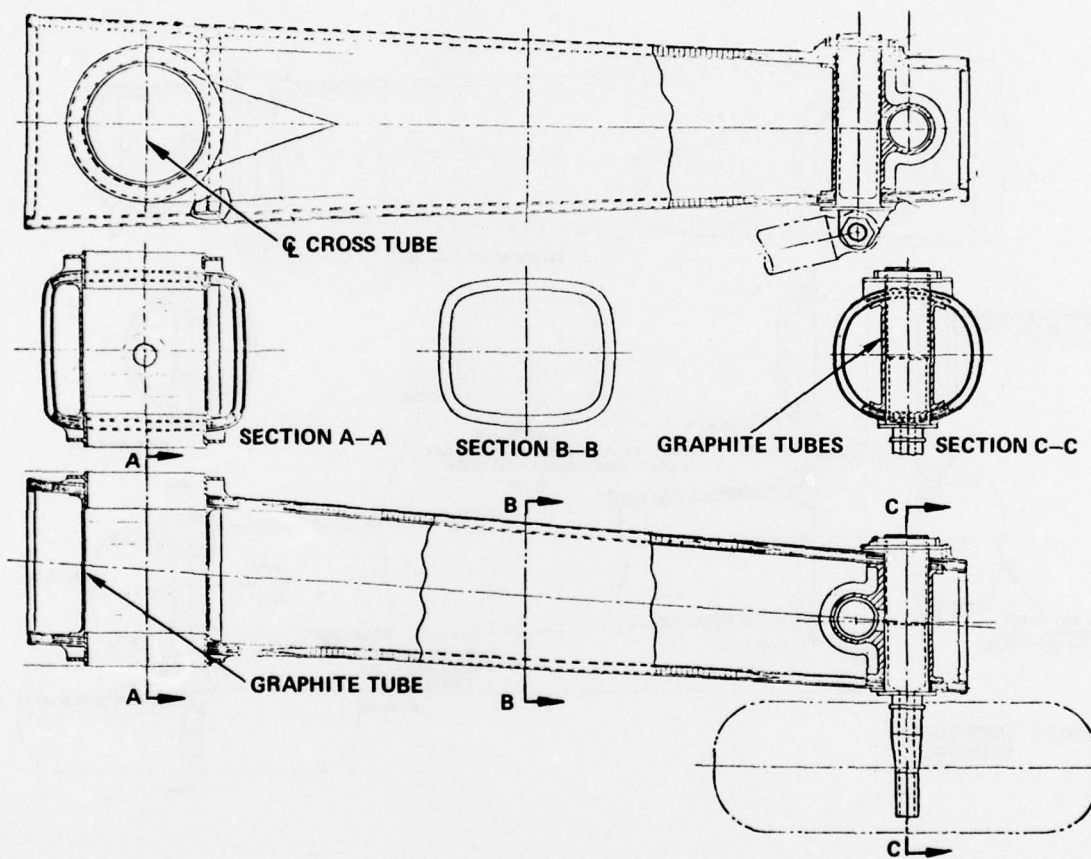


Figure E-9. Configuration 6.

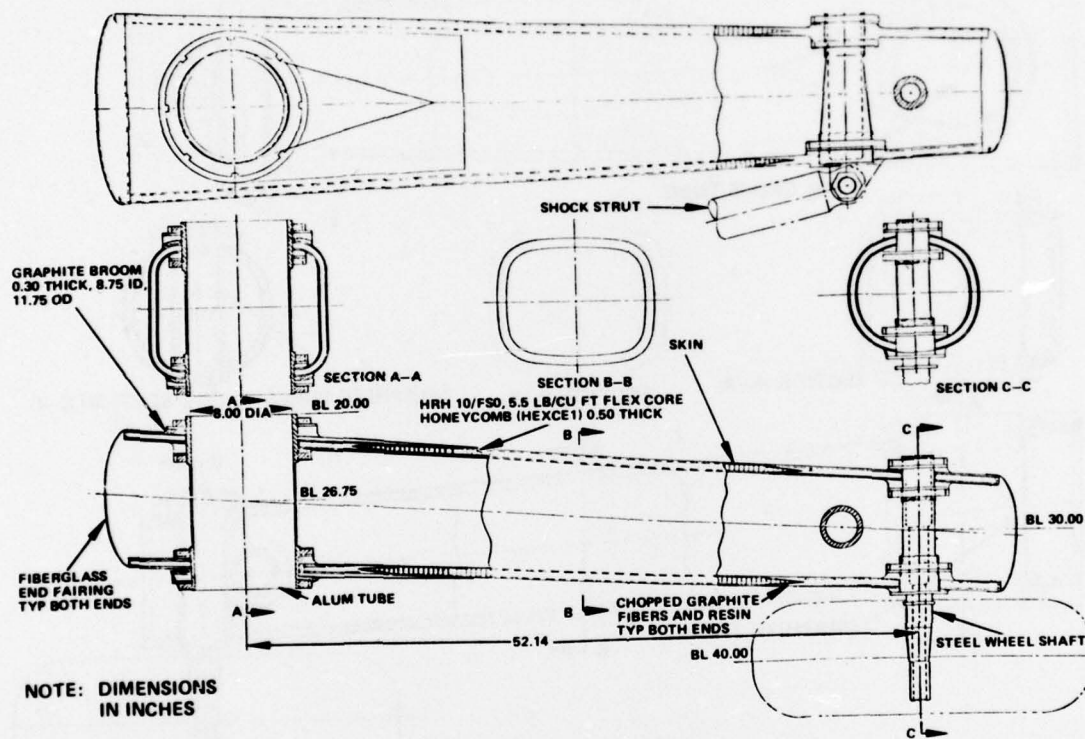


Figure E-10. Configuration 6A.

WINDING SEQUENCE-TRAILING ARM (3)

OPERATION	TOP ° FITTING	R" THICKNESS	ADD TO TOP, BOT, & SIDES AS FILLERS AT BROWN LAYERS	CENTER ° THICKNESS AVERAGE	BOTTOM ° FITTING
1	90°	.0328			90° .0328
2	90°	.0082		90° .0082	90° .0082
3	45°	.0328		15°	.0328
4	90°	.0328			
5	15°	.0328		15° .0396	15° .0458
6	BROWN	.0738	± 45°	.0986	15° .0328
7					90° .0328
8	45°	.0328		45° .0396	45° .0458
9	BROWN	.0738	± 45°	.0656	90° .0328
10					15° .0328
11	15°	.0328		15° .0396	15° .0458
12					15° .0328
13				.50	.0328
14					15° .0328
15	15°	.0328		15° .0396	15° .0458
16					15° .0328
17	BROWN	.0738	± 45°	.0656	90° .0328
18	45°	.0328		45° .0396	45° .0458
19					90° .0328
20	BROWN	.0738	± 45°	.0986	15° .0328
21	15°	.0328		15° .0396	15° .0458
22	90°	.0328			90° .0328
23	45°	.0328			
24	90°	.0082		90° .0082	90° .0082
25	90°	.0328			90° .0328
				7632	7632

* FULL LENGTH LAYERS

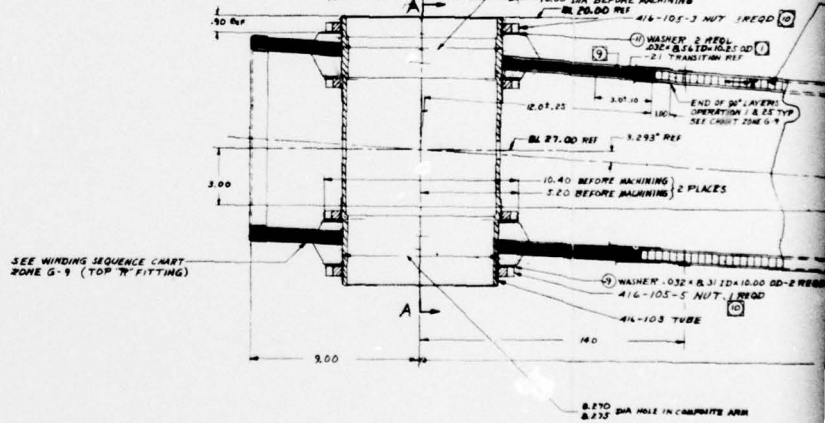
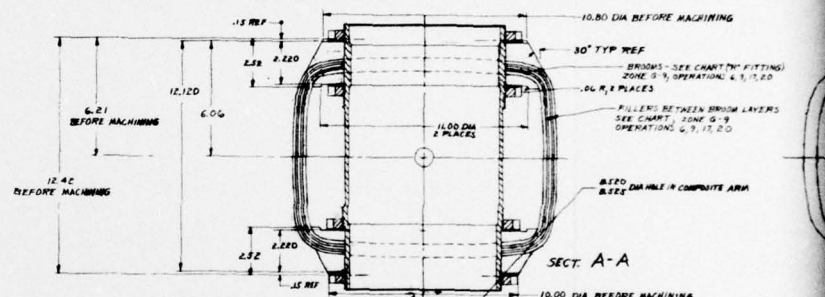
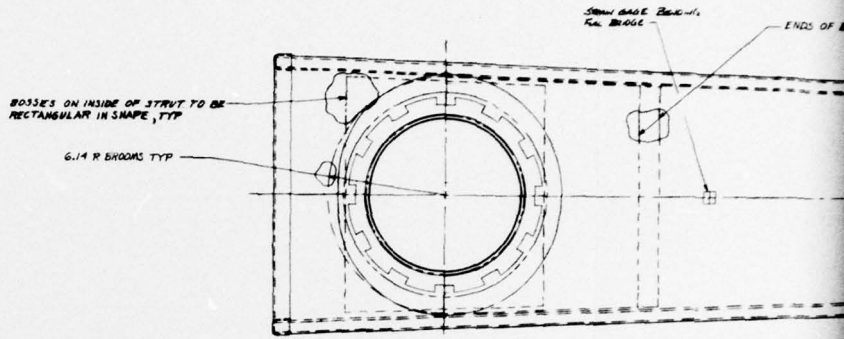
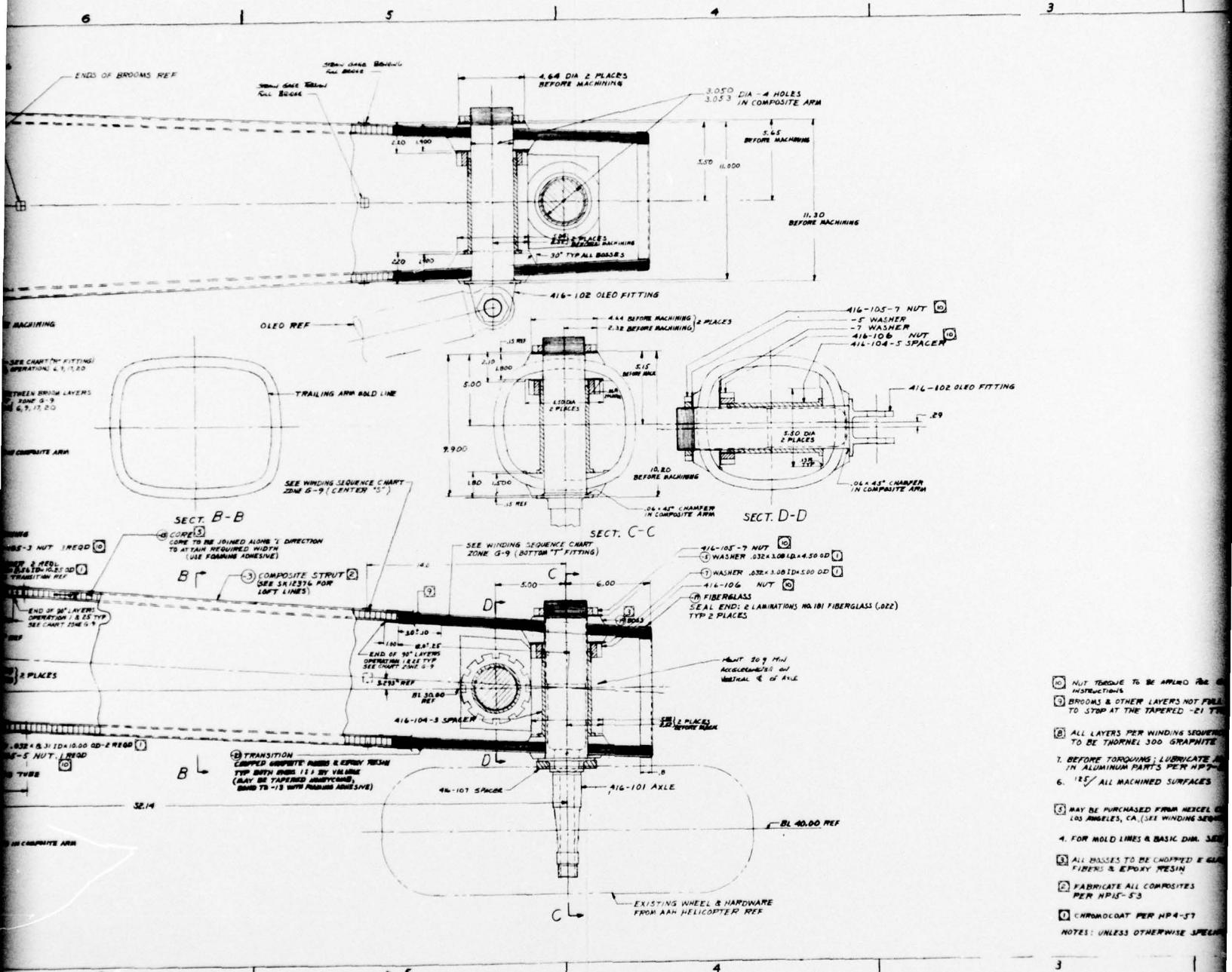


Figure E-11. Arm Assembly, Main Landing Gear.



- 10 NUT TORQUE TO BE APPLIED PER INSTRUCTIONS
 - 11 BROOMS & OTHER LAYERS NOT PERMITTED TO STOP AT THE TAPERED -21 TYP.
 - 12 ALL LAYERS PER WINDING SEQUENCE TO BE THORNEL 300 GRAPHITE
 - 13 BEFORE TORQUING: LUBRICATE ALL ALUMINUM PARTS PER HP4-53
 - 14 ALL MACHINED SURFACES
 - 15 MAY BE PURCHASED FROM MERCER INDUSTRIES, LOS ANGELES, CA. (SEE WINDING SEQUENCE)
 - 16 FOR MOLD LINES & BASIC DIM. SEE
 - 17 ALL BROUSES TO BE CHIPPED & GLASS FIBERS & EPOXY RESIN
 - 18 FABRICATE ALL COMPOSITES PER HP4-53
 - 19 CHROMODAT PER HP4-53
- NOTES: UNLESS OTHERWISE SPECIFIED

2

APPENDIX F

WEIGHT ANALYSIS

COMPOSITE TRAILING ARM WEIGHT BREAKDOWN (LB)

CONFIGURATION 1

Composite tube	38.0
Upper T fitting	23.3
Lower axle and nut	11.26
Shock strut fitting	<u>8.69</u>
TOTAL	81.25

CONFIGURATION 5

Composite tube	99.36
Axle (2)	14.80
Fuse attach fittings (2)	16.80
Shock strut fitting	<u>9.20</u>
TOTAL	140.16

CONFIGURATION 6A

Composite fittings	36.60
Skins	13.71
Honeycomb	2.42
Bosses, covers, etc	2.00
Metal fittings	<u>14.00</u>
TOTAL	68.73

WEIGHT ANALYSIS OF FINAL COMPOSITE TRAILING ARM (LB)

Upper fitting	23.75
Lower fitting	20.14
Skins	11.33
Honeycomb	1.77
Bosses, covers, etc	2.50
Adjust for holes, etc	<u>-7.42</u>
TOTAL, graphite arm	52.07
Shock strut fitting	5.80
Axle	7.00
Hardware	<u>1.55</u>
TOTAL, trailing arm assembly	66.42

APPENDIX G

TEST PLAN

- SCOPE:** This procedure describes the plan for static and dynamic testing of a composite landing gear trailing arm. The static and impact loads are directly comparable to those of the metal gear of the YAH-64 helicopter.
- DOCUMENTS:** HH Drawing 416-100, Arm Assembly
Figure G-1, Basic Dimensions
- EQUIPMENT:** Menasco test equipment, YAH-64 shock strut plus wheel and tire (bailed from YAH-64 program).
High speed (500 frames/sec) photographic equipment.
- INSTRUMENTATION:** The following gages or instruments, located on Drawing 416-100, shall be used.
1. Strain gages for bending, one bridge at two locations, to be used for dynamic and static testing.
 2. Strain gages for torsion, one bridge to be used for dynamic and static testing.
 3. A linear accelerometer for measuring vertical g loads during dynamic testing.
- STATIC TEST:** The arm will be loaded for a two-wheel landing with an outboard side load. All deflections will be measured relative to the axle and wheel center line in the fully extended position.
- The following limit loads will be applied at the wheel:
- | | | |
|--------------------|---|-----------|
| Vertical load | = | 22,000 lb |
| Outboard side load | = | 11,000 lb |
- Deflection measurements will be taken in at least six increments between 10 and 100 percent of the preceding loads. Upon attaining 100-percent load,

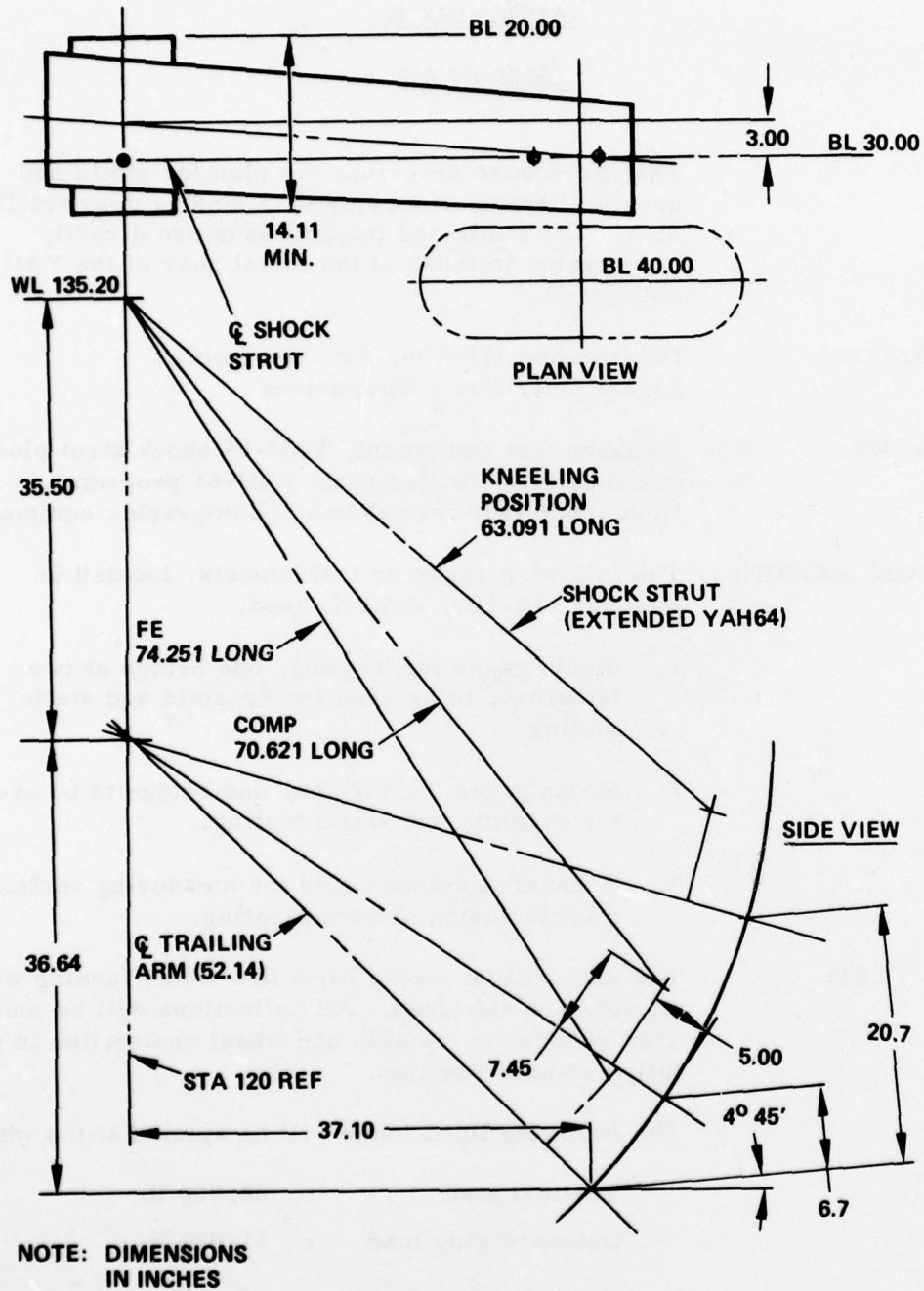


Figure G-1. Basic Dimensions.

the loading shall be reduced to zero and then the deflection measured at 10-percent load. After determining the permanent set, the strut shall be loaded to failure or to the maximum load permissible with the test apparatus.

DYNAMIC TEST:

The gear will be dropped to obtain the vertical impact loads associated with limit and reserve energy dropping of the YAH-64 gear. The drop weight and vertical ground reaction are to be recorded. A time history recordation of the stresses and accelerations shall be attained using the gages and accelerometer listed under "Instrumentation." High speed photographs are to be taken of the 32,000-lb (4.5g) reserve energy drop. The following conditions shall be used:

Helicopter Wt. (Ref only)	=	13,950 lb
Drop Wt.	=	To be determined
Ground Load Factor (Ref only)	=	3 and 4.5
Vertical Ground Reaction Limit	=	21,300 lb
Reserve E	=	32,000 lb
Tire Pressure (No load)	=	105 ± 2 psig
Platform Angle	=	Level
Helicopter Attitude	=	3-point

REPORT:

A simplified final report shall contain:

- Results of data measurements acquired during static and dynamic tests
- Four photographs of each test setup
- Description of all test history pertaining to the capability of the gear, including failures, discrepancies, and changes
- A brief comparison with the YAH-64 gear regarding general capabilities

WITNESS:

All testing shall be conducted by Menasco and witnessed by HH representatives and, if possible, Eustis Directorate personnel.

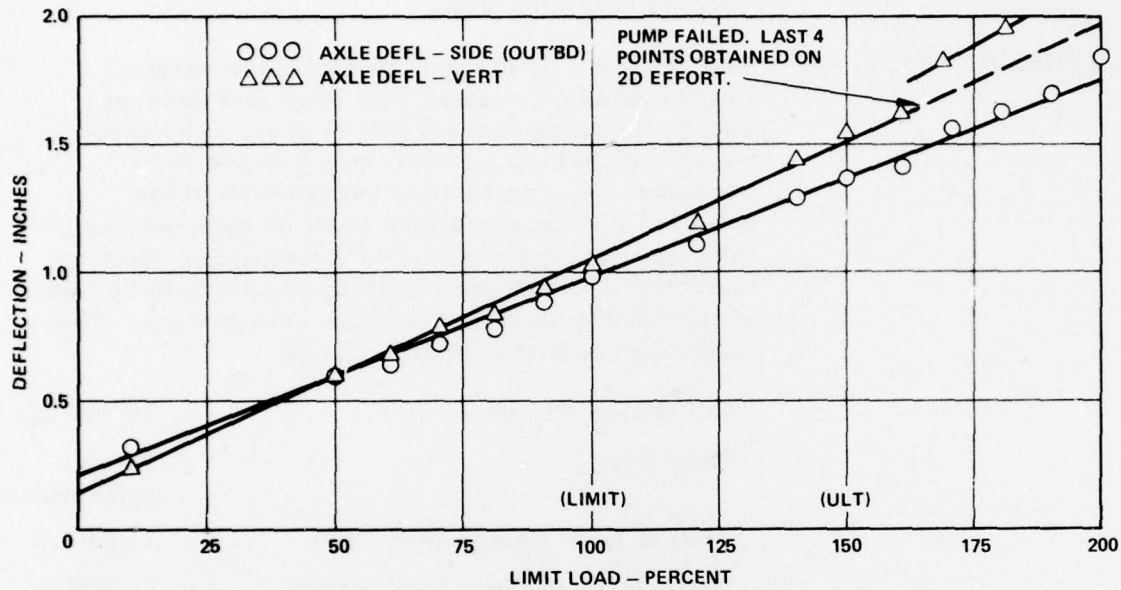


Figure G-2. Static Load Deflection Curve.